

RNI: DELENG/2005/15153

Publication: 15th of every month

Posting: 19th/20th of every month at NDPSO

No: DL(E)-01/5079/14-16

Licensed to post without pre-payment U(E) 28/2014-16

Rs.100

ISSN 0973-2136

www.mycoordinates.org

Coordinates

Volume XI, Issue 02, February 2015

THE MONTHLY MAGAZINE ON POSITIONING, NAVIGATION AND BEYOND

Positioning **N**avigation **T**iming *governance* **Required Improvements**



GNSS • GEODESY • LIDAR

Count On It

NEW
FOR 2015



Nikon Quality

There are things you can still count on in this world. The sun will rise, taxes will be levied, surveyors will be working, and Nikon total stations will be right there with them day after day. Your customers count on you and surveyors have always relied on Nikon total stations to provide quality results.

Nivo™ C Series features a Windows CE touchscreen interface and powerful Survey Pro, Layout Pro and Survey Basic with Roads field software.

Nivo M+ Series uses the intuitive Nikon onboard field software and is available in 2", 3" and 5" models. Point memory size has been increased to 25,000 points and a USB port added for convenient and portable data transfer.

NPL-322+ and DTM-322+ Series offer economical choices with Nikon quality and precision. Available in 2" and 5" models, Bluetooth is now standard and point memory has been increased to 25,000 points.

Visit www.nikonpositioning.com to choose the model that is right for you. Your jobs. Your choice.

Simply Nikon Quality

AMERICAS

Spectra Precision Division
10368 Westmoor Drive
Westminster, CO 80021, USA
+1-720-587-4700 Phone
888-477-7516 (Toll Free in USA)

EUROPE, MIDDLE EAST AND AFRICA

Spectra Precision Division
Rue Thomas Edison
ZAC de la Fleuriaye - CS 60433
44474 Carquefou (Nantes), France
+33 (0)2 28 09 38 00 Phone

ASIA-PACIFIC

Spectra Precision Division
80 Marine Parade Road
#22-06, Parkway Parade
Singapore 449269, Singapore
+65-6348-2212 Phone

©2015, Trimble Navigation Limited. All rights reserved. Nikon is a registered trademark of Nikon Corporation. All other trademarks are the property of their respective owners. (2015/1)



Scan the QR
code to receive a
FREE brochure



Visit www.nikonpositioning.com for the latest product information and to locate your nearest distributor.



Man the Unmanned

with centimeter- to decimeter-level accuracy.



THE ASHTECH MB-ONE — A NEXT GENERATION COMPACT, POWERFUL GNSS OEM RECEIVER MODULE

Impressive GNSS and RTK technology paired with Ethernet support in a miniature, power-saving design achieves centimeter- to decimeter-level accuracy for unmanned applications and more.

MB-ONE RECEIVER: FOR HIGH-PERFORMANCE, CENTIMETER-LEVEL POSITIONING IN A MINIATURE, POWER-SAVING DESIGN

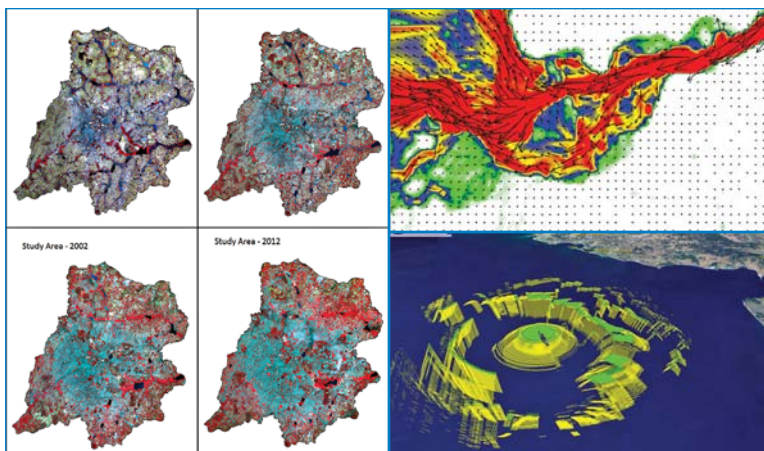
- Precise Heading + Pitch/Roll
- Precise Point Positioning using L-Band services
- 240 Channel Dual Core Engine with Ashtech Z-Blade Technology
- L1-only RTK and L1/L2 RTK with Precise Platform Positioning (P³) including Heading

The MB-ONE's extremely compact, dual-core design enables low power consumption and high performance. Count on accurate GNSS-based heading and attitude for static and dynamic applications. Man the unmanned and more with the full range of Ashtech's GNSS receivers from Integrated Technologies, a division of Trimble.

ashtech[™]

Trimble GNSS OEM

InTech.trimble.com



In this issue

Coordinates Volume 11, Issue 02, February 2015

Articles

- Positioning, Navigation, and Timing (PNT) Governance – Required Improvements** DANA ALLEN GOWARD 8
- Survey requirements for river flood assessment and spatial planning** ENRICO C PARINGIT, LOUIE P BALICANTA AND CZAR JAKIRI SARMIENTO 13
- 3D+t Acoustic Fields Modelling Based on Intelligent GIS** VASILY POPOVICH, YURI LEONTEV, VICTOR ERMOLAEV, DMITRY CHIROV AND OKSANA SMIRNOVA 18
- Tracking satellite footprints on Earth's surface** NARAYAN PANIGRAHI AND RAJ GAURAV 23
- A new approach for real-time structural monitoring** E BENEDETTI, M BRANZANTI, G COLOSIMO, A MAZZONI, M MORONI AND M CRESPI 37
- Monitoring the declination of surface water bodies using NDWI technique** AJAYA S BHARADWAJA AND PROF SYED ASHFAQ AHMED 46
- On module framework of VieVS and data processing for teaching and research** ERHU WEI, SHENQUAN TANG 50

Columns

My Coordinates EDITORIAL 6 **News** GALILEO UPDATE 22 GIS 55 IMAGING 56 GNSS 58 INDUSTRY 60

Mark your calendar MARCH 2015 TO SEPTEMBER 2015 62

This issue has been made possible by the support and good wishes of the following individuals and companies A Mazzoni, Ajaya S Bharadwaja, Czar Jakiri Sarmiento, Dana Allen Goward, Dmitry Chirov, E Benedetti, Enrico C Paringit, Erhu WEI, G Colosimo, Louie P Balicanta, M Branzanti, M Crespi, M Moroni, Narayan Panigrahi, Oksana Smirnova, Raj Gaurav, Shenquan TANG, Syed Ashfaq Ahmed, Vasily Popovich, Victor Ermolaev, and Yuri Leontev; Antcom, Effigis, HiTarget, Javad, Microsoft Vexcel, Microsurvey, Nikon, Navcom, Pentax, Rohde & Schwarz, Trace Me, Trimble, and many others.

Mailing Address

A 002, Mansara Apartments
C 9, Vasundhara Enclave
Delhi 110 096, India.

Phones +91 11 22632607, 98102 33422, 98107 24567

Fax +91 11 22632607

Email

[information] talktous@mycoordinates.org

[editorial] bal@mycoordinates.org

[advertising] sam@mycoordinates.org

[subscriptions] iwant@mycoordinates.org

Web www.mycoordinates.org

Coordinates is an initiative of cGIT that aims to broaden the scope of positioning, navigation and related technologies.

cGIT does not necessarily subscribe to the views expressed by the authors in this magazine and may not be held liable for any losses caused directly or indirectly due to the information provided herein. © cGIT, 2015. Reprinting with permission is encouraged; contact the editor for details.

Annual subscription (12 issues) [India] Rs.1,200

[Overseas] US\$80

Printed and published by Sanjay Malaviya on behalf of Centre for Geoinformation Technologies at A221 Mangal Apartments, Vasundhara Enclave, Delhi 110096, India.

Editor Bal Krishna

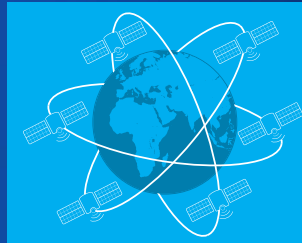
Owner Centre for Geoinformation Technologies

Designed at Spring Design (ajay@springdesign.in)

Printer Thomson Press India Ltd., B 315, Okhla Phase I, New Delhi - 110020, India

This issue of Coordinates is of 64 pages, including cover.

Gain perspective in real-world GNSS simulation



The GNSS simulator in the R&S®SMBV100A vector signal generator

Expensive, inflexible simulation of GNSS scenarios is a thing of the past. Now you can easily and cost-effectively test your satellite receivers under realistic conditions.

- Comes with a variety of predefined environment models such as "rural area", "urban canyon", "bridge" and "highway"
- Allows flexible configuration of realistic user environments including atmospheric modeling, obscuration, multipath, antenna characteristics and vehicle attitude

The R&S®SMBV100A generates all relevant communications and broadcasting standards such as LTE, HSPA+, WLAN, HD Radio™ and FM stereo.

To find out more, go to

www.rohde-schwarz.com/ad/smbv-gnss



R&S®SMBV-GNSS



Illegal signals?

According to the Federal Communication Commission (FCC),

Russia and other international GNSS service providers

Need to apply for authorization

Before their navigation signals can be legally used in the United States.

In addition, manufacturers are required

To get multi-constellation receivers certified for US use.

When there is a need to strengthen the efforts in the direction

That favors more conducive, compatible and interoperable multi GNSS scenario

Such developments not only strike a chord of discontent

Among various GNSS service providers,

But may also become a stumbling block

In encouraging free and fair usage of GNSS signals.

Bal Krishna, Editor
bal@mycoordinates.org

ADVISORS Naser El-Sheimy PEng, CRC Professor, Department of Geomatics Engineering, The University of Calgary Canada, George Cho Professor in GIS and the Law, University of Canberra, Australia, Professor Abbas Rajabifard Director, Centre for SDI and Land Administration, University of Melbourne, Australia, Luiz Paulo Souto Fortes PhD Associate Director of Geosciences, Brazilian Institute of Geography and Statistics -IBGE, Brazil, John Hannah Professor, School of Surveying, University of Otago, New Zealand

ZTS-360R

Total Station

Compact, lightweight design

High-performance MCU STM32

Powerful 600m reflector-less measurement capability

Dust and water protection IP66



FC CE  IP66

HI-TARGET

Surveying the world, Mapping the future.

www.hi-target.com.cn
info@hi-target.com.cn

Positioning, Navigation, and Timing (PNT) Governance – Required Improvements

Governance must ensure that sufficient rules, awareness systems, and operational capability exists to prevent most service disruptions, and to respond to the disruptions that do occur



Dana Allen Goward
President, Resilient
Navigation and Timing
Foundation, USA

The motion picture “Gravity” begins with a series of cascading failures. The destruction of one satellite creates orbiting debris. This debris sweeps through space destroying multiple satellites, which makes much more debris and destroys many more satellites. One imagines the process continuing until the entire orbital sphere contains nothing but fragments of fragments.

The film is instructive for government leaders and PNT policy professionals in two ways. First it reminds us that, simply because satellites dwell high above the earth, they are not immune to mishap. Severe space weather, cyber-attack, asteroids, and other misfortunes - including cascading showers of debris - could damage or cripple even the most robust constellation. Secondly, it is a dramatic example of progressive failures. It shows how the failure of one component of a system, if not contained, can ripple outward wreaking extensive destruction.

For many nations, GNSS is a single point of failure that can cause cascading failures across society. Because it is highly precise and free for use by anyone with an inexpensive receiver, clever (and economy minded) engineers have incorporated GNSS navigation and timing signals into nearly every facet of modern life. Financial transactions are marked with a GNSS time stamp. IT systems, cell phone networks and many synchronized electrical grids depend upon GNSS time and/or frequency for proper functioning. Agriculture is reputed to

be 30% more efficient and productive in many places because of GNSS technology. And, of course, GNSS signals are essential for modern transportation systems and networks. They are even used to synchronize traffic lights on some busy city streets, and in the engine controls of some vehicles and vessels.

GNSS has become an essential, silent, utility, like running water. It is possible, with some discomfort, and reduction in safety and efficiency, for modern societies to do without it for short periods. Extended outages could be disastrous.

Space systems, by their very nature, transmit very faint signals that are easy to disrupt. This is a vulnerability that many militaries are able to exploit by jamming GNSS over wide areas. North Korea has repeatedly done this to South Korea. Recognizing that signals from space are so faint and easy to disrupt, Russian military doctrine assumes that space systems will not be available to its forces in combat. The US military is also very concerned, and regularly holds exercises such as “A Day Without Space.”

Until now, though, most non-military GNSS disruptions have been fairly localized and confined to areas of several square kilometers or less. Some of these disruptions have been accidental. For example, novice US Navy technicians have accidentally jammed significant portions of the San Diego and Norfolk metropolitan areas at various times.

The most important
function of government is
protection of its citizens

The great majority, of such incidents, though, have been as a result of individuals with “Personal Protection Devices” or “PPDs.” Illegal in most countries, but inexpensive and easy to obtain from on-line sellers, these devices can operate from a small battery or a vehicle’s lighter/power outlet. Many are able to completely disrupt GNSS reception within tens or hundreds of meters. PPDs are becoming increasingly popular among individuals who don’t wish to be tracked by their spouses, employer, or governments.

Though few formal monitoring programs exist, authorities in the UK, US and elsewhere report that PPD usage is on the rise. Such devices have been responsible for interfering with airport systems, cellular communications, and stock exchanges. In fact, few systems that use GNSS have been spared at least minor disruptions. Many GNSS professionals are familiar with the incidents at the Newark International Airport in the United States that disrupted aircraft landing systems. Less well known is that the airport detects approximately 5 jamming devices a day passing by on a highway it abuts. More recently, French authorities monitored over 2,100 GNSS jamming incidents during a six month period on the A1 highway that runs through Charles de Gaulle International Airport.

More insidious, and potentially more problematic and dangerous, spoofing has also been revealed as a vulnerability for many GNSS users. Spoofers have effectively assumed control of both surface vessels and unmanned aircraft by transmitting signals only slightly stronger than those from GNSS. While advances have been made in receiver and antenna technology to reduce this threat, the nature of GNSS signals and the proliferation of inexpensive receivers means that spoofing will be a potential problem for many years to come.

Governments' responsibilities

The most important function of government is protection of its citizens. Yet, in spite of PNT’s criticality, few governments recognize it as critical infrastructure, or have even formally

acknowledged its importance. Fewer still are organized to ensure PNT services, and by extension, its citizens, are protected.

The United States presented an incredible gift to the world by making GPS available to all. Other GNSS

are following suit. Unfortunately, as the only sources of precise, wide area, wireless PNT for many nations, these free gifts have become like the first samples of a highly addictive drug. They have rapidly created a broad dependency upon space that, if it was no longer available, could cause the user extreme distress. Governments have a responsibility to protect their citizens and reduce this, potentially life threatening, dependence.

One of the important ways governments protect their citizens is by providing and preserving “common goods.” Things like defense forces, diplomatic services, etc., that benefit all, but that individuals and small groups are unable, unwilling, or shouldn’t do on their own. With many nations providing, or planning to provide, space-based PNT (GNSS) free of charge and available to all, PNT services have become widely seen as a common good. But nations that do not have adequate PNT governance suffer from “the tragedy of the commons” in this area. Like the world’s other commons - space, the oceans, cyberspace - everyone wants to use PNT, but no one wants to pay for and maintain it.

PNT services, which are necessary for so many different things, and touch people in so many different ways, must be coherently governed, if the public good they provide is to be preserved.

A Governance Model

In order to think systematically about the actions governments should and

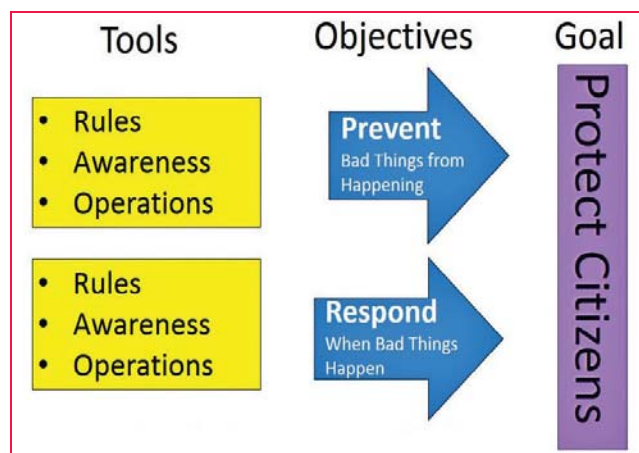


Figure 1: Generic Governance Model

must take to reverse this situation and ameliorate the threat, it is helpful to first think about how they work. Governments protect their citizens by (1) preventing adverse incidents when they are able, and when they are not, by (2) responding to ameliorate damage and restore things to normal. For example, governments take steps to prevent hazardous chemical spills. When spills do occur, they protect citizens by ensuring a rapid response to clean it up.

“Prevention” and “response” efforts can be classified as falling within one of three categories – Rules, Awareness, and Operations.

- Rules - approved and preferred behaviors articulated in laws, regulations, best practices, etc.
- Awareness – being able to sense the environment, determine if the rules are being followed, and discover information that would inform action (examples: Being aware of adverse trends to be reversed to prevent an adverse event, or, in a response, information needed to aid restore normalcy). This includes collecting, storing and analyzing data so that it can become information and knowledge.
- Operations – interacting with the real world to:
 - Encourage or compel adherence to the rules
 - Shape the environment to prevent adverse incidents
 - Restore the environment to the desired state.

Using this model, we can discover and organize the kinds of things governments should do to protect its citizens from adverse PNT-related events.

Prevention and response

Prevention

Video of helicopters braving storm winds to rescue hapless victims is very dramatic and plays well in the media. Yet, it is also evidence of a failure to prevent the incident in the first place.

Preventing bad things from happening, in addition to eliminating human pain and suffering, is almost always more economical than responding to and recovering from an adverse event. For the price of one ship and the rescue of its crew by helicopter, for example, a whole fleet of vessels could be inspected to ensure their hulls are strong, and their bilge pumps in working order.

Rational governments put the majority of their efforts into preventing bad things from happening so as to avoid societal damage and costly response operations.

For our purposes, the “bad thing” to be prevented is disruption of PNT services. The following list provides a starting point for the kind of Rules, Awareness, and Operations a government should have in place as part of its prevention efforts:

Prevention rules

(Laws, regulations, best practices, etc.) – These should:

- Ban or strictly limit the manufacture, import, export, sale, possession, and use of jamming and spoofing devices. To be effective, such rules must provide for penalties sufficient to deter the proscribed actions. Penalties vary widely across the globe. In Australia, use of a jammer is punishable by time in jail. In the United States, it is a civil (as opposed to criminal) offense punishable by a monetary fine. Some nations have no laws or

Rational governments put the majority of their efforts into preventing bad things from happening so as to avoid societal damage and costly response operations

regulations on the topic whatsoever.

- Require owners and operators of critical infrastructure and critical applications that rely upon GNSS signals to have and use a second navigation and/or timing source that has different characteristics and failure modes. *Requiring systems with different failure modes is essential for resilience so that one disruption event does not impact both systems. Using GLONASS or Galileo, for example, to complement GPS does not provide much added resilience as all are faint, space-based signals that operate in the same frequency band. Also, such requirements should be carefully structured so as to avoid “economical, malicious compliance” that meets the letter of the mandate, but does not increase resilience. For example, governments may wish to include a requirement for the non-GNSS system to be able to sustain operations for 60 or more days in the absence of GNSS services.*
- Require major commercial consumers of GNSS services to actively participate in jamming and spoofing prevention and response efforts. *This could include mandatory reporting of disruption incidents, required participation in detection networks, etc.*
- Establish industry standards for GNSS receivers used for critical systems that reduce their susceptibility to jamming and spoofing. *Many receivers, for reasons of economy, are designed to minimal standards and are subject to regular*

and predictable disruption from known and legal sources. For example, some receivers malfunction when authorities activate known, authorized, but non-routine, GNSS functions. This is because it would have been more expensive to design and build the receiver otherwise.

- Establish spectrum management standards that protect GNSS frequencies.

Prevention awareness

(The ability to detect, develop data and records, and analyze trends) – This should include the ability to:

- Detect illegal manufacture import, export and sale of jamming and spoofing devices.
- Detect use of jamming and spoofing devices. *While scattered, localized capability exists in many nations now, it is ad hoc, there are few organized networks, and few records are kept. Given the broad use of GNSS across societies, greatly broadening, networking and systematizing jamming and spoofing detection should be relatively easy and inexpensive. For example, if every cell tower had the capability to detect potential jamming or spoofing, an automated reporting network could easily be created. The cost of establishing such a system would be miniscule compared to the value of just the cellular infrastructure it protected.*
- Understand the use, performance and reliability of all PNT sources. *The goal of each nation should be to have a “healthy navigation and timing eco-system” that includes multiple sources with different failure modes that simultaneously support each other and fill the needs of all users. A complete understanding of each PNT sources is needed to ensure the resilience of the nation’s overall PNT capability and resilience. These sources include GNSS, VOR/DME, TACAN, Loran/eLoran, local positioning systems, inertial systems, clocks of all types, dead reckoning, compasses, etc.*
- Analyze trends and to inform improvements in rules, awareness and operations.

Prevention operations

(The use of information gained through Awareness, to encourage or compel compliance with Rules) - This requires sufficient enforcement and administrative capability to:

- Terminate illegal manufacture, import, export, sale, and possession of jamming and spoofing devices.
- Ensure PNT consumers, especially those with critical infrastructure and applications, comply with resilience Rules (standards, regulations, etc.)
- Ensure those who violate the Rules are appropriately processed and sanctioned.
- Ensure compliance with spectrum and equipment standards.
- Analyze prevention failures and modify Rules, Awareness and Operations to help avoid similar adverse events in the future.

Response

Even with the best prevention efforts, bad things will, inevitably, happen. When they do, governments must ensure sufficient capability and be ready to respond, recover and restore critical systems. Wise and efficient governments focus their response efforts on small, low level infractions as a way of creating an orderly environment and forestalling more serious offenses. Just as New York City authorities aggressively enforce requirements to replace cracked windows as a way of deterring neighborhood crime, governments should vigorously pursue individuals using "Personal Protection Devices" as a way of averting larger incidents and protecting critical infrastructure.

Response rules

These should dictate, who has the authority to act, where capability should reside, and how responses should be coordinated and conducted. - They should:

- Make manufacture, sale, possession and use of jamming and spoofing devices an offense at all levels of government. The great majority of law enforcement resources for many nations exist

Just as New York City authorities aggressively enforce requirements to replace cracked windows as a way of deterring neighborhood crime, governments should vigorously pursue individuals using "Personal Protection Devices" as a way of averting larger incidents and protecting critical infrastructure

at the state and local, vice federal, levels of government. Being able to leverage local Awareness and Operations capabilities depends upon local officials having the authority to participate in enforcement. Having this authority could be of great interest to local law enforcement. Detecting the presence of an active jammer during a routine traffic stop, for example, could be an indication of other illicit activity and aid community policing (pocket-sized jammer detectors are commercially available).

- Provide the authority for information sharing, joint operations and coordination among all private, commercial, and government organizations.
- Designate an organization to lead development of standard operating procedures, best practices, recommended equipment, etc. for responses.
- Outline priorities and responsibilities for recovery operations.

Response awareness

The ability to understand the extent of an incident and the condition of PNT services nationwide, to locate disruption sources in real time, and to know the location, status and activities of enforcement resources. This capability should include:

- Rapid location and identification of disruption sources, including those on moving platforms. *Most disruption sources are mobile. Static detection networks need to be able to track their movement in real time and communicate that to enforcement personnel. Enforcement*

personnel must also have mobile detection capability in order to precisely locate and identify the source of a disruption. A nightmare scenario for many authorities is a jamming device suspended from a weather balloon set adrift in light winds over a densely populated area. Not only would it wreak havoc on numerous systems, it would be very difficult to locate and disable. Location of mobile jammers on the land, sea, and in the air should be part of the awareness capability suite.

- The ability to understand the state of PNT services nation-wide. *As a national, critical infrastructure utility, wide area PNT services should be monitored for outages and to support rapid response and recovery. Having this "big picture" also helps authorities triage between localized issues and larger, perhaps more sinister and serious problems, and gauge their responses accordingly.*
- The location, status and activity of all enforcement resources.
- Communications and information sharing between response forces.

Response operations

The ability to promptly terminate a disruption, apprehend wrongdoers, restore the system, and help those impacted rapidly recover. This requires:

- Sufficient resources to effectively respond to and terminate disruptions *This includes the ability to operate on the land, sea, and in the air. Also the capability and capacity to apprehend, process and sanction those involved.*
- Sufficient resources to promptly

recover the system from a disruption and restore services.

- Preparation, exercise and training for response personnel.

The structure of governance

This author is tempted to postulate that the actual organizational structure of PNT governance is irrelevant. As long as it ensures quality services, prevents and responds to disruptions, what does it matter how the shapes on an organization chart are arrayed?

Yet organization charts mean things. They describe roles and, more importantly, relationships. They greatly influence how, and if, things get done. This is important because governance cannot be a static, “one shot and you are done,” endeavor. It must be dynamic and adapt to changing environments and realities.

Attributes for Good Governance

So structure can be important. While it may take many forms, good PNT governance must be organized such that:

- The views of all users are regularly heard, understood and considered
- Authorities and responsibilities of all participants are clear.
- Policies and plans to ensure reliable PNT services are developed and implemented. These include:
 - Prevention of service disruptions
 - Response to service disruptions that include system restoration and recovery
 - Ensuring the long term health and improvement of services
- One official is designated the primary leader for national PNT governance. The leader and his or her organization should have:
 - Ensuring national PNT services as a part of their core missions
 - The technical expertise and stature to be a credible leader
 - The ability to act as the secretariat for PNT stakeholders and users
 - The organizational status and budget authority to carry out their responsibilities.

The greatest return on investment – Five things every nation should do now

PNT has become supremely important. These services are a matter of national and economic security for every country. All should be more than eager to make every effort to ensure they are sufficient and reliable. Yet the long list of tasks for governments provided in this paper could seem overwhelming. Not all of the tasks and conditions are of equal importance, though. Implementation of a select few will enable any nation to realize great benefit from improved PNT governance and resilience.

- 1) **Publicly recognize and designate PNT as critical infrastructure.** PNT is critical infrastructure by almost any conceivable definition. Saying this out loud helps move it from being an unappreciated, silent utility and into the public consciousness. It will help garner support for governance efforts, and inspire innovation and contributions from unexpected quarters.
- 2) **Appoint a principal leader for national PNT.** Governance of services critical to a nation’s security, sovereignty, and economic well-being should be led by a prominent, respected official whose success or failure is tied to quality, resilient, uninterrupted services. PNT resilience should be part of the core missions of his or her organization. And, of course, this official should have the authority, status, and capability to carry out their responsibilities.
- 3) **Criminalize manufacture, import, export, sale, ownership and use of jamming and spoofing devices.** – Jamming and spoofing can lead to loss of life and extreme economic disruption. Monetary penalties do not have the same deterrent effect as the potential loss of personal liberty. Criminalizing these offenses is also a powerful public policy statement recognizing the importance of PNT, and the nation’s resolve to defend it.
- 4) **Establish a network to detect PNT jamming and spoofing.** – Just knowing the extent of the problem will help prevent more serious

disruptions and foster innovative solutions. Ignorance is dangerous in any context, while transparency can energize stakeholders and lead to quickly correcting the behavior.

- 5) **Ensure the availability of a national, difficult-to-disrupt, precise, wide area, wireless PNT source to be used alongside GNSS.** Simply requiring owners and operators of critical infrastructure and critical applications to be able to continue operations for 60 days in the absence of GNSS is insufficient if they are unable to comply at a reasonable cost. PNT has become a common good, and governments must ensure that it is resilient. A second source of wireless PNT greatly increases national resilience by ensuring services to critical infrastructure and applications continue during GNSS disruptions. It also helps minimize the overall number of incidents by deterring those who would otherwise deliberately disrupt services.

End Note – PNT Governance within Commercial Organizations

The success or failure of many large and well capitalized commercial organizations is entirely dependent upon uninterrupted, precise PNT. While this paper has focused on the need for PNT governance at the national level, many companies should consider the question as well. For example, when I asked a senior leader at a global package delivery company for a contact to discuss PNT, he was quite taken aback. Their aviation division dealt with navigation issues. Their process control people were concerned with tagging, wirelessly tracking and time-stamping packages. The CFO dealt with electronic financial transactions, and, of course, the CIO’s office was involved with spectrum and IT issues. This major company’s lack of focus on PNT, not only failed to recognize PNT as a critical component of its success, and therefore a potential area of risk, but also prevented it from effectively engaging with the government on PNT resilience and governance issues.

The paper was presented in ENC-GNSS 2014, Rotterdam, Netherlands, 15-17 April. ▴

Survey requirements for river flood assessment and spatial planning

Experiences from river hydrographic measurements and LIDAR surveys in the Philippines



Enrico C Paringit
Chair, UP Department
of Geodetic Engineering
and Director of the
TCAGP, University of the
Philippines, Philippines

Louie P Balicanta

University of the Philippines, Nationwide
Disaster Risk and Exposure Assessment for
Mitigation (DREAM) Program, National
Engineering Center (NEC), Philippines



Czar Jakiri Sarmiento
University of the
Philippines, Nationwide
Disaster Risk and
Exposure Assessment
for Mitigation (DREAM)
Program, National
Engineering Center (NEC), Philippines

Rivers are important sources of fresh and flowing inland water vital to the socio-economic functioning of society mainly for agricultural and urban service applications. Measurement and survey of river characteristics is therefore an indispensable exercise if any plans to develop, conserve and sustain resources found in river systems are to be drawn. In surveying, various methods for the measurement of geometric and hydrographic properties as well as the tenurial conditions of rivers have been established for different purposes ranging from power generation, water supply, irrigation and navigation. Surveys of rivers are also performed to serve as basis for planning, designing and implementing mitigation strategies to prevent, reduce or control riverine floods.

The Philippines River Systems and its Flooding Woes

In the Philippines, there are about 421 major river basins, 18 (>1,400 km²) of which are considered principal due to their economic value and social benefits they bring to the local communities. By international scales, the Philippine rivers are comparatively short due to the archipelagic configuration of the country. However, due to the vast and extensive use of river resources, citizens opt to live near rivers, streams and creeks.

Every year, the Philippines experiences devastating river-related disasters such as floods, rainfall-triggered landslides, debris flow and mudflows. According to

World Risk Index 2012, the Philippines places third out of 173 countries ranked according to their “risk score” or their exposure to hazards such as floods and storms, drought and sea level rise (Muckle, 2012). Riverine floods are technically pure water hazards in contrast to landslides, debris flows and mudflows which carry with them solid materials such as sediments, boulders and trees.

In order to address the flooding problems, there is a need to gather information on river characteristics as critical inputs to the formulation of both structural and non-structural measures to mitigate flooding hazards. It is necessary to incorporate the effect/influence of other development plans for an entire river system in the formulation of an overall flood control plan. For example, the height of levee will affect the design height of bridge. Likewise, the design riverbed profile will affect the design of the irrigation intake/canal and other related facilities.

The Philippine government undertook a massive effort to generate detailed elevation dataset and develop early flood warning for 18 major river systems throughout the country (Paringit et al, 2012). The Nationwide Disaster Risk and Exposure Assessment for Mitigation (DREAM) program employed airborne (Light Detection and Ranging) LIDAR technology to generate detailed topography of major river systems. Coupled with aerial surveys, ground surveys were also performed to capture parameters that cannot be obtained from airborne sensors.

River survey approaches for flood assessments

River surveys and investigation are typically conducted to generate the basic data and information necessary for the subsequent flood assessment and planning. From an infrastructure point of view, precise river surveys are conducted for the design and construction of appropriate river training structures and bank protection works. It is noted that the appropriateness of a particular plan/design rely much on the veracity and accuracy of available basic data and information. In addition to ground-based surveys, aerial photography has been traditionally used to generate topography, infer land uses and interpret geology.

We revisit the ground and aerial survey activities typically required for assessing river flooding conditions. These include control surveys, river cross-sections, profile surveys, bathymetry, hydrometric measurements and how aerial surveys, particularly with the use of airborne LIDAR, serve to supplant some of the spatial data requirements. We then present the methods we employed following the prescribed techniques and modification as the need arises. Lastly, we show the results and products of survey, processing and modeling exercise.

Ground Surveys

Control Surveys

The force of gravity, and hence water flow, depends on precise determination of elevation in and around rivers must be precisely known. Otherwise, backflows and wrong assessments of water dynamic behavior may occur.

Vertical control points or elevation benchmarks are typically established near river banks with the use of calibrated digital levels and observed Third Order Vertical Control (Type 2) standards: $error \leq 12mm \times \sqrt{D}$ where distance D is given in kilometers). These control points were referred to the mean sea level (MSL) referenced from the nearest benchmark, initially established by the national mapping agency - the National Mapping and Resource

Information Authority (NAMRIA). In the DREAM Program, the use of GNSS receivers was carried out in situations where a known control point was too distant from the survey site for a conventional leveling line to be established. Established horizontal control or reference points were also used as vertical control points provided proper connection through conventional or GNSS-based leveling is conducted.

River Cross-Section Surveys

For the development of master plans, river cross-sections at typical sites are done every 500 m to 1,000 m intervals along the stretches of a river of interest, depending on the size of the river from topographic maps (DPWH and JICAa, 2003, DPWH and JICAa, 2003). However, for implementation of typical river structure projects, finer scale surveys are conducted with horizontal scale of 1:500 to 1:2,000 depending on the size of the river. Vertical scales are of 1:100 to 1:500 depending on the topographic condition. Measurement of the interval between cross section survey ranges from 100 m to 1,000 m. The width of survey area is typically extended at least 20m beyond both banks, but may be further widened provided the location is still a flood prone area (e.g., based on best available flood hazard maps). The interval of measurement along the river-cross section ranges from 2m to 5m on narrow rivers and 5m to 20m for wide rivers.

For the case study presented here, GNSS-based kinematic-based techniques are employed to capture the river cross-section data in both upper and lower banks, and on both sides of the river. Traversing the river itself by wading through or riding a small boat or raft, the pole-mounted GNSS poles are carried by the survey or manually and an assistant to help clear out the section path. GNSS reading frequencies are set by distance moved, rather than by time interval. For shallow rivers, the surveyor has no choice but to wade through the river to cross the river channel.

River Profile Surveys

River profiles describe the longitudinal configuration of the river necessary

to determine the slope/grade and configuration. The profile along the upper bank and lower bank on both sides of the river are typically generated to fully describe the channel geometry. Again, a GNSS-based kinematic mode survey technique was employed. A combination of GPS-depth meter with vertical and horizontal resolutions of 10cm and 100 meters, or finer, respectively were utilized in the river profile surveys. Ground control points were used for post-survey correction of survey tracks. Whenever possible, river profile surveys were done simultaneously with the cross section surveys to make use of the same reference and control point.

River Bathymetry Surveys

Echosounders equipped with GNSS receivers installed in a rubber boat or motorized *banca* are utilized for surveying the river bed profile of the main river channel. The combined echo sounder GNSS setup records the position and depth at half meter (0.5m) horizontal distance intervals with vertical (depth) precision of 10 cm with a time stamp (time of measurement) record for later synchronization with the GNSS-based position and time. Depth is measured from the echosounder transducer towards the bottom (river bed) surface less the draft length of the transducer. Two depth measurement passes are captured. The first is a sinusoidal path going from one side of the river to the other typically at a wave period of about 50m. The second is by running the sounder-equipped boat along the thalweg - the deepest part of the river channel. Either way, the ability to follow the target path depends on the skill of the boat driver, the presence of obstructions and river current. Data from the two measurement paths are combined during the processing and adjusted for effect of tide.

Hydrometric Surveys and Monitoring

Inflows or incoming waters from the upper catchment area are measured for a continuous period in order to establish relationship of rainfall amount with flow in terms of magnitude and peak flow arrival

time. Rain gauges are installed to measure rain intensity and time of occurrence in the catchment. For river water velocity, two instruments are used: the first is the typical propeller meter, while the other makes use of an Acoustic Doppler Current Profiler (ADCP). ADCP intended for river surveys, are typically designed to measure either horizontal or vertical profile of the flow.

Continuous measurement of depth of water at a fixed point is done by a data-logging pressure gauge or by recording the water level from an automated water level sensor (AWLS). Traditionally, water levels are manually read in a staff gauge strip painted or attached to the bridge pile/pier in the river. However, digital pressure gauges and AWLS have become popular alternatives due to reduced cost operation, reliability and safety. Data from the AWLS are transmitted to a server via a short message system (SMS) protocol over the mobile telephone network. The latter holds the distinct advantage of being valuable for real-time monitoring and decreases risk to personnel conducting the measurements during high-flows.

The cross-section of a river is measured where the velocity sensor/gauge is placed to compute for the flow across the section by trapezoidal method. Depending on the orientation of the ADCP, the velocities may vary horizontally or vertically and consequently the method to compute for the flow assumes that either the vertical or horizontal component of the velocity is held constant respectively.

Manual velocity measurements are conducted even without rainfall to establish base flows. During rainfall events however, the frequency of measurements are increased to 10-minute intervals in order to capture the rise of water as rainfall runoff comes down from the catchment. The AWLS measures the stage at 10-minute intervals.

Flow measurement records are used mainly for calibrating and validating the discharge models. Water level measurement obtained from the staff gauges or AWLS installed in the area of interest must also be tied to the MSL in

order to establish the relative difference in elevation at different segments of the river. Applying a single reference system for the stage enables the observation and analysis of the cascading flood waters.

Aerial Surveys

Ground elevation is one of the most important datasets for conduct of flood modeling. For the case study presented in this project, LIDAR data at 2m points per m² density was acquired in April 2013 through the DREAM Program (Paringit, et al, 2012). The LIDAR point clouds were then processed to produce 1m-resolution digital terrain model (DTM). The LIDAR dataset was post-processed to remove features captured by the LIDAR that may artificially impede flow of water along the river such as bridges during the flood simulation. The positional accuracy of LIDAR data was later evaluated using the cross section data gathered, as described in the previous section.

Since the topographic LIDAR system is not able to penetrate water and capture depth, the bathymetry of the river that was surveyed using the methods employed in the previous sections, was 'burned' into the LIDAR-derived DTM. This integration process also serves as one of the quality assessment procedures for ensuring that the LIDAR DTMs are properly calibrated.

Uses of river survey data for flood modeling, mapping and monitoring

All the geometry data coming from different survey modes described above come together as input data for flood modeling. As was mentioned, the profile and cross section measurements are used to augment the river geometry along the river channel extracted from the LIDAR DTM data. This fused elevation data formed the basic geometric input of the flood model. Other datasets would be rainfall as the source of flooding and the tide measurement, if the downstream end of the river that was being modeled came from tide gauges or a predicted tide table. Surface roughness was obtained from the LIDAR measurements.

The river flood modeling program used in this paper is based on shallow water solution of the St Venant equation that simulates water flow along the river. Popinet (2003) implemented the shallow water equations using an adaptive mesh projection method for the time-dependent incompressible Euler equations. In order to take advantage of the availability of multicore computer processors, the computation domain may spatially discretized using quad/octrees and a multilevel Poisson solver (Popinet 2012). Complex solid boundaries are represented using a volume-of-fluid

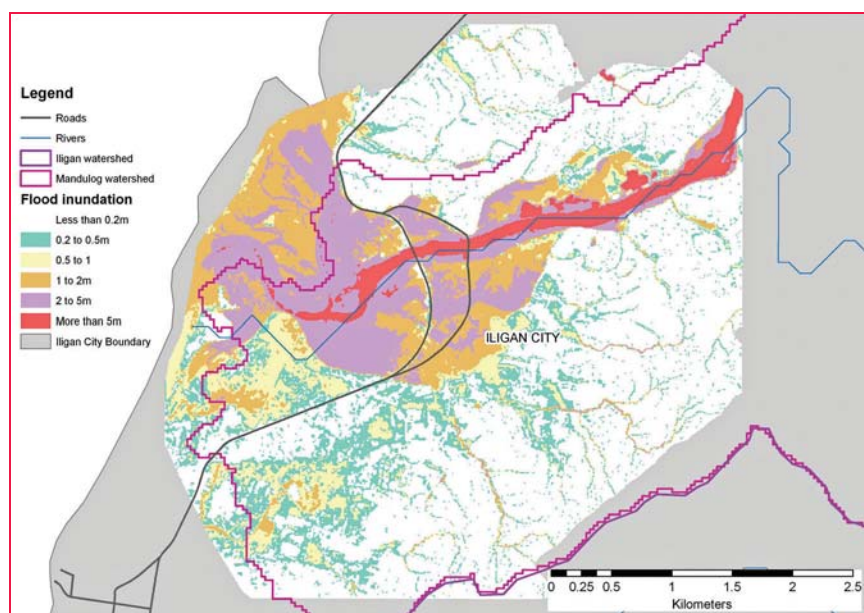


Figure 1: Flood depth inundation map of Mandulog River and flood plain.

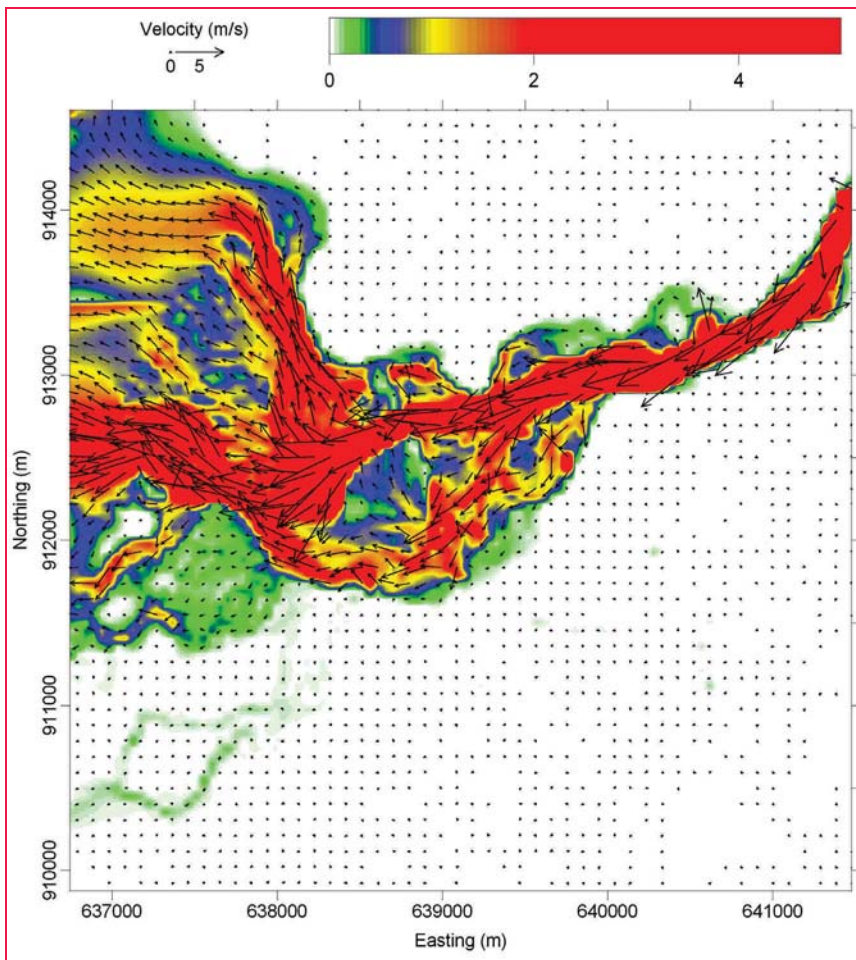


Figure 2: Velocity vector map for the lower reaches of Mandulog River for a 100-year return period. The arrow lengths indicate the speed (m/s) and the color of the magnitude of the speed.

approach. Second-order convergence in space and time is implemented on regular, statically and dynamically refined grids.

Aside from flood depths, the determination of speed of the rushing water is important for assessing flood hazards (Kelman and Spence, 2004). In this case, the depth-averaged velocity of the flooding is also captured during the simulation runs. The maximum velocity is assessed from the time series data.

Case studies

Iligan City River Flood Models and Maps

Our case study area, Iligan City in southern Philippines experienced 180mm of rainfall overnight, more than 60 percent of their average monthly rainfall pouring one event when Typhoon ‘Sendong’ (International

Name: ‘Washi’) hit the country on the night of 17 December 2011. Gushing waters from the two rivers (Mandulog River and Iligan River) located in the city coincided with the high tide which restricted the flow of flood waters, the steep topography of the catchment, and the debris into the river exacerbated the impact of flash flood that contributed to the disaster. Deaths reached 492 with 90,285 persons affected, and economic losses amounted to \$345 million (NDRRMC, 2011) for the entire area.

At total of 13 cross-section measurements were conducted. The bathymetry measurements, based on the surveys and LIDAR overflight data, high-resolution flood hazard map with 3D-rendition helps answer these questions. The map gave the spatial extent of flooding in the two rivers of Iligan City from rainfall that have 5-, 25-, 50- and 100-year rain return periods. It identifies in greater detail what communities

will be affected at various flood depths since it could be plotted in a greater scale than what was previously available.

An example of a depth map is shown in Figure 1. The ranges (0.2m to 0.5m, 0.5 to 1.0m, 1 to 2m, 2m to 5m and >5m) were so selected so as to illustrate the possible physical impact of the inundation. The velocity map is shown in Figure 2.

The flood hazard maps basically defined the carrying capacity of the river. This is important in land use planning and zoning since it identifies decision zones where development and location of communities must be regulated. It also guides investment decisions such as what flood and drainage control facilities must be put in place, and how will they be designed to withstand future impacts of climate change. It also directs priorities for watershed management by influencing policies on managed production while protecting the upland areas. The flood inundation model which simulates the velocity of water flow will also guide the integrated flood monitoring and early warning system that the government intends to put in place.

By being able to pinpoint areas that are of highest risk to future flood events, local governments will be able to prioritize their programs and projects to address the vulnerability of communities therein, come up with better preparedness programs, and ensure the safety of all.

Final remarks

This paper discussed the different surveys employed in order to produce the data required to perform detailed flood hazard mapping and assessment. The flood hazard mapping exercise was able to define in greater detail the flooding susceptibility of the four river systems based on a combination of various survey techniques employed on ground and in air. The newly generated spatial information serves as a valuable input for land use planning and zoning since it identifies decision zones where settlement and development activities must be regulated. The flood scenarios also guides investment decisions such as what flood

and drainage control facilities must be put in place, and how will they be designed to withstand future impacts of climate change. It will also guide priorities for watershed management by influencing policies on managed production while protecting the upland areas. The flood inundation model, which simulates the velocity of water flow, can guide the integrated flood monitoring and early warning system that government intends to put in place. By being able to pinpoint areas that are of highest risk to future flood events, local governments will be more equipped in prioritizing their programs and projects that will address the vulnerability of communities therein, come up with better preparedness programs, and ensure the safety of the citizens.

References

Department of Public Works and Highways (DPWH) and the Japan International Cooperation Agency (JICA) (2003), Manual on Flood Control and Planning, JICA, 135 pp.
Department of Public Works and Highways (DPWH) and the

Japan International Cooperation Agency (JICA) (2003), Technical Standards and Guidelines for Planning and Design, 177 pp.
Kelman, I. and Spence, R. (2004), An overview of flood actions on buildings, Engineering Geology 73, 297–309.
Muckle, P. (2012), Disaster Risk, Environmental Degradation and Global Sustainability Policy, in World Risk Report 2012, Allied Development Works, pp. 5–10.
National Disaster Risk Reduction and Management Council (NDRRMC) (2011), Final Report on the Effects and Emergency Management Tropical Storm “SENDONG” (Washi), url: <http://www.ndrrmc.gov.ph/attachments/article/358/Final%20Report%20re%20TS%20Sendong,%2015%20-%2018%20December%202011.pdf>; accessed: 18 December 2012.
Paringit, E. C. and Fabila, J. L. F. and Santillan J. R. (2012), High-resolution digital elevation dataset derived from airborne lidar for flood hazard assessment and mapping applications. Proceedings of the 33rd

Asian Conference on Remote Sensing (ACRS), Phuket, Thailand (in DVD).
Popinet, S. (2003), Gerris: a tree-based adaptive solver for the incompressible Euler equations in complex geometries, Journal of Computational Physics, 190(2), pp. 572–600.
Popinet, S. (2012) Adaptive modelling of long-distance wave propagation and fine-scale flooding during the Tohoku tsunami, Natural Hazards and Earth System Sciences, 12: 1213–1227.

Acknowledgements

The DREAM Program was supported by the Department of Science and Technology (DOST) Grant-in-Aid Program for the financial support to undertake this research program. The authors also thank the various agencies and local government units which made the surveys and measurements possible.

The paper was presented at FIG Congress 2014, Kuala Lumpur, Malaysia, 16-21 June 2014. ▴

IT'S IN OUR DNA...

...to engineer and manufacture the broadest and most trusted range of GNSS ANTENNAS for the most demanding Positioning, Navigation and Timing applications the world over.

Antcom produces GNSS antennas optimized for Agriculture, Aviation, Military, Marine, Survey and Network Timing applications. Our antennas are precision crafted to the highest metrics and to the most rigorous operational certifications.

Turn to Antcom for GNSS antenna capability, knowledge, and readiness to customize its antenna product line to customer-specific needs. For all of this and more, **ANTCOM KNOWS NO EQUAL.**

antcom.com | Excellence in Antenna and Microwave Products



3D+t Acoustic fields modelling based on Intelligent GIS

The approach described in this paper considers the development and implementation of the W2 concept and technology for the underwater acoustics' problems solving



Vasily Popovich

St. Petersburg Institute for Informatics and Automation, Russian Academy of Sciences, St. Petersburg, Russia



Yuri Leontev

St. Petersburg Institute for Informatics and Automation, Russian Academy of Sciences, St. Petersburg, Russia



Victor Ermolaev

St. Petersburg Institute for Informatics and Automation, Russian Academy of Sciences, St. Petersburg, Russia



Dmitry Chirov

St. Petersburg Institute for Informatics and Automation, Russian Academy of Sciences, St. Petersburg, Russia



Oksana Smirnova

St. Petersburg Institute for Informatics and Automation, Russian Academy of Sciences, St. Petersburg, Russia

Currently a lot of basic and applied research in hydroacoustics mainly considers resources of various types, including models' and calculated problems' libraries. Similar to the Internet and network resources, the hydro acoustic models development is an actual task.

The above selected problem is a component of a process that solves a problem of developing the IGIS modeling environment for acoustics as stated in [1]. The cornerstone in this research chain specification (statement) was laid in an attempt to develop a dynamic and adaptive computer model for the acoustic fields calculation by some combined complex methods (beam/ ray and wave acoustics) developed by Konstantin Avilov [2, 3]. The biggest problem of Avilov's approach is a need to possess actual data about many phenomena in the water, surface, air and bottom. Today as a rule there exist no statistical data accurate enough; also only several possibilities are available that provide the current data about real time conditions from real time systems, for instance, like 'Argo' [4].

The given paper attempts to demonstrate the advantages of W2 implementation for solving the above hydroacoustics problem. As an example of tasks, the passive location has been selected; the IGIS case study based on the paper authors' experience has been selected to illustrate the W2 capacities [5].

Main essentialities (entities) of the passive location equations and their decomposition are considered. Such decomposition gives a possibility to see the dependence of equations on the

current data from geo media. At that, the notations of equations by Urlick R J [6] are taken as a source description. The material presented in this paper proposes a subject domain description composed together by non-programming mathematical and acoustics experts. One can see a complex geo medium structure of the selected subject domain and a need to have distributed and heterogeneous W2 network (Intranet or Internet).

Short description of the W2 network and some requirements are given in Section III. As a result of this consideration, a conclusion is achieved that W2 network should be developed under Network Centric Operations principles.

A discussion on the IGIS implementation of W2 network as systems of some interfaces and as a container of the network web services has also been suggested. Also there are presented visual 3D representation results of modeling on IGIS and illustration of complexity of the geo media as an argument in favor of developing the W2 technology.

Fundamental basis

Let us discuss the main equation of an acoustic location and detect the dependence of some parts of the equation on hydroacoustics environment. According to Urlick R J [6], the active and passive-sonar equations look as follows:

The active-sonar equation:
 $SL - 2TL + TS = RL + DT;$

The passive-sonar equation:
 $SL - TL = NL - DI + DT, \quad (1)$

where:

- SL - Projector Source Level;
- TL - Transmission Loss;
- NL - Self-Noise Level;
- DI - Receiving Directivity Index;
- DT - Detection Threshold.

The object-oriented analysis of (1) has shown that first of all, it is necessary to perform an object-oriented decomposition based on the following 'class' notion. So, main classes of the passive sonar equation (1) are:

Sonar System, Sources of Sound and Medium. From this point of view, parts of equation (1) can be collected as follows.

1. Equipment (Sonar System):

- Projector Source Level (SL);
- Self-Noise Level (NL);
- Receiving Directivity Index (DI);
- Detection Threshold (DT).

2. Medium:

- Transmission Loss (TL);
- Reverberation Level (RL);
- Ambient-Noise Level (NL).

3. Target:

- Target Strength (TS);
- Target Source Level (SL).

According to the above information, there exist three main parts of the equation (Sonar System, Targets and Medium) that in the general case depend on each other. And it is important to know data about the defined area. It should be noted that data regarding the defined area are changing in various time scales: during the day periods, from season to season, and from year to year. This information is important and allows us to detect time of observation for receiving actual data. Type of information (data) and period of observation form a set of requirements for the W2 devices and technology. Relevant information can be helpful for understanding requirements for the measurement devices' locations: water (depth of installation), air, space, land, link type (wireless or traditional), requested period of time and other.

The sea and its boundaries (surface, bottom) form a remarkably complex medium for sound propagation.

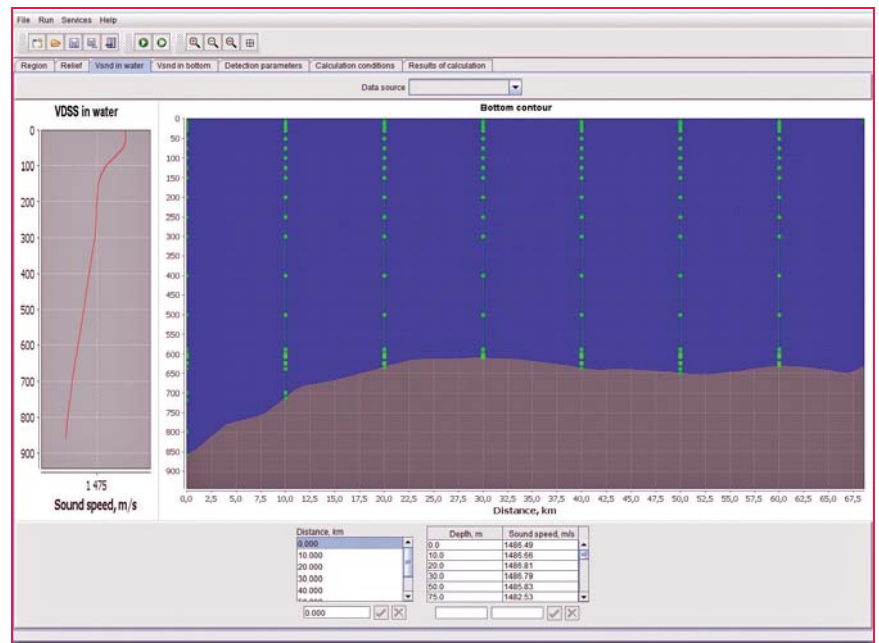


Figure 1: Vertical and horizontal distribution of sound velocity along one direction.

Parameter of *transmission losses* expresses the magnitude of one phenomenon of many associated with the sound propagation in sea, and is caused by:

1. spreading loss (a geometrical effect representing the regular weakening of the sound signal as it spreads outwards from the source);
2. attenuation loss (includes some effects as follows: absorption, scattering, diffraction and refraction);
3. sound scattering layers; and
4. boundaries.

An example of velocity distribution is shown in Figure 1.

It is difficult to develop really useful equations or experimental data of transmission losses (TL) in a general case. As a rule, it is necessary to consider at least the following three phenomena.

Shallow water

TL is calculated for three regions, each region is characterized by their own averaged decay law. Parameter H which provides the definition of these regions' boundaries is calculated using Marsh's and Shulkin's formula [9]:

$$H=0.58(h+h_o)^{\frac{1}{2}}$$

where h – water depth; h_o – thickness of isothermal layer.

The spherical decay law is applied to the distance $r \leq H$. At the distance $H \leq r \leq 8H$ TL varies in inverse proportion to the distance raised to the power of three halves and depends heavily on boundary conditions. At the distance $r \leq 8H$ the averaged decay law is cylindrical with increasing influence from the additional attenuation.

The dominating influence on the losses value in the shallow water has frequency, thickness of the water layer and bottom type. Rough water effect at the low frequencies is insignificant. As the frequency increases, the heaving of sea begins to tell when its value is more than 4-5 on Beaufort scale.

Deep sea

The main factors, which define sound propagation conditions at the deep sea, are speed of sound distribution in depth. Different hydrologo-acoustic conditions determine following acoustic phenomena in the deep sea:

- surface sound channel;
- antiwave sound propagation;
- underwater sound channel;
- regional field structure.

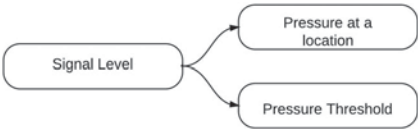
Variable channel along the range of propagation

In this case, bottom relief, speed of sound distribution at the depth and bottom property exercise significant influence over TL. Given phenomena are typical for:

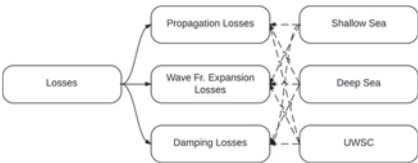
- sound propagation on the long distance (more than 1,000 km);
- sound propagation in the coastal wedge;
- crossing frontal zones by sound energy.

The given below graphic representation is used as a descriptive version instead of algebraic equations.

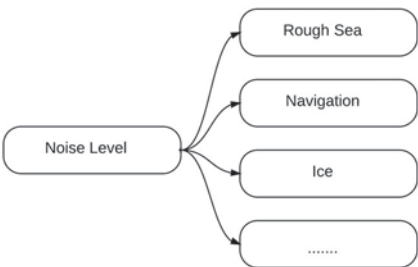
3.1. Signal level.



3.2. Losses.



3.3. Noise level.



3.4. Directivity index.



3.5. Detection.



In the general case TL could be represented as a picture, see Figure 2.

Web & Wireless capabilities

The given pictures clearly indicate the dependence of the parts of main acoustic equation on different input data. Conventionally, for most input hydroacoustic data, these data are of

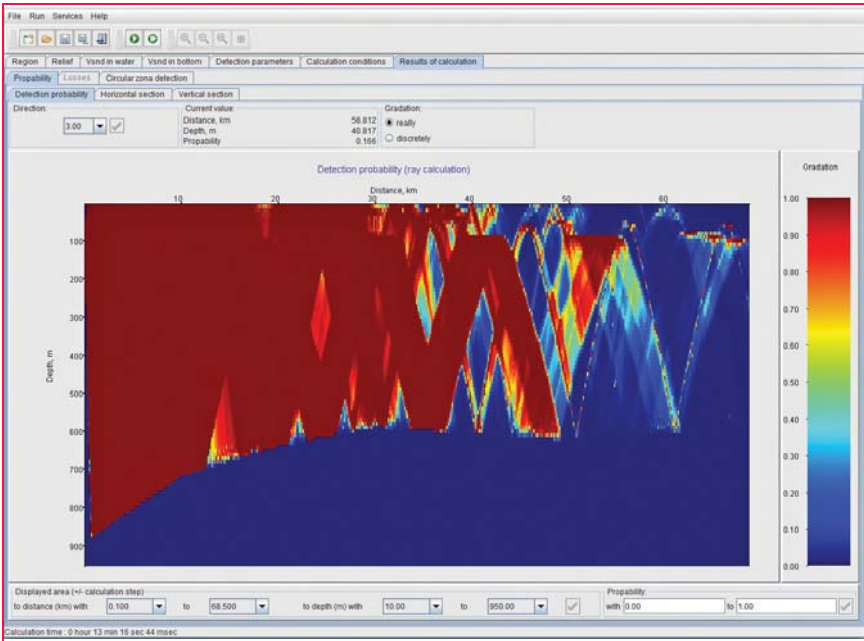


Figure 2: TL along one direction.

statistical nature. So, evidently the received results are not accurate enough. To assure the input data, it is necessary to have the right information at the right time, and it is only possible to receive such information using the distributed hybrid network. Figure 3 gives 3D representation of hydroacoustic conditions in some parts of the ocean (near the Strait of Gibraltar). It is quite easy to form a link between the equations (sections 3.1-3.5) and environment phenomena in the sea. It is worth emphasizing again that to receive real data in real time for sure it is necessary to have a distributed hybrid network available. For the problem selected in the paper at least the following network types will be required: satellite, cell (traditional network), underwater cell and special hydroacoustic networks. At that, it will be necessary to operate with a fairly big volume of data and data of the different time scales as well as with the sources of hybrid network On the data flow side, a situation is similar to the Global Internet, at the same time, certain new requirements arise for the general case of underwater acoustics, and most important are: very large volume of data from underwater sound channel, bottom, surface conditions, etc. This is why every information source and receiver should have web&wireless interfaces and work as an element of global or local network.

So in short, the web & wireless networks for underwater acoustics problems should be developed based on the Network Centric Operations principles. According to those principles, it is needed to collect information from different sources and also to furnish other customers with the information processed. According to the so far existing experience, it is possible to use information from Automatic Identification System (AIS) [7]. As a rule, this information covers well enough conditions on sea routes and ports (cell network), satellite images (space network), weather conditions at sea, ice line, etc. Complementary information about surface conditions and ships come from the radars. One important experimental conclusion is that for some information sources it is possible to use several various networks instead of a single one. So, the customer has a possibility to choose using one or several networks. Also, it is needed to evaluate the network costs and the data transfer rate. While developing monitoring system for regions like the Baltic Sea, the conclusion was made that cell networks are somewhat preferable for AIS and radars at identifying the surface conditions. Indeed, the decisions regarding a configuration and architecture of the network should be made for the defined region, goals and costs. On

the whole, the situations can be more complex in case of underwater and bottom properties and conditions, since it is difficult to maintain continuous data channel. Underwater cell network turns out to be too complex and expensive. However, for military purposes some countries, for instance, the USA, support investigations in developing the underwater cell networks of the kind.

Intelligent GIS capabilities

It had been already noted [8] that Geographic Information Systems (GIS) are a key technology for up-to-date information systems and especially for underwater acoustic systems. GIS could be used in different ways as a friendly interface, as a special system for control and processing heterogeneous data, and as a container of web interfaces and services. The proposed GIS handy tools allow the end users or decision-makers to graphically fuse different information, and Figure 3 gives an example of such a fusion. In Figure 3, the ship under study is located in the center of a green circle, and from the green circle's center the ship's signals are propagated in different directions from 0 to 360, and the distribution of the sound energy differs in accordance with the conditions of the geo medium. The energy level (Signal Level) is a complex function that depends on a number of factors as discussed in Section II. Environmental factors depend on the coordinates that unfortunately are time-varying. So, the distributed network should be used for assuring the receipt of true results that would assist the decision-makers. The network is expected to provide the right information at the right place and real time as has been discussed in Section III. GIS should at least provide the following services in order to: control network; check conditions and state of the input data sources; run a system of hydroacoustics field modeling; provide recommendations for decision-makers; collect and store initial data; provide initial and processed data to other customers; generate visual representation of situation on maps in 2D (2D+t) or 3D (3D+t) versions.

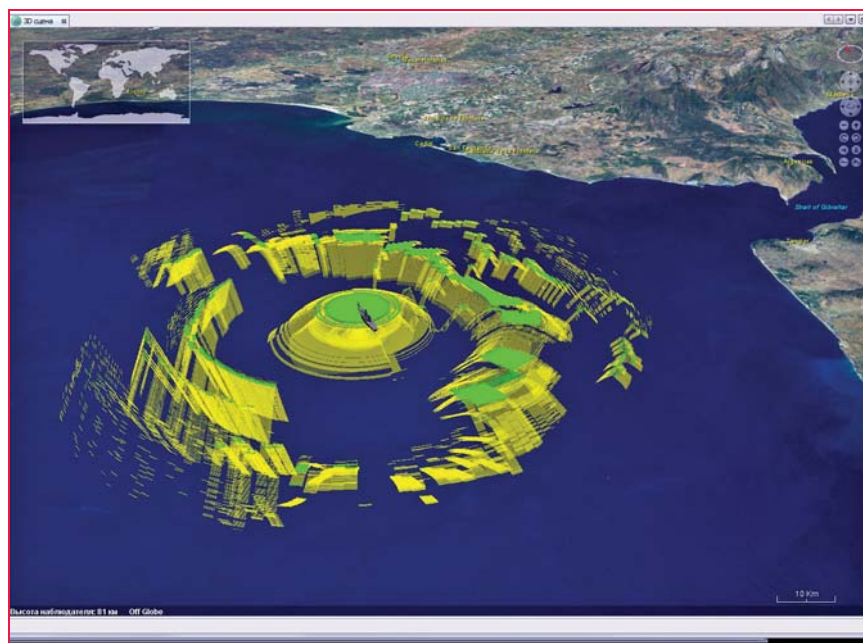


Figure 3: Visual representation of sound propagation in Strait of Gibraltar region.

Intelligent extensions turn GIS (IGIS) into truly advanced information systems; say, for underwater acoustics problem, IGIS is a revolutionary technology that allows the regular users to investigate hydroacoustic problems in their work place without extra obligations to communicate elite laboratories and companies. It is also evident that the W2 technologies enable optimistic opportunities for many researchers in developing and investigating various acoustics problems under real data and real time conditions, and using their personal computer/network means. To match this optimistic prognosis, the GIS system should incorporate certain new properties and capabilities; most important of them are: well developed system of web services (at least three levels: system, application & data base, and end users); input and output systems for receiving and sending data by different wireless networks; structured system of ontology for data harmonization, integration and fusion.

Conclusion

Web&Wireless technology plays an important role in everyday life and affects the fundamental science and hi-tech. The approach described in this paper considers the development and implementation of

the W2 concept and technology for the underwater acoustics' problems solving. Needless to say that the above approach demonstrates a fusion of different science and technology: W2, GIS, Intelligent GIS and underwater acoustics.

Currently, the studies in the complex hydroacoustic calculations' models are pursued based upon the existing accomplishments of different companies interested in solving the problem under consideration. It is assumed that the approach proposed here will allow, along with accounting for the medium objective parameters, detection means and systems to account for the factors like: who uses the calculation system (remote terminal, sophisticated user or other), what are the time constraints (real-time or imposed time constraints), availability of information resources for calculations (current measurements, statistic or processes data), etc.

References

- [1] V. V. Popovich, V. A. Zaraisky, R. M. Yusupov, Multi Agents Approach for Underwater Sound Equations Solution, *Proc. of the Sixth International Conference on Theoretical and Computational*

Galileo update

Galileo service interruption planned for system upgrade

Galileo's navigation messages will shortly stop being updated to enable the migration of a new release for Galileo's ground mission segment, announced the European Space Agency.

Although the actual navigation signals will continue to be transmitted, the generation and uplink of the navigation message — which renews the contents of the signal — will be interrupted during the last week of January for about five weeks.

The accuracy of the navigation message received by users will slowly degrade, or in case of a reset in the satellite signal generator the message content will be dummy material. The users will be informed accordingly through a warning flag in the disseminated message, or through the online Notice Advisory to Galileo Users.

“The main benefits of this migration from V1.2 to V2.0 of the Galileo Ground Mission Segment are better overall performance and availability, increased robustness and improved operability,” explained ESA's Martin Hollreiser, who is overseeing the mission segment's development with Thales Alenia Space France as prime contractor. “The latter is achieved through enhanced operator interfaces, increased access to performance data and the automation of procedures.

“Various ‘non-conformances’ identified by operators over time have been fixed, while overall security has been further strengthened through treatment plans,” Hollreiser said. “This is in particular true for the Public Regulated Service, or PRS, the most secure Galileo class of signal. Finally, the number

of Galileo Sensor Stations will increase from 12 to 15 worldwide and the number of Galileo Uplink Stations from four to five.

“The new Sensor Stations will be on Santa Maria in the Azores, Ascension Island in the mid-Atlantic and Kiruna in the Swedish Arctic. The additional Uplink Station will be on Papeete, in French Polynesia. Such system improvements have always been part of our planning since the contract began in 2011.”

Galileo's worldwide ground mission segment is one of the most complex developments ever undertaken by ESA, with twin European Galileo Control Centres and a network of sensor and uplink stations deployed on remote sites across the world. They are all interconnected via a robust satcoms realtime network.

While satellite control and housekeeping are performed by Galileo's Ground Control Segment in Oberpfaffenhofen, Germany, the Ground Mission Segment that provides the navigation and timing services and related performances is operated from a separate centre in Fucino, Italy.

ESA to launch six navigation satellites in 2015

Six Galileo satellites are to be put into orbit in 2015, European Space Agency (ESA) Director General Jean-Jacques Dordain said.

He also added that the satellites will be put into orbit by Ariane 5 and Soyuz carrier rockets. ▴

Acoustics (ICTCA), Honolulu, Hawaii, August, pp. 464-474, 2003

- [2] K. V. Avilov, Pseudodifferential Parabolic Equations of Sound Propagation in the Slowly Range-Dependent Ocean and their Numerical Solutions, *Acoustic Journal*, Vol. 41, No. 1, 1995, pp. 5-12
- [3] K. V. Avilov, O. E. Popov, The Calculation of the Signal from a Broadband Point Source Arbitrarily Moving in the Range-Dependent Ocean, *Proc. of the XIV-th L.M. Brekhovskikh's Symposium*, Moscow, 1998
- [4] V. Popovich, V. Ermolaev, N. Hovanov, D. Chirov, P. Konuhovsky, S. Vanurin, Acoustics Field's Calculation Optimization on the Combined Approach Basis, *Proc. of the European Conference on Underwater Acoustics (ECUA)*, Istanbul, Turkey, July, 2010
- [5] P. N. Volgin, V. I. Guchek, V. I. Ermolaev, V. V. Popovich, S. N. Potapichev, Visual Representation of Sonar's Possibilities for 2D Heterogeneous Medium, *Proc. of XI-th Conference "Applied Technologies of Hydroacoustic & Hydrophysics"*, pp. 63-65, St. Petersburg, Russia (in Russian), 2012
- [6] R. Urlick, Principles of Underwater Sound for Engineers, McGraw-Hill, New-York, 1975
- [7] V. Popovich, V. Ermolaev, Y. Leontev, O. Smirnova, Hydroacoustics phields modeling on an Intelligent GIS Base, *Artificial Intelligence and Decision Support*, No. 4, 2009, pp. 37-44
- [8] Object-Oriented Geoinformation Systems Laboratory of SPIIRAS. www.oogis.ru
- [9] Marsh H.W. and Schulkin M. (1962) Colossus II Shallow-Water Acoustic Propagation Studies, USL Report No. 550, 1. ▴



Tracking satellite footprints on Earth's surface

A coordinate transformation method to compute ECEF coordinate of a satellite revolving in Keplerian orbit in TEME coordinate



Narayan Panigrahi
Scientist, Center for Artificial Intelligence and Robotics, DRDO, C.V Raman Nagar, Bangalore, India



Raj Gaurav
Navigation-System research enthusiast, Indian Institute of Surveying and Mapping, Survey of India, Uppal, Hyderabad, India

Reference systems are used in Geodesy, Astronomy and Spatial information science extensively. In addition to well established systems like ICRF, MOD, TOD, and WGS84, various other systems are available that arise from intermediate or approximate transformations [6]. Computing the footprint of a revolving satellite or space object in terms of ECEF (Earth Centred Earth Fixed) coordinate on the Earth's surface is an interesting problem. This problem has been solved by Vallado D. A. [1], and macros for equivalent transform are in MATLAB.

A key objective of this work is to develop a coordinate transformation method to compute terrestrial coordinate in a geocentric reference frame given its corresponding celestial coordinate. This is also an instance of coordinate transformation from 'inertial' frame of reference to a coordinate in 'Earth Centered Earth Fixed' frame of reference. The two line element dataset hosted by NORAD (North American Aerospace Defense Command) of all the satellites and space debris is the source of obtaining the inertial coordinate of a satellite. The ephemeris of a celestial object in TEME (True Equator Mean Equinox) coordinate system is obtained after processing TLE data. TEME is an

inertial coordinate system conceptualized in space for location of satellites with respect to earth's frame of reference. An exact operational definition of TEME coordinate system is very difficult to find in literature, but conceptually, its primary direction is related to the 'uniform equinox' (Seidelmann, 1992:116, and Atkinson and Sadler, 1951). The direction of the uniform equinox resides along the true equator 'between' the origin of the intermediate PEF (Pseudo Earth Fixed) and TOD (True of Date) frames [4].

In this paper we have proposed an algorithm which transforms TEME coordinate of celestial objects obtained from the NORAD TLE to a well defined ECEF (Earth Centered Earth Fixed) coordinate system.

The solution obtained through this algorithm is required in many different applications such as controlling the satellite from Earth station, acquisition of remotely sensed data of a pre-designated location on Earth surface, etc. The usefulness of this proposed method is very high when we want to visualize the footprint of a celestial object on a digital map in GIS environment as depicted in Figure [1].

The NORAD TLE which is maintained in the website 'www.celestrak.com/NORAD/elements' mentions the classical orbital parameters of celestial objects, like satellites and debris revolving in Keplerian orbit. The orbital parameters which define the instantaneous position of the celestial objects are known as Classical Orbital Elements (COE). The COE describes the orbit in the form

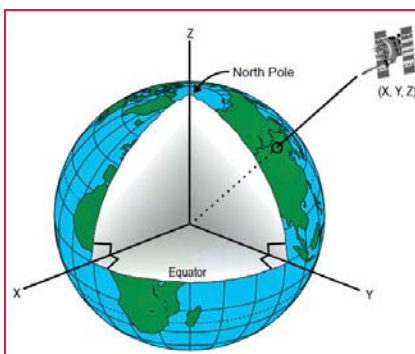


Figure 1: Satellite tracked in ECEF frame

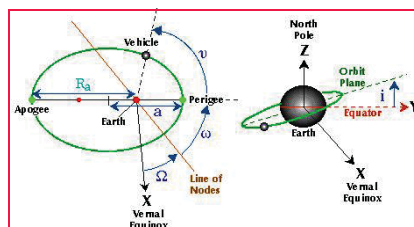


Figure 2: Classical Orbital Elements (COE) in Space

of these parameters given by $\langle a, e, I, \Omega, \omega, \nu \rangle$ as depicted in Figure [2].

a - Semi-major axis - A constant defining the size of the orbit.

e - Eccentricity - A constant defining the shape of the orbit (0=circular, Less than 1=elliptical).

i - Inclination - The angle between the equator and orbit plane.

Ω - Right Ascension of the Ascending Node - The angle between vernal equinox and the point where the orbit crosses the equatorial plane.

ω - Argument of Perigee - The angle between the ascending node and the orbit's point of closest approach to the earth (perigee).

ν - True Anomaly - The angle between perigee and the vehicle (in the orbit plane).^[5]

TEME coordinate system lies in celestial and inertial frame of reference Figure [3] and is based on mean equinox. TEME is not fixed to earth surface and hence does not rotate along with rotation of Earth. If we want to see the location of any celestial object on a digital map in 2D or in the surface of a digital globe in 3D, there is a coordinate system required which is fixed with Earth rotation. Therefore to visualize the footprints of a revolving celestial object around the Earth, whose instantaneous position can be specified through the TEME coordinate obtained from NORAD TLE, a coordinate

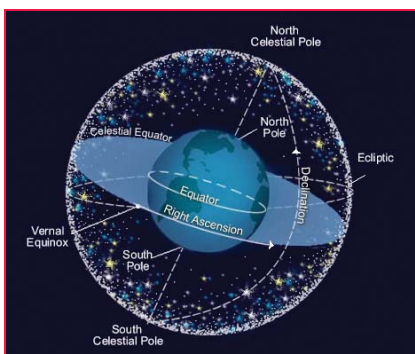


Figure 3: A celestial reference frame

transformation is required which can transform the TEME coordinate of the satellite to the ECEF coordinate of the earth. Hence the basis of this computational problem is to develop a coordinate transformation which will transform the TEME Coordinate to ECEF coordinate of the celestial object. In the next section, the explanation of TEME and ECEF coordinate is given followed by the transformation algorithm later.

The TEME coordinate system

There are two consideration of visualizing TEME (True Equator Mean Equinox) coordinate system:

- i) TEME of Date
 - ii) TEME of Epoch
- i) TEME of Date: The TEMED system is a less common reference system that is aligned with the true equator and the mean equinox at the time of consideration. Its z-axis is parallel to the instantaneous rotation axis of the Earth (i.e., z-axis along the true rotation axis of the Orbit Epoch), but the x-axis points into the direction of the mean vernal equinox at the concerned time. The TEMED system arises implicitly in an orbit determination program, when true sidereal time is substituted by mean sidereal time in the transformation of measurements from the Earth-fixed frame to inertial frame. The difference between mean and true sidereal time (or likewise the difference between the mean and true equinox) amounts to roughly $15''=1s$ at maximum, and varies with the longitude of the Moon's ascending node on the ecliptic. The TEMED system is for, e.g., applied in the generation of NORAD elements.^[6] In this, epoch of the TEME frame is always the same as the epoch of the associated ephemeris generation time.^[4]
- ii) TEME of Epoch: In this system, the Z points along the true rotation axis of the Coordinate Epoch,^[5] and X points toward the mean vernal equinox. The epoch of the TEME frame is held constant.^[4]

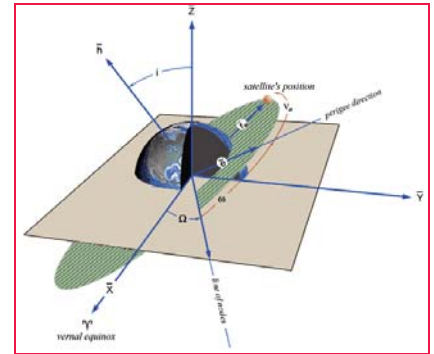


Figure 4: TEME Coordinate in Space

[Source: <http://spaceflight.nasa.gov/realdata/elements>]

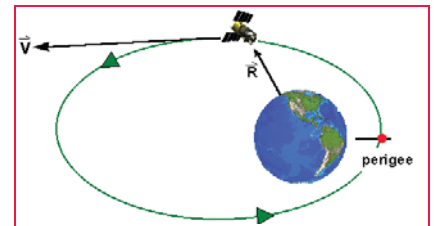


Figure 5: TEME representation in Cartesian form

[Source: www.public.iastate.edu]

TEME can use both Cartesian and COE elements for representation of coordinate.^[5] In COE, position and velocity can be defined by six Keplerian elements as depicted in Figure [2]:

$$a, e, I, \Omega, \omega, \nu$$

The corresponding Cartesian coordinate is represented by position vector \mathbf{r} (x, y, z) and velocity vector \mathbf{v} ($\dot{x}, \dot{y}, \dot{z}$) as depicted in Figure [5]:

The ECEF coordinate system

ECEF (Earth-Centered Earth-Fixed) is a Cartesian coordinate system, and is sometimes known as a 'conventional terrestrial reference frame' system. The origin (0, 0, 0) is defined as the center of mass of the Earth, hence the name Earth-Centered. Its axes are aligned with the International Reference Pole (IRP) and International Reference Meridian (IRM) that are fixed with respect to the surface of the Earth, hence the name Earth-Fixed.

The z-axis points towards the north but it does not coincide exactly with the

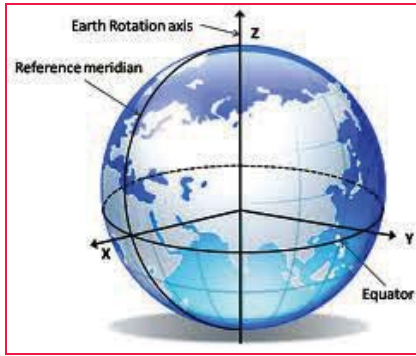


Figure 6: ECEF reference frame
[Source: http://gnss.be/systems_tutorial.php]

instantaneous Earth rotational axis. The slight 'wobbling' of the rotational axis is known as **polar motion**. The x-axis intersects the sphere of the Earth at 0° latitude (Equator) and 0° longitude (Greenwich) **Figure [6]**. This means ECEF rotates with the earth and therefore, coordinates of a point fixed on the surface of the earth do not change. [7]

ECEF uses only Cartesian element for representation of position and vector [5]:

Position can be represented by:

$$\mathbf{r} \rightarrow x, y, z.$$

Velocity can be represented by:

$$\mathbf{v} \rightarrow \dot{x}, \dot{y}, \dot{z}.$$

Problem Definition

Since TEME lies in an inertial frame and we have to transform it in an Earth fixed frame, so, the main problems we observe are:

- Rotating x_{TEME} towards x_{ECEF} .
- Rotating instantaneous pole of TEME towards IRP of ECEF.

Relation between TEME and ECEF coordinate System

In defining a coordinate system, in general, we choose two quantities: the direction of one of the axes and the orientation of the other two axes in the plane perpendicular to this direction. The latter orientation is often specified by requiring one of the two remaining axes to be perpendicular to some direction.

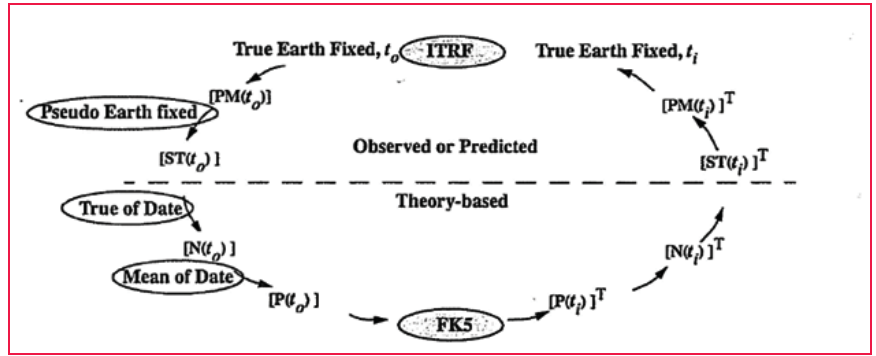


Figure 7: Relation between body fixed (ITRF) and inertial (FK5) frame
[Source: Fundamental of Astrodynamics (David A Vallado)]

In the case of TEME and ECEF the same is followed. For transformation of ECEF from TEME, first we need to transform TEME to PEF (Pseudo Earth Fixed) Coordinate system. We will see all the coordinate systems which fall in between TEME and ECEF in a single frame shown in Figure [7]:

$$\text{PM}(t_i) = \text{ROT1}(y_p), \text{ROT2}(x_p)$$

$$\text{ST}(t_i) = \text{ROT3}(-\theta_{\text{AST}})$$

This figure depicts the transformation of a state vector in the body fixed to inertial frame. PEF (Pseudo Earth Fixed), ToD (True of Date), MoD (Mean of Date) are intermediate frames. FK5 defines the Celestial Reference Frame and ITRF defines Terrestrial Reference Frame. If we go through the FK5 to ITRF ellipse depicted in Figure [7], we will find the transformation frame through which we can solve our objective. Although in our case of TEME to ECEF we will not follow exactly what is mentioned in the Figure [7]. But it is very close.

$$\text{P}(t_i) \rightarrow \text{Precession at epoch}$$

$$\text{N}(t_i) \rightarrow \text{Nutation at epoch}$$

$$\text{ST}(t_i) \rightarrow \text{Sidereal Time at epoch}$$

$$\text{PM}(t_i) \rightarrow \text{Polar Motion at epoch}$$

The same relation will be used when we will process the transformation between TEME and ECEF. Because ECEF is a body fixed and TEME is a celestial coordinate system.

Solution approach

The transition from Space Fixed Inertial System (CIS) to Conventional terrestrial System (CTS) is realized through a sequence of rotation that account for:

- Precession
- Nutation
- Earth rotation including polar motion

These can be described with the matrix operations. For a point on a sphere, described through a position vector \mathbf{r} , the equation is:

$$\mathbf{r}_{\text{CTS}} = \text{SNP} \mathbf{r}_{\text{CIS}} \quad [3]$$

$\mathbf{r}_{\text{CTS}} \rightarrow$ Position vector i.e. x, y, z of terrestrial system (for our case it is ECEF)

S \rightarrow Sidereal Time, N \rightarrow Nutation, P \rightarrow Precession

$\mathbf{r}_{\text{CIS}} \rightarrow$ Position vector i.e. x, y, z of inertial system (for our case it is TEME).

Precession and Nutation

Earth axis of rotation and its equatorial plane are not fixed in space, but rotate with respect to an inertial system. This results in some gravitational attraction of the Moon and the Sun on the equatorial bulge of the Earth. The total motion is composed of a mean secular component (Precession) and a periodic component (Nutation). [3] Corrections to the Nutation parameters ($\delta\Delta\psi_{1980}$ and $\delta\Delta\epsilon_{1980}$) supplied as Earth Orientation Parameters (EOP) from the IERS are simply added to the result. These corrections also include effects from Free Core Nutation (FCN) that correct

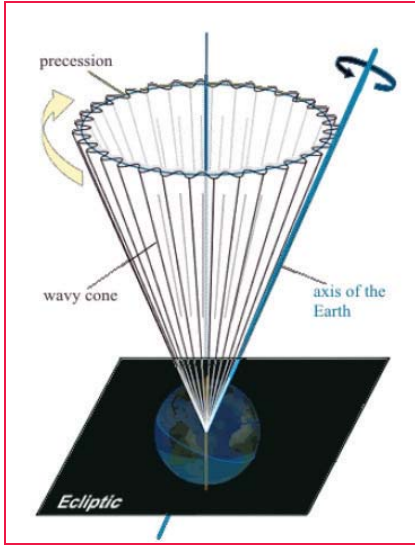


Figure 8: Precession and Nutation
[Source: A satellite footprint visualization tool: Patrick Daum]

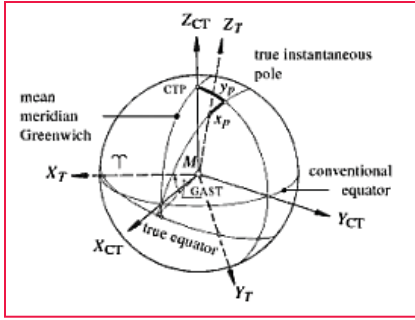


Figure 9: True instantaneous and a conventional terrestrial Pole
[Source: Satellite Geodesy (David Gunter Seeber)]

errors in the IAU-76 precession and IAU-80 nutation. However for TEME, these corrections do not appear to be used.^[4]

$\delta A\psi 1980 \rightarrow$ Nutation in longitude

$\delta A\epsilon 1980 \rightarrow$ Obliquity of the ecliptic

Sidereal Time

It is a measure of time defined by Earth's diurnal rotation with respect to the vernal equinox.^[8] This is responsible for most of time dependency of the vector components. This process is usually coupled with Polar Motion. It transforms the non rotating frame to a rotating coordinate system. It addresses the variability in sidereal time and requires the Greenwich Apparent Sidereal Time

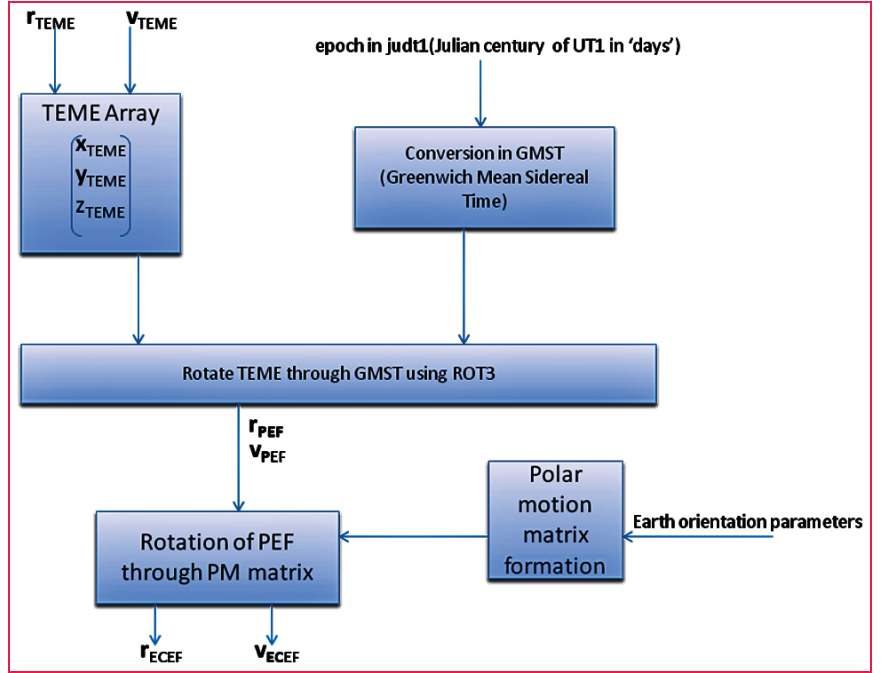


Diagram 1: Block Diagram for Conversion of TEME coordinate system

(GAST), because the rotating frame references the Earth's actual equator of date, which is the true equator. GAST is measured on the true equator relative to the true equinox. And Greenwich Mean Sidereal Time is measured along the true equator relative to the mean equinox. The difference between two times is called equation of equinox.^[1]

The rotation matrix is then:

$$r_{PEF} = ROT3(\theta_{GMST}) r_{TEME} \quad (1)^{[4]}$$

$$v_{PEF} = ROT3(\theta_{GMST}) v_{TEME} \quad (2)$$

Eq. (1) can be written as:

$$r_{PEF} = \begin{bmatrix} \cos\theta & \sin\theta & 0.0 \\ -\sin\theta & \cos\theta & 0.0 \\ 0.0 & 0.0 & 1.0 \end{bmatrix} \times \begin{bmatrix} x_{TEME} \\ y_{TEME} \\ z_{TEME} \end{bmatrix} \quad \theta = GMST$$

Similarly for Eq. (2).

Earth Rotation and Polar Motion

For the transition from an instantaneous space-fixed equatorial system to a conventional terrestrial system, we need two further parameters. They are called Earth Rotation Parameters (ERP) and Earth Orientation Parameters (EOP), namely

$x_p, y_p \rightarrow$ the pole coordinates.

Unlike precession and Nutation, Earth rotation parameters cannot be described through theory but must be determined through actual observations by an international time and latitude service. The Earth Orientation Parameters (EOP) describe the irregularities of the Earth rotation with respect to a non-rotating reference frame.^[9] The IERS (International Earth Rotation Services) has been maintaining these parameters from 1988.

The Earth Fixed system is realized through the conventional orientation of a cartesian $(x, y, z)_{CT}$ system. The z_{CT} axis is directed towards the conventional terrestrial pole CTP, and x_{CT} axis towards the mean Greenwich meridian. The relative position of the instantaneous true pole with respect to the conventional terrestrial pole CTP is usually described through pole coordinates x_p, y_p . x_p, y_p describes the polar motion with respect to the crust.^[9]

The polar transformation matrix is:

$$r_{ECEF} = ROT2*(x_p) * ROT1*(y_p) * r_{PEF} \quad (3)$$

$$v_{ECEF} = ROT2*(x_p) * ROT1*(y_p) v_{PEF} \quad (4)$$

The multiplications of transformation matrix of pole coordinate x_p and transformation matrix of pole coordinate

y_p with r_{PEF} gives the required coordinate r_{ECEF} . And similarly v_{ECEF} will be obtained.

Block Diagram and Algorithm for TEME to ECEF conversion

Diagram 1 explains the process flow of coordinate transformation:

Algorithm

TEME_TO_ECEF (
 (r_{TEME}, v_{TEME}) , jdut1, eopfile.txt
 (r_{TEME}, v_{TEME}) , jdut1, eopfile.txt)

This function takes the TEME Coordinate (r_{TEME}, v_{TEME}) and Coordinate Epoch (in jdut1) as an input, and the ECEF Coordinate is generated after conversion.

$r_{TEME}(x, y, z) \rightarrow$
 Position vector of date

$v_{TEME}(\ddot{x}, \ddot{y}, \ddot{z}) \rightarrow$
 Velocity vector of date

Table-1: Comparison of Ephemeris Computed by the coordinate transformation algorithm Observation epoch: 2012 3 23 3:22:24.999987

Input (r, v)	TEME	PEF	ECEF
x	4671.58251041	4966.8088	4966.808800
y	-3933.40827657	3553.335639	3553.335639
z	-3475.801715	-3475.801715	-3475.801715
\dot{x}	-3.578379765	-2.291693	-2.291693
\dot{y}	1.451590645	-3.108064	-3.108064
\dot{z}	-6.457583702	-6.457584	-6.457584

jdut1 \rightarrow Julian century of UT1 in 'days'

eopfile.txt: file contains the nutation daily values used for optimizing the speed of operation. It can be obtained from- <http://www.celestrak.com/SpaceData>.
 Step 1. [VARIALE DECLARATION]

Var $(r_{TEME}, v_{TEME})(r_{TEME}, v_{TEME})$
 //Position vector of TEME in km
 and velocity vector TEME in km/s

Var $(r_{PEF}, v_{PEF})(r_{PEF}, v_{PEF})$

Var $(r_{ECEF}, v_{ECEF})(r_{ECEF}, v_{ECEF})$

Var time // Coordinate epoch

Var x_p //Polar motion
 coefficient xp in arc sec

Var A1[3][3] // xp rotation matrix

Var y_p // Polar motion
 coefficient yp in arc sec

Var A2[3][3] // yp rotation matrix

LINERTEC

LGP-300 Series
 WinCE Reflectorless
 Total Station

LTS-200 Series
 Reflectorless
 Total Station

LTH-02/05
 Electronic
 Theodolite

LGN-200 GNSS

A-100 Series
 Automatic
 Level

Cutting-Edge Technology
 at an Affordable Price

TI Asahi Co., Ltd.

www.tilinertec.com | contact us at trade@tilinertec.com
 Contact in India: Premier Optical Pvt. Ltd. - poplpremier@gmail.com

Var PM[3][3] //Polar Motion Matrix

Step 2. [INPUT_TEME]

Input (r_{TEME}, v_{TEME}
 $r_{TEME}, v_{TEME}, time$);

/* This function takes input for r_{TEME} and v_{TEME} and time from the output obtained after processing the NORAD TLE dataset */

Step 3. [TIME CONVERSION]

- [Conversion of coordinate epoch in 'jdut1']
- [Conversion of 'jdut1' in GMST]

Step 4. [TEME_TO_PEF]

$(r_{PEF}, v_{PEF}) = ROT3\theta * (r_{TEME}, v_{TEME})$

/* This is the multiplication of r_{TEME}, v_{TEME} with ROT3 θ matrix where θ = GMST :

$$\begin{bmatrix} \cos\theta & \sin\theta & 0.0 \\ -\sin\theta & \cos\theta & 0.0 \\ 0.0 & 0.0 & 1.0 \end{bmatrix} \times \begin{bmatrix} x_{TEME} \\ y_{TEME} \\ z_{TEME} \end{bmatrix}$$

Similarly for v_{TEME}, v_{TEME} */

Step 5. [PEF to ECEF CONVERSION]

$x_p = \text{ReadXp}(\text{eopfile.txt});$

$y_p = \text{ReadYp}(\text{eopfile.txt});$

// Here ReadXp() and ReadYp() are two simple file reading functions that are specified to read Polar-motion Coefficients (x_p, y_p) from a special text file 'eopfile.txt'.

$A1 = ROT2 * x_p;$

$A2 = ROT1 * y_p;$

/* ROT1 and ROT2 are standard rotation matrices likewise ROT3 defined above, details are given in the glossary */

$PM = A1 * A2;$

$(r_{ECEF}, v_{ECEF}) = PM * (r_{PEF}, v_{PEF})$

/* A1 variable stores the rotation matrix of xp and A2 stores the rotation matrix of yp. And product of $A1 * A2$ gives the PM (Polar Motion) Matrix. When we multiply PM with r_{PEF} and v_{PEF} , then corresponding r_{ECEF} and v_{ECEF} is obtained.*/

Step 6. Return (ECEF); // This function is returning the ECEF ephemeris.

Step 7. [FUNCTION END].

This test is done after producing NORAD element data set and obtaining TEME ephemeris.

The TEME coordinates were the input in our proposed system and tabulated the observation in PEF and ECEF coordinate system.

Application & future works

The main reason behind this conversion is to visualize the moving object on a 2D map. NORAD element set was able to generate x, y, z but in unknown coordinate system, i.e. - TEME. So, we developed this conversion system which is able to convert TEME into ECEF coordinate system. This coordinate conversion will be proven very beneficial for entire GIS community, especially while working with celestial object.

As far as future work is concerned, it can be further converted into geographic coordinate system (i.e., - Lat., Long., and Alt.).

Conclusion

In this paper, a method of conversion of an inertial frame to non-inertial frame has been discussed. In this case we have taken a coordinate system TEME, for which no proper definition is available. We have opted first to transform TEME to PEF coordinate system using GMST, and then transform PEF to ECEF using polar motion

coefficient. In this, time conversion method has been used and polar motion parameters have been taken from the <http://www.celestrak.com/SpaceData>.

Acknowledgement:

A Sincere thanks due to Sir David A. Vallado, for his valuable suggestion, while working on this problem. The success of this algorithm was possible because of his insightful instructions.

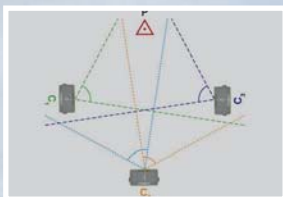
References

- [1] Vallado D. A., McClain Wayne D., "Fundamental of Astrodynamics and Application", 2nd Edition, Microcosm Press: USA and Kluwer Academic Publishers: The Netherlands, 2001.
- [2] AIAA Astrodynamics Standard: Propagation Specifications, Test Cases, and Recommended Practices, American Institute of Aeronautics and Astronautics.
- [3] G. Seeber, "Satellite Geodesy", 2nd Edition, Walter de Gruyter: Germany, 2003.
- [4] Vallado D. A, Crawford Paul, Hujak Richard, Kelso T. S., "Revisiting Spacetrack Report #3", AIAA 2006-6753.
- [5] Gorman Shaun, "A Brief Introduction to Astrodynamics", www.public.iastate.edu/~fchavez/.
- [6] Montenbruck, E. Gill, Th. Terzibaschian., "Note on the BIRD ACS Reference Frames", DLR-GSOC TN 00-01.
- [7] <http://en.wikipedia.org/wiki/ECEF>
- [8] Vallado D. A, Seago John H., "The coordinate frames of the US space object catalogs".
- [9] Bizouard Christian, Gambis Daniel, "The combined solution C04 for Earth Orientation Parameters consistent with International Terrestrial Reference Frame 2008", Observatoire de Paris, SYRTE, 61 av. de l'Observatoire, Paris, France. ▴

In the issue

▶ New Photogrammetry

Get about 2 cm accuracy
with TRIUMPH-LS



▶ Angle Measurement

Quickly measure angles
with TRIUMPH-LS



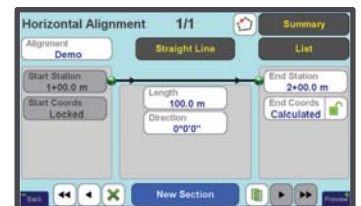
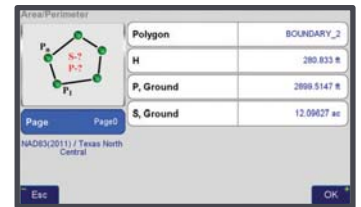
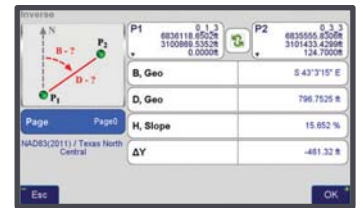
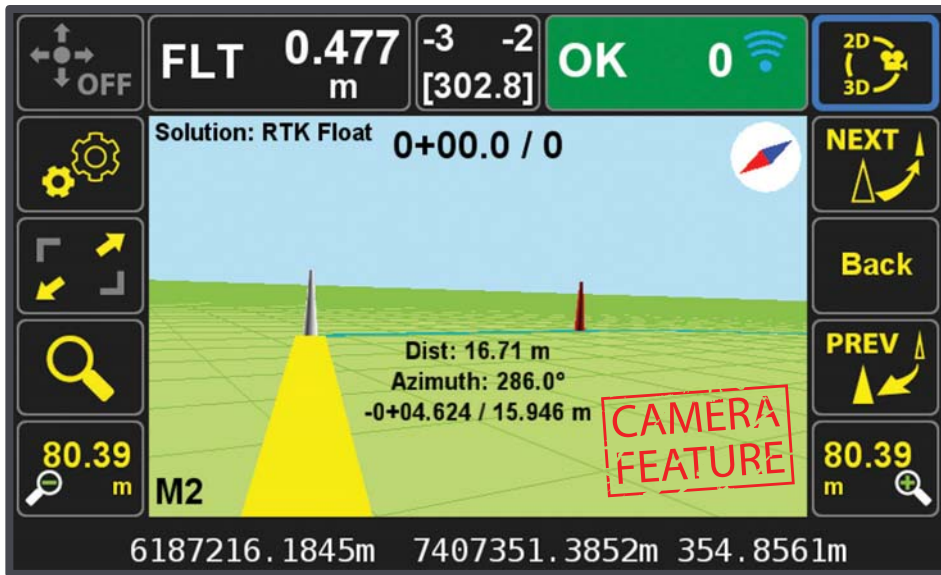
▶ Letter

from Kelly



WWW.JAVAD.COM





Store and Stake

Introducing GUIDE data collection in the TRIUMPH-LS. Visual Stake-out, navigation, six parallel RTK engines, over 3,000 coordinate conversions, advanced CoGo features, rich attribute tagging on a high resolution, large, bright 800x480 pixel display.

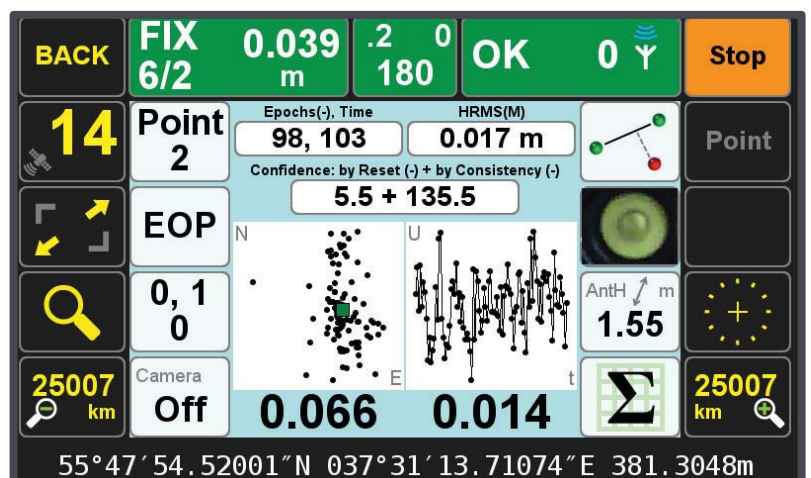
Versatile attribute tagging, feature coding and automatic photo and voice documentation.

The TRIUMPH-LS automatically updates all firmware when connected to a Wi-Fi internet connection.

View and Document your level

The downward camera of TRIUMPH-LS scans and finds the liquid bubble level mounted on the pole. Then focuses on the circular bubble automatically and shows its image on one of the eight white buttons of the Action Screen. You can:

- View the liquid bubble level on the screen.
- Document survey details including the leveling by taking automatic screen shots of the Action Screen, as shown here.
- Calibrate the electronic level of TRIUMPH-LS with the liquid bubble level for use in Lift and Tilt and automatic tilt corrections.



All these camera features are possible only in TRIUMPH-LS where camera, and GNSS antenna are co-located and all other modules integrated.

OMEGA

Rugged GNSS Unit



OMEGA is the most advanced GNSS receiver. It does not include integrated antenna and controller. It is suited for applications like **machine control** and in **marine** and **avionics** applications.

Adding GrAnt and Victor-LS makes a complete RTK system.

It is well suited for **monitoring and network stations**.

A variety of Radio Modems Bluetooth and USB in all JAVAD radios



JLink 3G



JLink 3G BAT



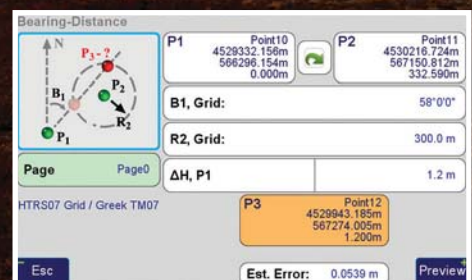
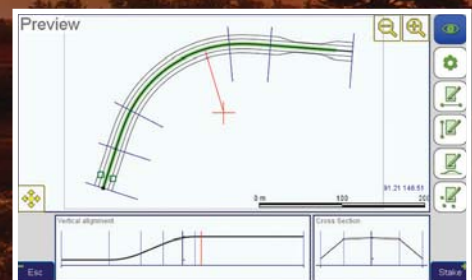
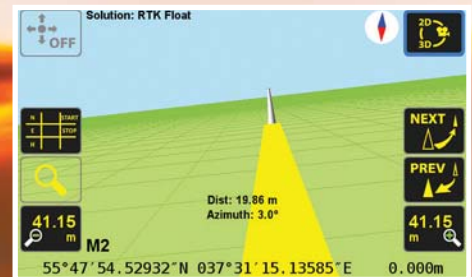
HPT435BT/HPT135BT/
HPT225BT

TRIUMPH-LS

Receiver+Antenna+Radio Modem+Controller+Pole



- 864 Channels for all GNSS signals
- 24 Hours Battery Life
- Interference monitoring of all GNSS and UHF channels
- Visual Stake out
- Lift & Tilt
- 6 parallel RTK engines



Victor-LS

The Rugged Field Controller



Victor-LS is a rugged field controller. It runs J-Field and can be used with TRIUMPH-1 and TRIUMPH-2.

Base	GEO	55°54'01.30723"N	037°23'50.26652"E	244.461m
	GRID	26021.015m	-6423.657m	244.191m
Rover	GEO	55°47'52.87472"N	037°31'20.76734"E	366.064m
	GRID	14623.098m	1406.924m	365.916m
Dir:	325°30'37"	Dist:13828.612m	ΔH:-121.603m	
FIX:5	Sats:7+5			
HRMS:0.008m	VRMS:0.010m	RMS:0.013m		
HDOP:0.988	VDOP:1.319	PDOP:1.648		
TDOP:1.082	GDOP:1.972			
95% Confidence Ellipse				
σ ₁ :0.014m	σ ₂ :0.013m			
0:33°47'16"	oh:0.020m			
Esc				



TRIUMPH-1M + Victor-LS



TRIUMPH-2 + Victor-LS

High performance Antennas

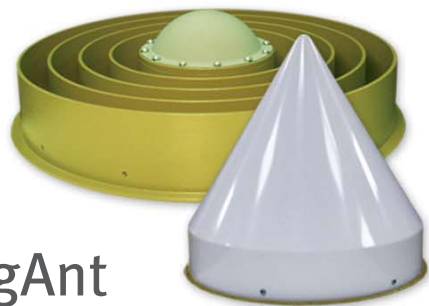
TriAnt



AirAnt



RingAnt



GrAnt

See details at www.javad.com



HPT404BT/
HPT104BT/HPT204BT



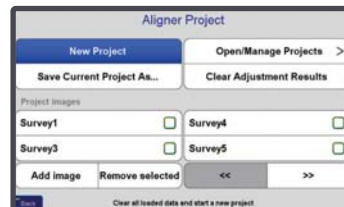
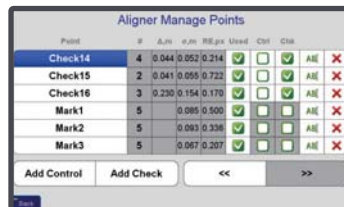
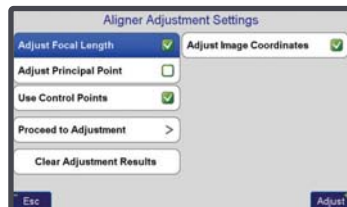
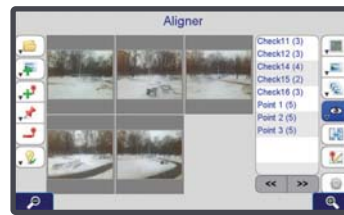
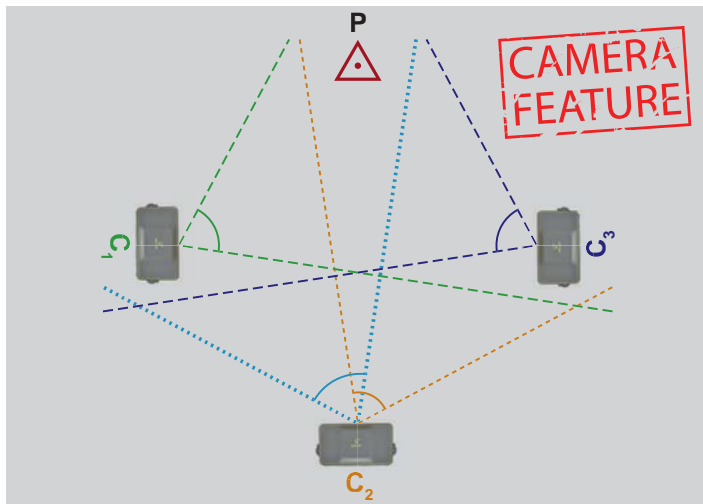
L-Band/Beacon/
Spread Spectrum



HPT401BT/HPT101BT/
HPT201BT

Offset Survey with built in camera

You can survey points with internal TRIUMPH-LS camera with accuracy of about 2 cm. Take pictures from at least three points. Leave a flag on points that you take pictures from, otherwise accuracy will be about 10 cm.

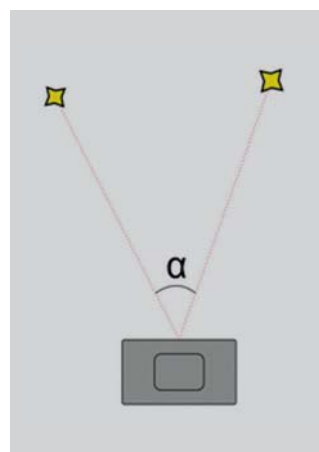


Visual Angle Measurement with Triumph LS

The new Visual Angle Measurement function of the TRIUMPH-LS allows measuring angles between points by using photos taken by the TRIUMPH-LS camera and use in CoGo tasks with the Accuracy of about 10 angular minutes.

To measure an angle:

- just take an image containing both objects of interest and open it in the Measure Angle screen
- select first and second point (using zoom to focus on necessary features)
- The angle between points is immediately displayed on the screen.



From:

V. Kelly Bellis, PLS

Horizon Surveying Co., Inc.

Ellsworth, Maine 04605

kellybellis@gwi.net

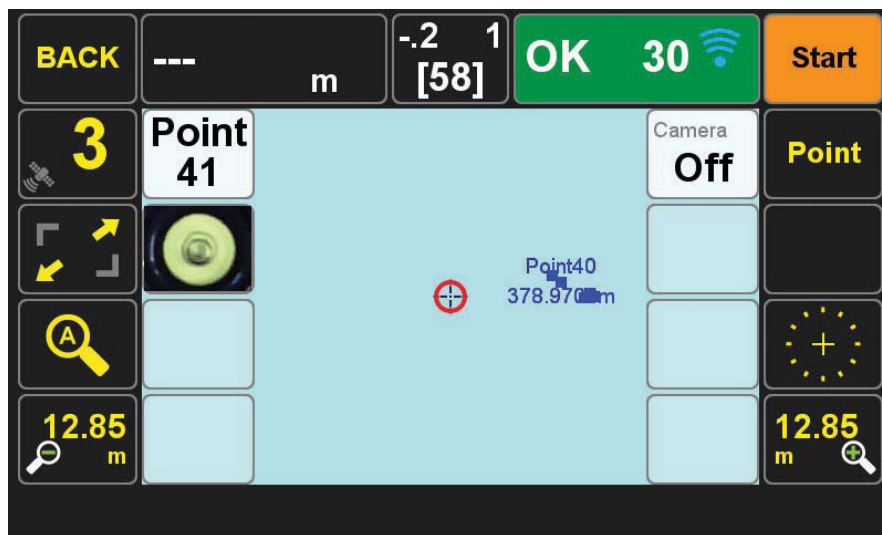


Without question, the Triumph-LS is the most mind-blowing piece of technology that I have ever held in my hands and being able to work with it is the highlight of my 40-year career in land surveying. Intertwined and commensurate with that highlight has also been the incredible honor and privilege in working with Javad Ashjaee, his amazing Moscow-based team of scientists and engineers, as well as some of the brightest surveyors in the United States, all in the shaping of the Triumph-LS and its graphical user interface, J-Field.

There are so many features of the Triumph-LS worth highlighting, it's difficult to know where to start; from the built-in frequency scanners for both UHF interference and GNSS interference, the automated shifting of project coordinates after the base file has

been submitted to DPOS (Javad's own version of OPUS for .jps files) and its adjustment received – all being done by J-Field, or to start by mentioning Visual Stakeout using J-Field's unique and way cool Guide feature. The ability to locate objects using photogrammetric methods is another exciting tool included in J-Field's extensive tool-set.

Being a person that has always gravitated to understanding things visually, J-Field's approach and graphical displays has aided my transition from strictly being an L1 guy for more than a dozen years; (6) ProMark2 Ashtech¹ receivers, to finally get with today's surveying using RTK. Of course, the Triumph-LS's very competitive price point also made this transition possible.



Shown here is just one example of the visual presentation of information given the surveyor. It includes being able to see at a glance the image of the rod bubble beneath the instrument's second camera and the textual display of Triumph-LS's internal pitch and roll values.

If I was limited to saying only one thing about the Triumph-LS that has impressed me the most, I'd have to say that it doesn't have anything to do with technology whatsoever. It has to do with a GNSS manufacturer that has so openly embraced the surveying profession during the development of a specific product, and most notably, professional land surveyors in the United States. As a matter of policy, Javad GNSS users are encouraged to suggest improvements and new features to all Javad GNSS products. And nowhere is that policy reflected more clearly than in J-Field.

The Javad PLS Support Network is an other reflection of Javad GNSS's commitment to supporting the U.S. Professional Land Surveyor and

their use of Javad equipment. Composed of a core group of licensed professional land surveyors scattered across the United States, the so-called 5PLS members stand ready to assist by phone or email. The best method of support is actually using the website's support forum (<https://support.javad.com/index.php>) which serves not only as a portal to quickly getting answers to questions from all of the licensed land surveyors, Javad GNSS geodesists, scientists, engineers and even Javad Ashjaee himself, but also ever increasingly the support forum serves as a reference source and suggestion box.

¹ Ashtech was the first GNSS company that was founded by Javad Ashjaee.

A new approach for real-time structural monitoring

This work addresses the feasibility of employing low-cost GNSS receivers and MEMS-accelerometers for structural and infrastructures monitoring purposes, in particular as regards vibrations recognition and characterization



Elisa Benedetti
PhD candidate, Geodesy and Geomatics Division, University of Rome "La Sapienza", Italy



Mara Branzanti
PhD candidate, Geodesy and Geomatics Division, University of Rome "La Sapienza", Italy



Gabriele Colosimo
Software Engineer, R&D Network and Reference Station team, Leica Geosystems, Heerbrugg, Switzerland



Augusto Mazzoni
Post-doctoral Researcher, Geodesy and Geomatics Division, University of Rome "La Sapienza", Italy



Monica Moroni
Researcher of DICEA, University of Rome "La Sapienza", Italy



Mattia Crespi
Full Professor, Faculty of Civil and Industrial Engineering, University of Rome "La Sapienza", Italy

In the context of structural monitoring, GPS technology made possible the structures behaviour monitoring in terms of absolute displacements, relative to a fixed global reference frame.

The accelerometers, typically employed in such a field, were in fact characterized by some limitations in displacement measurements being able to describe relative displacements with respect to their body fixed reference frame. In recent years, with the increasing development and dissemination of structures and infrastructures in urban areas, the response of huge structures to dynamic phenomena as earthquakes, severe winds, traffic loads and thermal behaviour is of great interest.

Monitoring networks which employ dual frequency GPS receivers are now commonly used (Yi et al. (2012)). These sensors are quite expensive; therefore widespread distribution cannot take place on such a structure. Hence, the employment of low-cost

single frequency receivers offers the possibility to overcome such a problem and the growing number of studies are focusing on this topic (Jo et al. (2012)).

In this work, we address the problem of fast oscillatory motions reconstruction through LIS3LV02DQ MEMS-accelerometer (LIS-MEMS), uBlox 6 (uBlox) single frequency and Leica Viva (Viva) dual frequency GPS receivers, in order to evaluate the performances of the three different sensors and the agreement among their solutions.

VADASE software for real-time displacements estimation

VADASE software has been used to process both dual and single frequency GPS data collected from the two GPS receivers (respectively, Viva and uBlox 6), during experimental trials. VADASE algorithm was successfully proposed in the Global Navigation Satellite Systems seismology (shortly indicated as GNSS seismology) context.

In Colosimo et al. (2011), a first demonstration of VADASE algorithm was presented; its effectiveness was confirmed with the application to the catastrophic Tohoku-Oki earthquake (USGS M = 9.0, March 11, 2011) (Branzanti et al. (2013)) and then to the Emilia earthquake in Italy (USGS M = 6.1, May 20, 2012) (Benedetti et al. (2014a)).

The software is based on the so-called variometric approach, applied on single phase observations continuously collected by a standalone GPS receiver.

Overall, the obtained results are quite promising for possible establishment of structural health monitoring through low-cost GNSS receivers and MEMS-accelerometers

Standard GPS broadcast products (orbits and clocks), available in real-time, are required. With receiver phase observations and broadcast products, VADASE estimates epoch-by-epoch displacements, basically equivalent to velocities. The velocities are then integrated over the considered time period and displacements are retrieved. Since VADASE does not require either additional technological complexity or a centralized data analysis, in principle, it can be embedded into the GPS receiver firmware and work in real-time.

For these reasons, it could represent a new and efficient strategy in structural monitoring field. In this work we handle only GPS data, but VADASE is capable of working also with GLONASS and Galileo constellations (Colosimo (2013), Benedetti et al. (2014b))”

VADASE analytical basis

To briefly recall the estimation model of the variometric approach (for a more detailed discussion, please refer to Colosimo et al. (2011), Branzanti et al. (2013), Colosimo (2013)), we start from the standard carrier phase observation equation (in length units):

$$\lambda \Phi_r^s = \rho_r^s + c(\delta t_r - \delta t^s) + T_r - I_r - \lambda N_r^s + p_r^s + m_r^s + \varepsilon_r^s \quad (1)$$

where subscript (r) refers to a particular receiver and superscript (s) to a satellite; Φ_r^s is the carrier phase observation of the receiver with respect to the satellite; λ is the carrier phase wavelength; ρ_r^s is the geometric range; c is the speed of light; δt_r and δt^s are the receiver and the satellite clock errors, respectively; T_r and I_r are the tropospheric and the ionospheric delays along the path from the satellite to the receiver, respectively; N_r^s is the phase ambiguity; p_r^s is the sum of the other effects (relativistic effects, phase center variations, phase wind-up); m_r^s and ε_r^s represent the multipath and the noise, respectively.

If we consider the difference in time (Δ) between two consecutive epochs (t and t+1) of carrier phase observations in the ionospheric-free combination (α

and β are the standard coefficient of L3 combination of L1 and L2 phases), we obtain the so defined variometric equation:

$$\alpha[\lambda \Delta \Phi_r^s]_{L1} + \beta[\lambda \Delta \Phi_r^s]_{L2} = (\mathbf{e}_r^s \bullet \Delta \xi_r + c \Delta \delta t_r) + ([\Delta \rho_r^s]_{OR} - c \Delta \delta t^s + \Delta T_r + [\Delta \rho_r^s]_{EIOI} + \Delta p_r^s) + \Delta m_r^s + \Delta \varepsilon_r^s \quad (2)$$

where \mathbf{e}_r^s is the unit vector from the satellite to the receiver at epoch t, $\Delta \xi_r$ is the epoch-by-epoch displacement (equivalent to velocity) of the receiver in the interval t and t+1, $[\Delta \rho_r^s]_{OR}$ is the change of the geometric range due to the satellite's orbital motion and the Earth's rotation and $[\Delta \rho_r^s]_{EIOI}$ is the change of the geometric range due to the variation of the solid Earth tide and ocean loading. The term $(\mathbf{e}_r^s \bullet \Delta \xi_r + c \Delta \delta t_r)$ contains the four unknown parameters (the 3D velocity and the receiver clock error variation $\Delta \delta t_r$) and $([\Delta \rho_r^s]_{OR} - c \Delta \delta t^s + \Delta T_r + [\Delta \rho_r^s]_{EIOI} + \Delta p_r^s)$ that is the known term that can be computed on the basis of known orbits, clocks and of proper well-known models.

The least squares estimation of the 3D velocities is based upon the entire set of variometric equations (2) written for two consecutive epochs. The number of variometric equations depends on the number of satellites common to the two epochs, and at least four satellites are necessary in order to estimate the four unknown parameters for each couple of epochs.

VADASE for single frequency observations

The variometric equation can be also expressed by considering L1 single frequency observations:

$$[\lambda \Delta \Phi_r^s]_{L1} = (\mathbf{e}_r^s \bullet \Delta \xi_r + c \Delta \delta t_r) + ([\Delta \rho_r^s]_{OR} - c \Delta \delta t^s + \Delta T_r - \Delta I_r + [\Delta \rho_r^s]_{EIOI} + \Delta p_r^s) + \Delta m_r^s + \Delta \varepsilon_r^s \quad (3)$$

The ionospheric term ΔI_r represents the variation of ionospheric delay during the interval (t, t+1) and in the current version of VADASE (Benedetti et al. (2014b)). It is modelled according to the Klobuchar model (Klobuchar (1987)) which requires approximate information as geodetic latitude, longitude, elevation

angle and azimuth of the particular GPS satellite considered, together with coefficients given by the navigational message. A possible alternative ionospheric model is NeQuick, recently proposed by Radicella (2009), and it will be considered in future developments of VADASE software.

Recent results in GNSS seismology field have shown VADASE software capability in handling single frequency data (L1).

For example, for the Emilia earthquake (Benedetti et al. (2014a)), 7 permanent stations data were processed with VADASE and the solutions were then compared with the ones obtained with other well-established strategies and software. VADASE software was used both applying L3 combination over dual frequency data, both considering L1 data only. The Root Mean Square Error for VADASE L3 solutions with respect to the reference ones are within 1.1 cm in horizontal and within 1.5 cm in height. The agreement in terms of RMSE of the difference between the two solutions (VADASE L3 and VADASE L1), over a 2 minute time interval, is 0.4 cm in horizontal and 1.7 cm in height.

The obtained results are very promising and they pave the way to the possibility of a massive use of low-cost GPS receivers for monitoring purposes, which is one of the main goals of this investigation.

Experiments and devices: goals and features

Several experimental tests were performed in order to investigate the capability of LIS-MEMS, Viva and uBlox GPS receivers in retrieving kinematic parameters of oscillatory motions and the solution agreement.

The main goal of this research is to determine the feasibility evaluation of adopting low-cost sensors (GPS receivers and accelerometers) for structural and infrastructural monitoring purposes and perform in future, data processing strategies to integrate the observables provided by the two sensors.

Some advantages of an integrated system based on these low-cost sensors can be summarized as follows:

- cheap sensors allow the possibility to set up dense network monitoring, suitable for structures and infrastructures with wide dimensions; redundant observations can be strategic to better describe extended dynamic phenomenon
- as regard the two different technologies, it is well known that accelerometers and GPS receivers can offer complementary contribution for monitoring purposes: for example, a temporary bad sky visibility can harm GPS receiver performances, while accelerometer is also capable of working indoors. In contrast, especially when operating under low acceleration conditions, the performances of MEMS-accelerometers can be influenced by thermal and mechanical noise characteristics (Mohd-Yasin et al. (2010))
- the different details of information provided by the two sensors are complementary: MEMS-accelerometers can usually work at a very high acquisition rate; for example, the LIS-MEMS, used in our trials, is capable to acquire a minimum frequency of 40 Hz, while the uBlox receiver can provide good quality observations, acquiring at (maximum) 5 Hz on the base of our experiences.

In the same time with a GPS sensor, it is possible to know the receiver position in a global reference frame together with accurate time information. Whereas MEMS-accelerometer information refers to a (X,Y,Z) body reference frame and no time stamps are usually given.

LIS-MEMS, Viva and uBlox GPS receivers have been tested with a simple vibrating table, able to realize one-dimensional oscillations, allowing different amplitudes (from 4 to 8 cm) and frequencies (from about 1 Hz to 5 Hz). Unfortunately, it is not possible to set precisely the vibration frequency, which can be roughly changed through a potentiometer.

As shown in Figure 1, the three sensors were located over the vibrating table; all the chosen oscillation frequencies were imposed during tests with durations of about 10-12 minutes.

Following, a brief description of the three devices and software interface.

Monitoring with image analysis for test system validation

The test system (vibrating table with uBlox, Viva and LIS-MEMS on board) has been validated using an independent image acquisition system (Figure 1). The goals of this validation were to control that the different sensors undergoing the same motion.

The image acquisition system consisted of a high-speed, high-resolution camera (Mikrotron EoSens) equipped with a Nikon 50-mm focal length lens capturing gray-scale images at up to 500 fps (frames per second) with a resolution of 1280x1024 pixels (for the present set of measurements, images were acquired at 250 fps) and a high-speed camera link digital video recorder operating in full configuration (IO Industries DVR Express® Core) to

Table 1: An example of retrieved frequency from image processing: the same frequency was found either when features of each element was separately seen (receivers, accelerometer or table) either or all features together (system) were considered.

Features Point from	Frequency [Hz]
Viva	5.8594
MEMS	5.8594
Ublox	5.8594
Table	5.8594
System	5.8594

manage data acquisition and storage. The captured images were transferred to a personal computer under the control of the Express® Core software.

Acquired images have been processed using an image analysis algorithm solving the Optical Flow equation, which defines the conservation of the pixel brightness intensity at time t ($I(\mathbf{x},t)$):

$$\frac{DI(\mathbf{x},t)}{Dt} = \frac{\partial I(\mathbf{x},t)}{\partial t} + \mathbf{u} \frac{\partial I(\mathbf{x},t)}{\partial x} + \mathbf{v} \frac{\partial I(\mathbf{x},t)}{\partial y} = 0 \quad (4)$$

where $\mathbf{x}=(x,y)$ is the generic pixel coordinate and $\mathbf{U}=(u,v)$ is the unknown velocity vector at location \mathbf{x} . Since (1) is insufficient to compute the two unknown velocity components (u,v)



Figure 1: Vibrating table with sensors on board, monitored by two high-resolution cameras.



Figure 2: Screenshot of the image processing with features highlighted trajectories.

associated to a single pixel, the equation is computed in a window $W=H \times V$ (where H and V are the horizontal and vertical dimension of the window respectively) centered at the pixel location and the solution, i.e., the displacement vector of the interrogation window between two consecutive frames, is determined through a least squares optimization (Moroni and Cenedese, (2005)).

The algorithm, namely PEP (Particle Extraction and Prediction), selects image features (image portions suitable to the tracked because their luminosity remains almost unchanged for small time intervals) and tracks those from frame by frame (Shindler et al., (2012)).

The trajectories are then employed to compute velocity vectors and those belonging to the same frame are arithmetically averaged to compute the time history of both velocity components.

By considering the results obtained from image processing, it is possible to state that the velocities of the different sensors and the vibrating table are homogeneous and therefore, fully comparable.

An example of these results is presented in Table 1 while in Figure 2 the velocity reconstructed in time by observing the trajectories of different features relating to each sensor are drawn.

Employed sensors

A Leica Viva GPS receiver was chosen to represent a solution reference to better understand the uBlox capability.

Leica Viva is a geodetic class receiver that is able to acquire in dual frequency from low (< 1 Hz) till very high (50 Hz) sampling rate. In these

experiments, an acquisition rate of 10 Hz was deemed sufficient.

uBlox 6 is a low-cost GPS receiver that is able to acquire in single frequency only, from low (< 1 Hz) to high sampling rate (10 Hz). On the basis of previous experiments, it has been set up to work with a frequency rate of 5 Hz, since the observations have to be stored in real-time through a USB connection in an external memory unit (i.e. laptop) and some stream managing problems have been noticed at higher acquisition rates.

The u-center program (available online), used in the 6.2.2.0 release, is a flexible tool for the uBlox/laptop interface and allows the evaluation, analysis and configuration of the receiver.

The LIS3LV02DQ MEMS-accelerometer, provided by STMicroelectronics, was used as integrated in the EK3LV02DQ Evaluation Kit. It is a low-power tri-axial linear accelerometer with an acquisition frequency from 40 Hz to 640 Hz and a full scale of $\pm 2g$ and $\pm 6g$.

The software interface used was Unico 0.7.0.5.

These sensors were massively used for manifold applications (O' Reilly et al. (2008)) as for crash safety, game controllers, personal computers, smartphones and cameras.

Recent studies have demonstrated encouraging results for the suitability of low-cost tri-axial MEMS-accelerometers in civil and geophysical fields, employable for the reconstruction of vibrations and ground motion (Cochran et al. (2009), Zhao M. and X. Xiong (2009), D'Alessandro A. and G. D'Anna (2013)).

Data processing: methods and results

Here, we present the strategy followed to evaluate the performances of the sensors in retrieving kinematic parameters of an oscillatory phenomenon.

MEMS data were analysed as recorded on a personal computer with Unico software interface: accelerations in MEMS body reference frame are given.

Dual and single frequency GPS data were both processed with VADASE software: as previously mentioned, the only input required are observations and navigational files available in real-time.

Starting from MEMS-accelerations and GPS-velocities, we proceeded to data analysis: three experimental tests are considered in this discussion.

From these tests, analysis corresponding to five different frequencies (from about 1 to about 2.2 Hz) will be presented. These frequencies have been chosen from a frequency interval where solutions of the different sensors coexist, in order to allow the comparison of the three sensors. The vibrating table was set at the smallest allowed displacement of 3.95 cm (amplitude 1.975 cm), measured with an accuracy of 0.005 cm.

Spectral analysis

A spectral analysis of MEMS-accelerations and GPS-derived velocities was carried out (Figure 3).

As above mentioned, because of the 5 Hz sampling rate of uBlox receiver (hence, Nyquist frequency is 2.5 Hz), all data were band-pass filtered within 1.0 - 2.5 Hz using a Butterworth filter.

The shape of power spectrum (Figure 3) suggests high correlation of the frequency content tracked by the three sensors. The power spectrum is of course dependent on the sampling frequency adopted (i.e., the MEMS-accelerometer solution power spectrum is much higher than that of uBlox receiver).

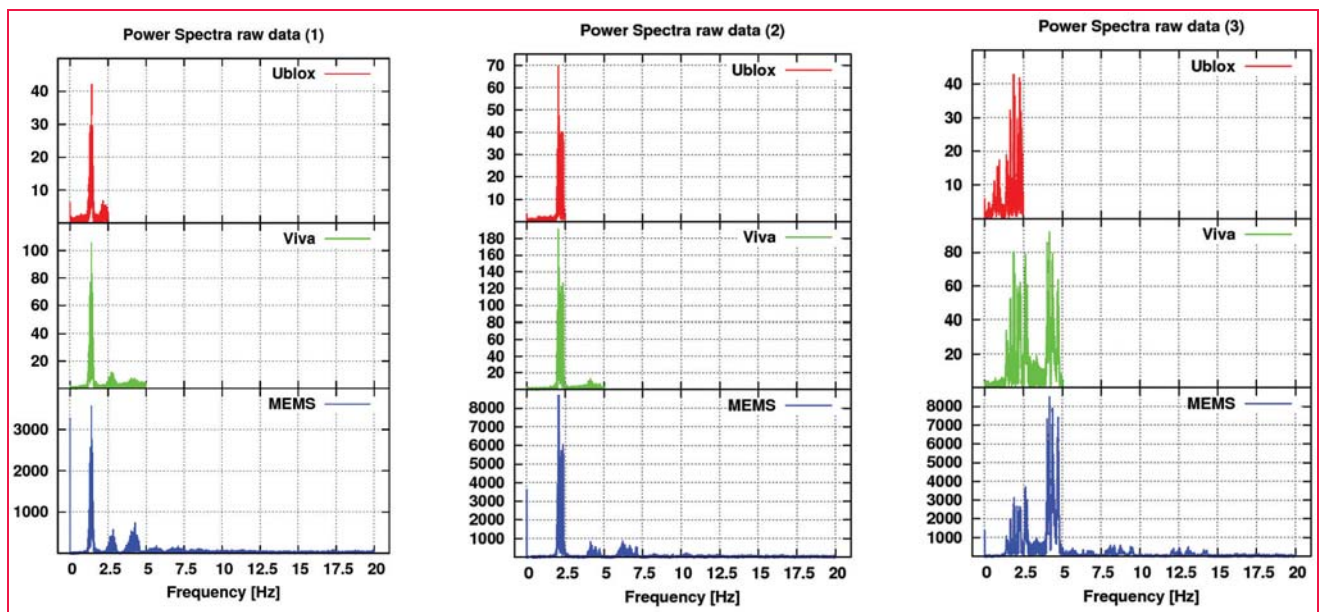


Figure 3: Three tests spectral analysis results refer to horizontal GPS-derived velocities receivers and horizontal MEMS-derived accelerations.

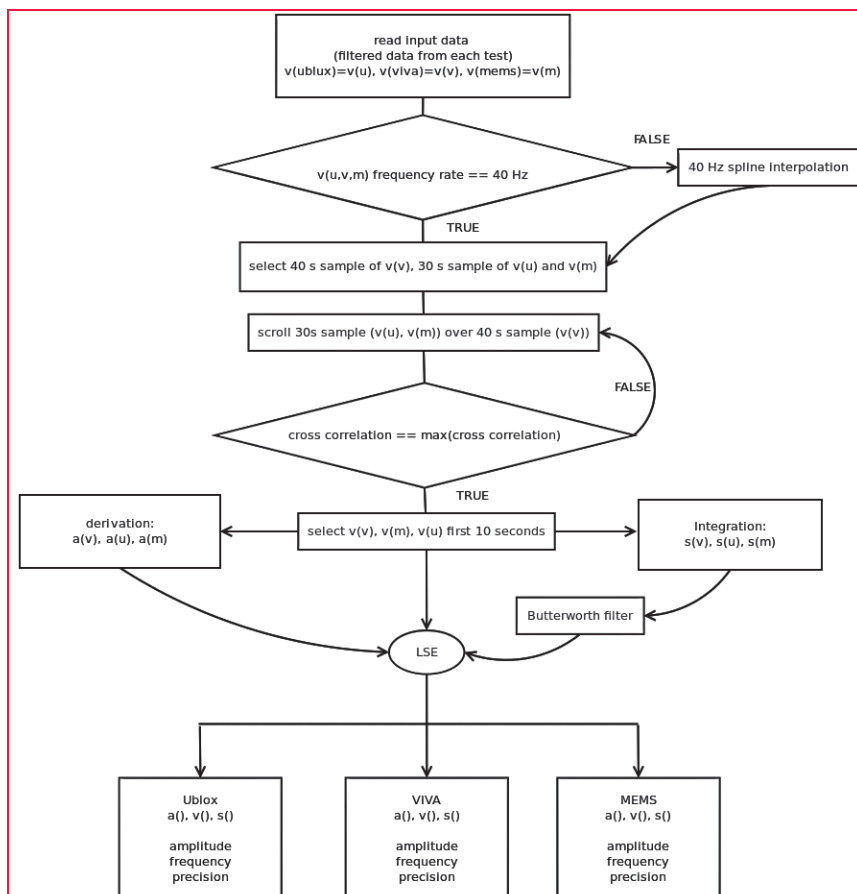


Figure 4: The flowchart describes all the steps followed to carry out the comparisons between sensors.

LIS-MEMS was fixed on board the table with its y-axis aligned along the direction of oscillation, hence only the y-direction was considered. As regard the GPS-derived velocities, VADASE solutions

provided East, North and Up components. They were hence combined to consider the motion along the vibration direction.

In Figure 3 the spectra of y-acceleration

of LIS-MEMS and GPS receivers planimetric velocities are shown.

Solutions comparison

We used a least squares motion estimation method (LSE) in order to quantify the agreement between the solutions and to estimate kinematic parameters (acceleration, velocity and displacement in a chosen time interval) of the oscillatory phenomenon.

The motion estimation method was formulated under the hypothesis of a constant sinusoidal motion, so that the residual phase shift, the main frequency and the corresponding amplitude were least squares estimated in accordance to the simple model:

$$x = A \cdot \sin[(2\pi f) \cdot t + \varphi] \quad (5)$$

where A , f and φ are respectively amplitude, frequency and phase of GPS (uBlox or Viva) or LIS-MEMS solutions (in Figure 4 the flowchart describing the steps followed to compare different solutions is shown). It is important to recall that the vibrating table is only roughly perfect harmonic oscillator. In this respect, with the aim to perform the estimation, it was necessary to select only short intervals (10 seconds), for which the frequency can be considered constant.

The input data at the beginning of the flowchart are the filtered velocities of the three sensors. As regards LIS-MEMS velocities in input to the Butterworth filter, they were previously obtained through the integration of the stored accelerations.

The GPS-derived velocities were resampled at 40 Hz (the rate of LIS-MEMS measurements) through cubic splines in order to allow solutions comparison.

As regards the time scale, it is necessary to remind that LIS-MEMS observations are given without the corresponding time stamps; for such a reason, these time stamps were a-posteriori reconstructed by adding 0.025 seconds for each observation, starting from the first one. Obviously, this choice does not guarantee that the LIS-MEMS reconstructed time scale is aligned with the GPS time scale, so that a synchronization problem has to be faced.

In detail, the possible time drift between these time scales was estimated and removed accordingly to the following equation:

$$t_{m_synchro} = [(\omega_u + \Delta\omega)/\omega_m] \cdot t_m + \Delta\phi/\omega_m \quad (6)$$

where the subscripts 'm' and 'u' refer respectively to LIS-MEMS and uBlox,

$$\Delta\omega = \omega_m - \omega_u = 2\pi(f_m - f_u) \quad (7)$$

$$\Delta\phi = \phi_m - \phi_u \quad (8)$$

and t_m , $t_{m_synchro}$ are respectively MEMS time stamps before and after the synchronization with uBlox, taken as reference. After the synchronization, the correlation between the signals related to positions, velocities and accelerations was computed.

The obtained positions, velocities and accelerations results respectively are reported in Table 2, while in Table 3, cross correlation results among the three sensors are summarized.

Discussion

From the results obtained considering five frequencies (from about 1 to 2.2 Hz) the following remarks can be drawn:

- the sigma0 obtained from the LSE suggests a good precision of the adopted method; the median value calculated among all the solutions amounts to 0.27 m/s², 0.025 m/s, 0.002 m as regards acceleration, velocity and displacement estimation respectively
- the estimated displacement can be compared with the real amplitude of the vibrating table (0.0198 m): MEMS-accelerometer displacement solutions deviate the reference value by $\pm 1\%$, except for the f5 frequency where the solution is underestimated for 5%; uBlox displacement solutions overestimate the reference value from about 2% to 17%, while overestimate 32% at the f5 frequency

where uBlox solutions suffer aliasing phenomenon; Viva displacement solutions are characterized by an overestimation from 9% to 15% in comparison with the reference value except for the f1 frequency where the underestimation is about 3%

- the correlation coefficients reported in Table 3 have been calculated by considering 10 seconds of data in input to the estimation method. However, they are representative of a general high correlation between all the results obtained. For tests considered in their entirety, at maximum the coefficients ($\rho_{(MEMS-uBlox)}$, $\rho_{(MEMS-Viva)}$, $\rho_{(Viva-uBlox)}$) are lower in percentage less than 3.5% with respect to the coefficient here presented
- looking at the obtained results, the 2 Hz frequency seems to represent a sort of threshold: if overcome (as from 1.95 to 2.15 Hz), the uBlox

Table 2: Acceleration (A_a), velocity (A_v), displacement (A_s) and frequency (f) estimations with corresponding precisions (sigma0).

		f Hz	A_acc m/s ²	sigma0_acc m/s ²	A_vel m/s	sigma0_vel m/s	A_disp m	sigma0_disp m
Viva	f1	1.34	1.353	0.232	0.161	0.021	0.019	0.002
Ublox		1.34	1.476	0.276	0.176	0.025	0.021	0.002
MEMS		1.34	1.396	0.196	0.166	0.019	0.020	0.002
Viva	f2	1.48	1.838	0.268	0.200	0.028	0.021	0.003
Ubox		1.48	1.990	0.290	0.216	0.028	0.023	0.003
MEMS		1.48	1.681	0.228	0.182	0.024	0.020	0.002
Viva	f3	1.89	3.350	0.189	0.287	0.016	0.024	0.001
Ubox		1.89	2.724	0.468	0.233	0.029	0.020	0.002
MEMS		1.89	2.762	0.179	0.236	0.015	0.020	0.001
Viva	f4	1.95	3.504	0.471	0.290	0.039	0.024	0.003
Ublox		1.95	2.989	0.701	0.248	0.047	0.020	0.003
MEMS		1.96	2.936	0.371	0.242	0.031	0.020	0.002
Viva	f5	2.15	4.250	0.258	0.321	0.019	0.023	0.002
Ublox		2.15	2.449	0.762	0.185	0.045	0.013	0.002
MEMS		2.15	3.450	0.214	0.260	0.016	0.019	0.001

Table 3. Correlation coefficients among velocities solutions of MEMS-accelerometer and Viva receiver (mv), uBlox and Viva receiver (uv), uBlox and MEMS-accelerometer (um), uBlox and MEMS-accelerometer synchronized (um synchro) respectively and the relative increment (um increment).

Correlation coefficient (%)					
	mv	uv	um	um synchro	um increment
f1	99.79%	97.75%	98.89%	98.99%	0.10%
f2	99.32%	99.07%	99.35%	99.42%	0.07%
f3	99.77%	97.13%	98.79%	98.98%	0.19%
f4	98.40%	98.30%	98.37%	98.40%	0.02%
f5	99.80%	94.60%	94.71%	94.73%	0.02%

Discover Freedom & Flexibility with



Five Centimeter Global,
Real-Time Accuracy...
without a base station



starfire.navcomtech.com

NAVCOM

A John Deere Company

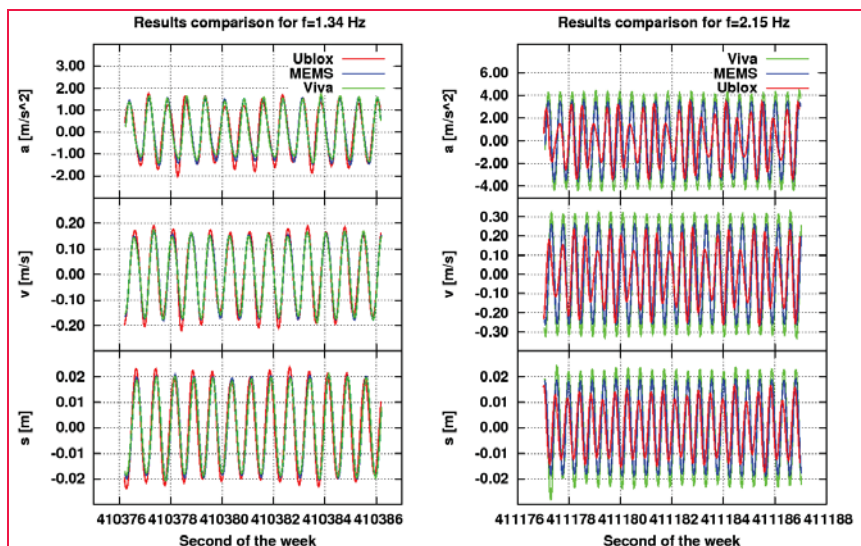


Figure 5: Comparison between accelerations, velocities and displacements retrieved by the three sensors are depicted. The solutions shown refer to the lowest and the highest frequency considered.

shows significant problems in reconstructing the oscillatory motion due to the aliasing phenomenon

- it is necessary to highlight the synchronization between uBlox receiver and LIS-MEMS observations must be considered as a preliminary attempt. In fact, it will be necessary to consider synchronization model under the hypothesis of different and variable time scale of LIS-MEMS and uBlox receiver.

However, it can be noted that the synchronization is more effective for low frequencies.

Conclusion

This work addresses the problem of fast oscillatory motions monitoring through LIS3LV02DQ MEMS-accelerometer, uBlox single frequency and Leica Viva dual frequency GPS receivers, in order to evaluate the performances of the three different sensors and their solution agreements.

Suitable tests were performed using a vibrating table able to shake the co-located devices with a frequency from about 1 to 5 Hz.

A first spectral analysis was carried out: Figure 3 show the spectra obtained for

three tests made and the similar shape suggests high concordance in terms of frequency content between the different solutions set. These starting solutions are accelerations of LIS-MEMS and velocities of the two GPS receivers obtained with VADASE software.

A pass-band filter was then applied in order to consider the frequency band common to the three devices. The filtered data were then given in input to an LSE model in order to estimate kinematic parameters representative of the considered oscillatory motion. Integrating and deriving the starting velocities, the analysis was extended to accelerations and displacements; five frequency oscillations were investigated.

The estimated solutions highlight the uBlox (set to acquire at 5 Hz) capability to reconstruct oscillatory motions with frequencies in the interval of 1 - 1.95 Hz.

The uBlox (5 Hz acquisition rate) displacement estimated amplitude differs from the real amplitude of vibrations (0.0198 m) ranging from 0 to 3.5 mm for frequencies from f1 to f4 (1 - 2 Hz), while for f5 (2.15 Hz), the difference is 6.5 mm due to the aliasing phenomenon.

The Viva (10 Hz acquisition rate) displacement estimated amplitude differs from the real one from 0 to 4 mm, while

LIS-MEMS solutions are close to the amplitude reference value within 1 mm.

High level of correlation has been obtained, in particular for frequency lower than 2 Hz where the correlation between LIS-MEMS and uBlox solution is always higher than 98.30%.

Overall, the obtained results are quite promising for possible establishment of structural health monitoring through low-cost MEMS-accelerometers and GPS receivers.

The combined and integrated use of these low-cost sensors in dense network monitoring represents a useful solution to better ensure a more detailed coverage of structures and infrastructures.

The use of low-cost single frequency receivers is allowed by the VADASE software which also ensures the employment of standalone receivers with the possibility to work in real-time.

A next step of this research which will be addressed in the near future, that could be represented by the formulation of MEMS-accelerometer and uBlox receiver data analytical integration.

References

- Benedetti E., M. Branzanti, G. Colosimo, A. Mazzoni, M. Crespi (2014b). VADASE: state of the art and new developments of a third way to GNSS Seismology. International Association of Geodesy Symposia, VIII Hotine Marussi Symposium (In Press).
- Benedetti E., M. Branzanti, L. Biagi, G. Colosimo, A. Mazzoni, M. Crespi (2014a). GNSS seismology for the 2012 Mw= 6.1 Emilia Earthquake: exploiting the VADASE algorithm. Seismological Research Letters, Volume 85, Issue 3, May-June 2014, pages 649-656, DOI: 10.1785/0220130094.
- Branzanti M., G. Colosimo, M. Crespi, A. Mazzoni (2013). GPS near real-time coseismic displacements for the great

Tohoku-Oki earthquake, IEEE Geoscience and Remote Sensing Letters, vol. 10, no. 2, DOI: 10.1109/LGRS.2012.2207704.

Colosimo G., M. Crespi and A. Mazzoni (2011). Real-time GPS seismology with stand-alone receiver: A preliminary feasibility demonstration, Journal of Geophysical Research, vol. 116, Issue 11, DOI: 10.1029/2010JB007941.

Colosimo G. (2013) VADASE: a brand new approach to real-time GNSS seismology, 180 pp., ISSN:9783845438382, Lambert Academic Publishing AG & Co KG.

Cochran E. S., J. F. Lawrence, A. Kaiser, B. Fry, A. Chung, and C. Christensen (2011). Comparison between low-cost and traditional MEMS-accelerometers: a case study from the M 7.1 Darfield, New Zealand, aftershock deployment, Annals of Geophysics, vol. 54, pp. 728–737.

D'Alessandro A. and G. D'Anna (2013). Suitability of low-cost three-axis MEMS-accelerometer in strong-motion seismology: Tests on lis331dlh (iphone) accelerometer,

Bulletin of the Seismological Society of America, vol. 103, pp. 2906–2913.

Jo H., S-H Sim, A. Tatkowski, Spencer Jr. B. F. and Nelson M. E. (2012). Feasibility of displacements monitoring using low-cost GPS receivers. Structural Control Health Monitoring, vol. 20, pages 1240-1254.

Klobuchar J. A. (1987). Ionospheric time-delay algorithm for single-frequency GPS users, IEEE Transactions on Aerospace and Electronic Systems, vol. AES-23, pp 325–331.

Mohd-Yasin F., D. J. Nagel and C. E. Korman (2010). Noise in MEMS, Measurement Science and Technology, vol. 21, n. 1.

Moroni M., A. Cenedese (2005). Comparison among feature tracking and more consolidated velocimetry image analysis techniques in a fully developed turbulent channel flow. Measurement Science and Technology 16, 2307-2322.

O'Reilly R., H. Tang, and W. Chen (2008). High-g testing of MEMS devices,

and why, IEEE Sensors Conference.

Radicella S. M. (2009). The NeQuick model genesis, uses and evolution, Annals of Geophysics, vol. 52, n. 3 - 4.

Shindler L., M. Moroni, A. Cenedese (2012). Using optical flow equation for particle identification and velocity prediction in particle tracking. Applied Mathematics and Computation, 218, 8684–8694.

Zhao M. and X. Xiong (2009). A new MEMS-accelerometer applied in civil engineering and its calibration test, Ninth International Conference on Electronic Measurements and Instruments (ICEMI '09).

Yi T H, Li H N, Gu M. (2012). Recent research and applications of GPS-based monitoring technology for high-rise structures. Structural Control Health Monitoring.

The paper was presented in ENC-GNSS 2014, Rotterdam, Netherlands, 15-17 April. ▴



13th South East Asian Survey Congress

Expanding the Geospatial Future

28 - 31 July 2015
Marina Bay Sands, Singapore



Registration information: <http://www.seasc2015.org.sg>
Congress Secretariat email: info@seasc2015.org.sg

Monitoring the declination of surface water bodies using NDWI technique

This paper presents the usefulness of Normalized Difference Water Index (NDWI) technique in monitoring the declination in surface water bodies in an urban scenario, with the case study of Bengaluru city



Ajaya S Bharadwaja
Air Traffic Controller,
HAL Airport,
Bangalore, India



Prof. Syed Ashfaq Ahmed
School Of Earth
Science, Central
University of Karnataka,
Gulbarga, India

The Normalized Difference Water Index (NDWI) is derived using similar principles to the Normalized Difference Vegetation Index (NDVI) to enhance the spectral reflectance of surface water bodies. NDVI was introduced by Rouse, et al (1973), where the comparison of differences of two bands, red and near-infra-red (NIR) is made with the following formula. $NDVI = \frac{(NIR-RED)}{(NIR+RED)}$, the resultant image will have the reflectance of vegetation enhanced. Gao (1996) has introduced the concept of NDWI. The normalized difference water index (NDWI) is derived using similar principles. It uses the following formula to assess the liquid water content of the vegetation canopy. $NDWI = \frac{(NIR-SWIR)}{(NIR+SWIR)}$, where SWIR wavelength is located in the region of vegetation canopy reflectance with water absorption. McFeeters 1996, has further modified NDWI to enhance the reflectance surface water bodies with the following formula $NDWI = \frac{(Green-NIR)}{(Green+NIR)}$. After this, many researchers were able to successfully delineate the surface water bodies from Landsat MSS, TM, and ETM+ imageries, using NDWI technique (McFeeters, 1996; Jain et al., 2005; Sethre et al., 2005; Xu, 2006;). Mapping of water bodies for different years using this technique will help in analyzing the water area changes.

In urban areas, lakes assume special importance in providing lung spaces, ambience, cooling, ground water recharge, habitat for various types of aqua flora and fauna (bio diversity), drinking water, bathing and washing, religious activities, cultural importance, tourism, recreation like boating, sailing, angling and fishing, giving rise to a lot of useful activities and livelihood for various people. Most important of all in the context of the present study, it provides flood mitigation during such an event. This kind of unplanned urbanization will result in the encroachment of surface water bodies. The decreased surface water bodies will induce water stagnation and urban flood. This makes it very important to study the surface water body degradation so that the corrective actions may be taken to sort out the issues. This paper presents the usefulness of NDWI technique in extracting surface water bodies using Landsat data. Applying this technique for data taken in different years will help in assessing the trend in areal extent of surface water bodies over the years.

Study area

Bengaluru is the IT capital of Southeast Asia. Due to the boom in the IT industry in the city, Bengaluru has grown by leaps and bounds in the last few decades. With the increase in the demand for urbanization, many of the agricultural lands and ecological features have been

NDWI images, a clear spectral enhancement of the water bodies can be seen, which is not so in the original image

converted into urban entities, which have made few areas of the city vulnerable to urban flooding. The areas close to the lakes that are subjected to urbanization are most vulnerable to water stagnation.

The city is located in the middle of the Mysore Plateau, a region of the larger Precambrian Deccan Plateau at an average height of 920 m (3,018 feet). 12.97° N 77.56° E is it's position. Bengaluru has a three valley system namely, Koramangala, Vrushabhavathy and Hebbal. The study area is so considered that it completely covers all the three valleys. It has no major rivers flowing in the district. The Arkavati River flows in the district for a small distance in the city's north taluk and the Dakshina Pinakini touches the borders of the district to the Northeast of the Anekal Taluk. Though there are no major rivers running through the city, it is blessed with many lakes.

There has been a growth of 632% in urban areas of Greater Bengaluru across 37 years (1973–2009). Encroachment of wetlands, flood-plains, etc., is causing a obstruction and loss of natural flood storage in the city. The number of water bodies reduced from 159 to 93. The lakes of the city have been largely encroached upon for urban infrastructure. As a result, in the heart of the city only 17 good lakes exist as against 51 healthy lakes in 1985.

The climate, affable local populace, availability of skilled man power in Bengaluru was conducive for urban development and today, the city sports a new label as Silicon Valley of India, having the unique distinction of producing the largest software professionals in the world. The growth of industries has seen a drastic increase in the population and the consequent pressure on the city's resources, including lakes.

City lakes

Bengaluru is also known as Lake City. Its surface water bodies have a phenomenal significance. The entire ecological balance is maintained by nature on the basis of this factor. Hence, any abnormality

will prove disastrous for the entire ecosystem. The lakes help in keeping monsoon waters for the drier periods of the year, canalize these important flows preventing water logging, inundation and erosion, and to ensure the refilling of groundwater. So the encroachment of lakes both legally and illegally is a major reason for water inundation in the city.

There have been many studies to assess the decline of lakes in Bengaluru city. Each study gives a different picture. According to Deepa, et al (1996), in 1973, there were 379 tanks in two taluks of Bengaluru urban district. Divided between them, 138 were located in the north taluk and 241 were located in south taluk. By 1996, they have come down to 96 in the former and 150 in the latter. This is a decline of 35.09% decline. A recent study shows that the areal

extent of the tanks, which was 2,342 ha in 1973, has reduced to 918 ha in 2007, which is a remarkable decline of 60.80%.

According to Karnataka State Pollution Control Board in 1960s, there were 262 lakes. Today it has declined to 81 out of which 34 has been recognized as live lakes. Satellite data collected by BMRDA in 2001 reveals that there are 2,789 tanks/ lakes in the BMRDA that are in different stages of decay, size varying from 2 hectares to 50 hectares and have a water spread area of 18,260.48 hectares.

There were 159 water bodies spread in an area of 2,003 ha in 1973, and this number has declined to 147 (1582 ha) in 1992, which further declined to 107 (1083 ha) in 2002, and finally, there are only 93 water bodies (both small and medium

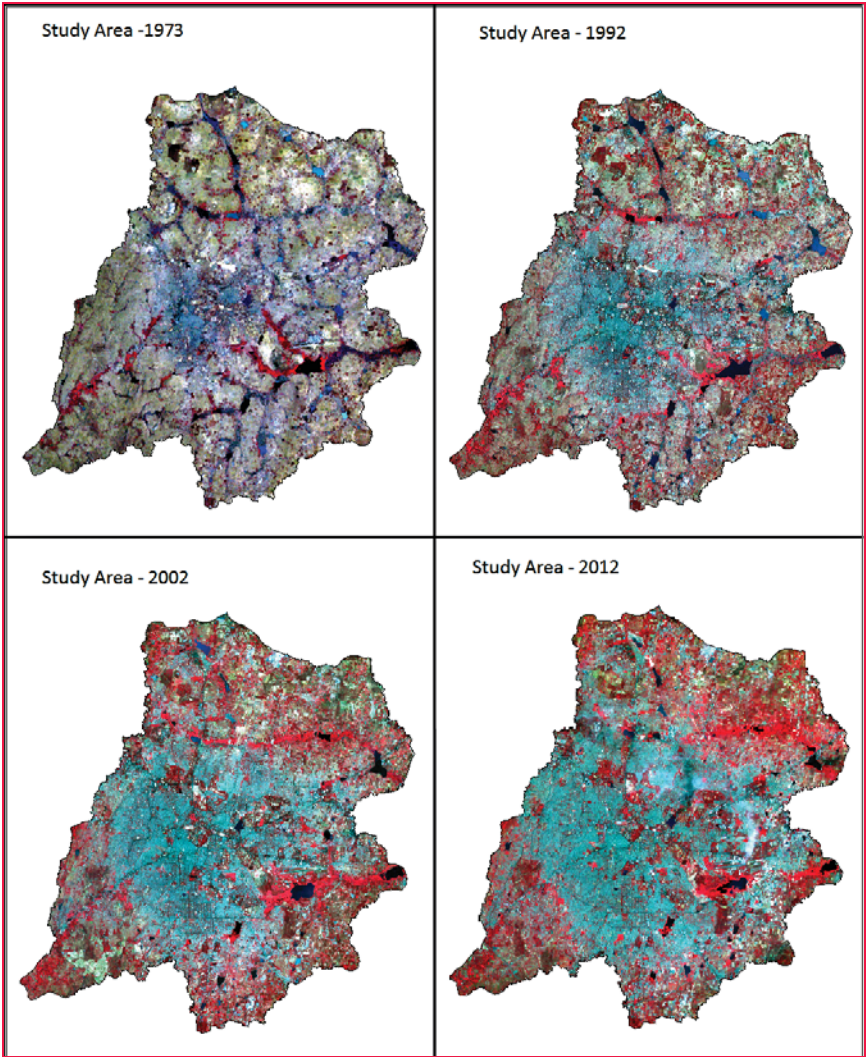


Figure 1: Landsat images of the study area for the years 1973, 1992, 2002 and 2012

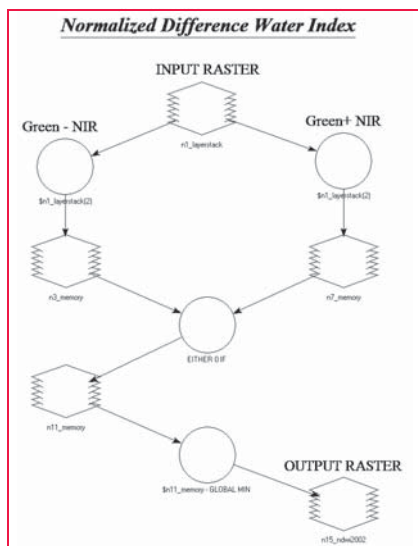


Figure 2: NDWI model created by modifying NDVI model in ERDAS 9.2., where 'layerstack' is the Landsat (TM) image for 2002 after layer stacking.

size) with an area of 918 ha in the Greater Bengaluru region in 2007 (Ramachandra T.V. and Uttam Kumar, 2008).

Apart from these, other studies and reports have also been reporting along similar lines. Though there are differences in the numbers and extents of the tanks/ lakes, all the studies accept one fact - there is a sharp decline in the number of lakes and extent of lakes in the city. All researches in this regard attribute this decline to rapid urbanization.

Disappearance of water bodies and a sharp decline in the number of water bodies in Bengaluru is mainly due to intense urbanization and urban sprawl. Many lakes were encroached for illegal buildings (54%). Field surveys (during July-August 2007) show that nearly 66% of lakes are sewage fed, 14% surrounded by slums and 72% showed loss of catchment area. Also, lake catchments were used as dumping yards for either municipal solid waste or building debris. (Ramachandra T.V. and Uttam Kumar, 2008).

Materials and methodology

Landsat MSS, TM, ETM+(SLC off) images were collected from the Landsat archive for the years 1972, 1992, 2002

Table1: Landsat bands and their spectral wavelengths

Bands	MSS (Landsat 1-3) Wavelength (micrometers)	MSS (Landsat 4-5) Wavelength (micrometers)	Landsat Thematic Mapper (TM) Wavelength (micrometers)	Landsat Enhanced Thematic Mapper Plus (ETM+) Wavelength (micrometers)
Band-1	NA	0.5 - 0.6	0.45-0.52	0.45-0.52
Band-2	NA	0.6 - 0.7	0.52-0.60	0.52-0.60
Band-3	NA	0.7 - 0.8	0.63-0.69	0.63-0.69
Band-4	0.5 - 0.6	0.8-1.1	0.76-0.90	0.77-0.90
Band-5	0.6 - 0.7	NA	1.55-1.75	1.55-1.75
Band-6	0.7 - 0.8	NA	10.40-12.50	10.40-12.50
Band-7	0.8-1.1	NA	2.08-2.35	2.09-2.35
Band-8	NA	NA	NA	0.52-0.90

and 2012 to carry out the intended work. Layer stacking for each image was done using ERDAS 9.2. De-striping of the Landsat data for 2012 was done with ENVI 4.5, using the technique developed by Scaramuzza, et al (2004). This is done because on May 31, 2003, the Landsat 7 Enhanced Thematic Mapper (ETM) sensor had a failure of the Scan Line Corrector (SLC). Since that time, all Landsat ETM images have had wedge-shaped gaps on both sides of each scene, resulting in approximately 22% of data loss. Figure 1 contains all the four images of the study area considered for the present study.

There is a ready NDVI model available in ERDAS 9.2. The same model was altered in model maker tool in ERDAS 9.2 to fit the NDWI formula $\frac{(Green-NIR)}{(Green+NIR)}$. The model is given in figure 2.

The model was run for each image. For every image while executing the model, there is a requirement to change the bands, number of bands and the wavelength of

those bands represent varies for MSS, TM and ETM+. The Landsat bands and their spectral wavelengths are given in table 1.

So for NDWI from Landsat MSS 1-3, band 5 and band 7 will be used whereas for Landsat ETM+, band 2 and band 4 will be used.

Figure 3 is the set of four images after NDWI model was run for all the images. When these images are compared with the original FCC images, a clear distinction between them can be made

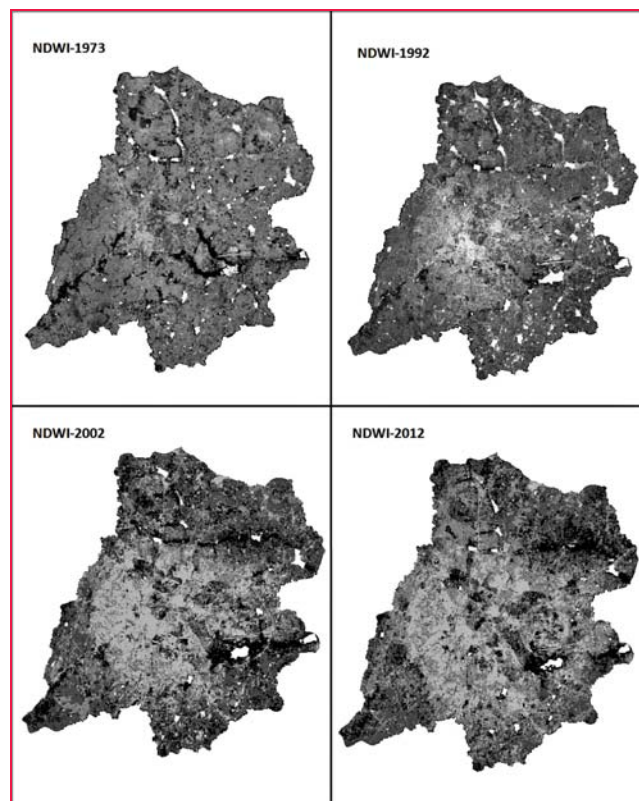


Figure 3: Images of study area after executing NDWI model for the years 1973, 1992, 2002 and 2012

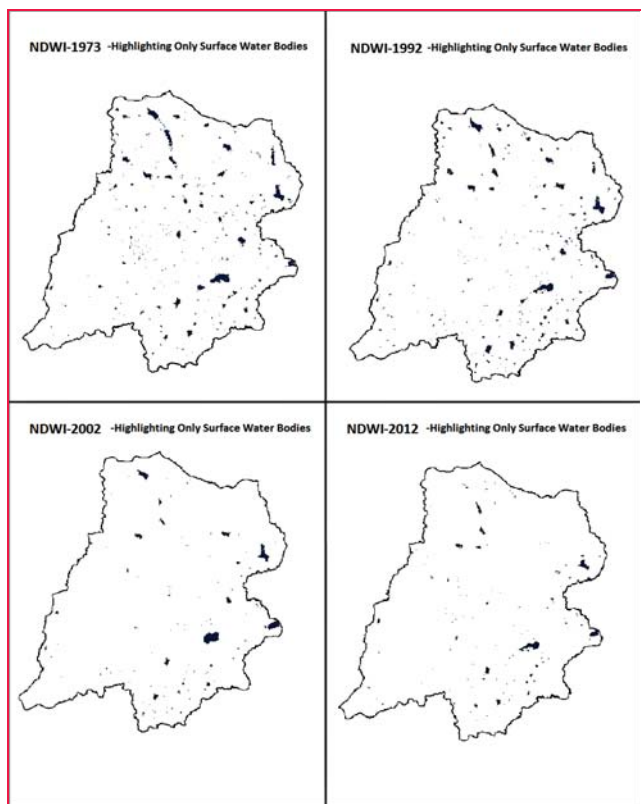


Figure 4: NDWI image after classification- highlighting only water bodies for years 1972, 1992, 2002 and 2012.

out. In NDWI images, a clear spectral enhancement of the water bodies can be seen, which is not so in the original image.

So the brightest portions those can be seen in the images are the water bodies in the study area. This image was then classified in ERDAS Imagine 9.2 using supervised classification technique. In the signature editor, the brightest features which represent surface water was considered as one class, and other classes were created as any other supervised classification. This classified image was then imported into ArcMap 9.2 and the display properties of this image theme was so changed that the class that represents water is set to blue and all other classes are assigned to no color. This makes the resultant images to have only surface water bodies and nothing else. The resulting image is given in Figure 4.

Results and discussions

The study shows the evident decline in the extent of surface water bodies in Bengaluru. The city now faces water

inundation problems even for relatively lower rainfall. Carrying out the same study, using high resolution images, can give much more detailed results. The results may vary depending on the season, as the NDWI operates on the reflectance values and not the elevation values. So it is suggested to use the images from the same season of different years to arrive at the result.

This study demonstrates the usefulness of NDWI technique for

monitoring the Declination of Surface Water Bodies. Especially in an urban area, where the surface water bodies act as storm water receivers, the decrease in the area of surface water bodies is alarming. RS and GIS techniques may effectively be used to monitor any such changes and take appropriate actions to restore the ecological balance or prevent such further occurrences.

This application of Remote Sensing and GIS in Hydrology is useful in many hydrological related studies. Apart from the current study, (i.e., flood risk assessment), this tool can be used in many other applications as well. As the model deals with spectral band combinations and not the elevation profile of the area, it will map any area containing water. Any hydrological feature like, lake, river, drainage, etc., can be mapped using this tool. Urban planning, Groundwater Prospects, Natural Resource Management, etc., are the few applications of this tool. This makes the tool widely used even after so many years since it was first used. The disadvantage of the model

is that it cannot be used to delineate the water bodies as the result of NDWI study is greatly influenced by different seasons.

References

- Deepa R.S, Ramachandra T.V., and Kiran R., 1996. Anthropogenic stress on wetlands of Bangalore. Bangalore: Centre for Ecological Science, Indian Institute of Science.
- Gao B., 1996. NDWI – A normalized difference water index for remote sensing of vegetation liquid water from space, *Remote Sensing of Environment*, 58(3):257–266.
- Jain, S.K, R.D. Singh, M.K. Jain, and A.K. Lohani, 2005. Delineation of flood-prone areas using remote sensing technique, *Water Resources Management*, 19(4):337–347.
- Ramachandra, T. V. and Uttam Kumar (2008), *Wetlands of greater Bangalore, India: automatic delineation through pattern classifiers*. *Electron. Green J.*, 2008, 1(26); <http://escholarship.org/uc/item/>
- Rousse, J.W., Haas, R.H., Schell, J.A., and Deering, D.W., *Monitoring Vegetation Systems in great Plain with ERTS*. In: *Proceedings of the Third ERTM Symposium*. US Government Printing Office, NASA Washington , DC, pp. 309-317
- Scaramuzza P, Micijevic E, Chander G (2004) SLC gap-filled products: phase one methodology. Available online at: http://landsat.usgs.gov/documents/SLC_Gap_Fill_Methodology.pdf , accessed on 15 July 2012
- Sethre, P.R., B.C. Rundquist, and P.E. Todhunter, 2005. Remote detection of prairie pothole ponds in the Devils Lake Basin, North Dakota, *GIScience and Remote Sensing*, 42(4):277–296.
- Xu, H., 2006. Modification of normalised difference water index(NDWI) to enhance open water features in remotely sensed imagery, *International Journal of Remote Sensing*, 27(14):3025–3033. ▴

On module framework of VieVS and data processing for teaching and research

VieVS is a new software for VLBI data processing, which has been a great help for research of Space Geodesy. Various solution modules and corresponding principles were introduced, steps were introduced for sake of experiment, and is may be helpful for teaching and research on VLBI data processing.



Erhu WEI
Professor, Ph.D, Ph.D
supervisor, School of
Geodesy and Geomatics,
Collaborative Innovation
Center for Geospatial
Technology, the

Key Laboratory of Geospace Environment
and Geodesy, Ministry of Education,
Wuhan University, Wuhan, China



Shenquan TANG
Master Candidate,
School of Geodesy and
Geomatics, Wuhan
University, Wuhan, China

VLBLI plays a unique role in the practical realization and maintenance of the International Celestial Reference Frame (ICRF) and International Terrestrial Reference Frame (ITRF), it is also the only technique which provides the full set of Earth Orientation Parameters (EOP)^[1]. Thus NGS format VLBI data processing is crucial. Previously, VLBI data processing software was mainly for OCCAM. However, duo to OCCAM being unable to adapt to the new international standards or update itself slowly, it now can't handle the current VLBI data. VieVS, a new software for VLBI data processing, was developed by Johannes Bohm, Schuh Harald of Geodesy and Geophysics Institute, Vienna University of Technology. VieVS is written in MATLAB language and it meets the IERS meeting that recommended the latest computing model. The latest version of VieVS is version 2.2.

- 1) The software is made fully consistent with the latest IERS Conventions (e.g., non-rotating origin and the corresponding partials for the nutation parameters).
- 2) It estimates the parameters as piece-wise linear offsets at integer hours, which makes the results more comparable with those from other space geodetic techniques like GNSS and SLR.
- 3) VieVS has GUI interface, the parameters can be set intuitively and MATLAB language makes VieVS more open. Users can modify corresponding code according to their needs.
- 4) VieVS has a 'batch' mechanism and select 'Save + Run' option in the user interface. You can perform batch processing of data without having to write your own 'batch' script, which greatly improves user productivity.
- 5) VieVS have a strong 'capacity expansion'. When the VLBI station or VLBI observations of radio sources change, you can create your own corresponding Superstation files and Supersource files to calculate, without waiting for software updates. VieVS also allows users to add external ionosphere and troposphere data files.

Main features of VieVS

Compared to OCCAM, VieVS in NGS format VLBI data processing has the following new features. These features make VieVS more competent in data processing tasks of VLBI.

VieVS module calculations and principles ^[3-6]

VieVS is composed of a plurality of modules. Fig. 1 shows the correlation between the VieVS each module, which also shows the whole of the operational flow of VieVS.

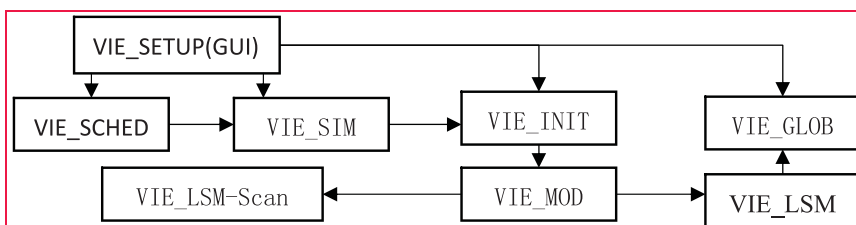


Figure 1: VieVS module framework

PENTAX

Scanning System S-3180V

3D laser measurement system



- + Integrated HDR camera allows combination of brilliant colours with high-resolution scan data
- + The fastest laser-scanner over 1 million points/second
- + Eyesafe laser class 1
- + IP53 dust & water resistance

TI Asahi Co., Ltd.

International Sales Department
4-3-4 Ueno Iwatsuki-Ku, Saitama-Shi
Saitama, 339-0073 Japan
Tel.: +81-48-793-0118
Fax: +81-48-793-0128
E-mail: International@tiasahi.com

www.pentaxsurveying.com/en/

Authorized Distributor in India

Lawrence & Mayo Pvt. Ltd.
274, Dr. Dadabhai Naoroji Rd.
Mumbai 400 001 India
Tel: +91 22 22 07 7440
Fax: +91 22 22 07 0048
E-mail: instmum@lawrenceandmayo.co.in

www.lawrenceandmayo.co.in

VIE_SETUP module

The purpose of this module is to provide a GUI interface for all computing modules of VieVS, allowing users to select the appropriate options and parameters. It reads Superstation.mat and Supersource.mat files, creates process_list.mat file for observation sequence which will be processed, and creates Runp.mat file to gather critical information of processing in WORK directory. It creates a parameter file for each processing sequence at DATA/LEVEL0 directory. E.g., 14AUG12XA_N004_parameter.mat, this means the treatment of NGS format observation sequence parameter file of August 12, 2014.

VIE_SCHED module

The first observation of a radio source known as a scan, scan length is calculated as follows:

$$scanlength = \left(\frac{1.75 \times SNR_{min}}{F_{obs}} \right)^2 \times \left(\frac{SEFD_1 * SEFD_2}{2 \times B \times N_{ch}} \right) + CORSSYNCH \quad (1)$$

F_{obs} is for the observed radio source strength, B is the bandwidth, N_{ch} is number of channels, CORSSYNCH for the extra time-related synchronization, SNR for the signal-to-noise, SEFD for the antenna sensitivity, it can be calculated by the following formula:

$$SEFD = \frac{2 \times k \times T_{sys}}{A_{eff} \times \eta \times 10^{-26}} \quad (2)$$

where k is Boltzmann's constant, T_{sys} for the system temperature, A_{eff} for the effective collecting area of the antenna and η is the processing factor. This module is used to monitor the effectiveness of the resulting scan, read the directory system files (.cat files) and local control file (.txt files). Among them, the directory system files include source.cat, flux.cat, antenna.cat, modes.cat, freq.cat, hdpos.cat, et al. The local control files include param.txt, down.txt, snrmin.txt, psource.txt, tagalong.txt, et al. For specifications of these files, please refer to the literature [5]. The NGS files of output are used to estimate the parameter, schedule file (.skd files) for real-time VLBI calculation, summary file for all aspects of the preliminary estimate of schedule, trf_sched.txt document for

solving the station location and crf_sched.txt file for solving radio source position.

VIE_SIM module

The three most important stochastic error sources in VLBI are zwd (troposphere zenith wet delay), station clock and measurement error. VIE_SIM module can be established for each epoch least-squares adjustment of the vector equation $o - c$ (observed value minus the calculated value), the vector $o - c$ is calculated as follows:

$$o - c = (zwd_2 \cdot mf(el_2) + clk_2) - (zwd_1 \cdot mf(el_1) + clk_1) + wn_{bst} \quad (3)$$

Where zwd_1 , zwd_2 respectively for troposphere zenith wet delay, $mf(el)$ is mapping function (elevation), clk is station clock, wn_{bst} for the white noise per baseline, $o - c$ produces artificial delay observation, favors testing new scheduling policy, the impact of the geometry of different network stations, antenna specifications and system effects. Read NGS format data and estimation parameters at DATA/TURB directory. Output scheduling test file, null file, application/omit valid documents which should be tested.

VIE_INIT module

This module reads data from observations NGS file, read the coordinates and velocity data from stations Superstation.mat file and read the radio source coordinates from Supersource.mat file. The outliers will be removed to a specified Outlier folder. These outliers include stations, radio sources, baselines; etc. Height cut-off angle will be introduced. Operation produces structural sequence of scan, antennas and radio sources. E.g. 14AUG12XA_N004_scan.mat, 14AUG12XA_N004_antenna.mat, and 14AUG12XA_N004_source.mat. These structural sequence files will be stored in DATA/LEVEL0 directory.

VIE_MOD module

According to the structure of the sequence generated by VIE_INIT, VIE_MOD module establishes a theoretical time delay and partial derivative, which is

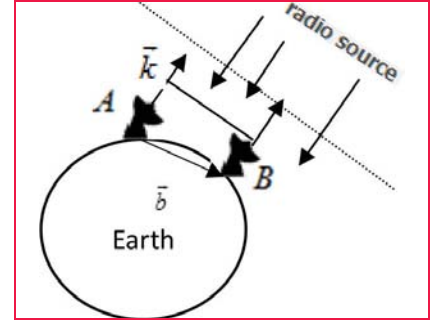


Figure 2: Schematic diagram of computing model.

the establishment of 'a priori model'. Computing model is as follows:

$$\tau = - \frac{\vec{b} \cdot \vec{k}}{c} \quad (4)$$

\vec{b} is for the linear vector between two VLBI stations and \vec{k} for a vector of station to the radio source. Figure 2 is a schematic diagram.

A calculation delay from VIE_MOD module minus observation delay is derived from NGS file, that will produce a vector of $o - c$. Adding delay information and partial derivative information structure sequence will output to DATA / LEVEL1 folder.

VIE_LSM module

VIE_LSM module uses the principle of least squares to estimate the corresponding parameters of the earth from VLBI observations, the adjustment of all parameters are based on PWLO (piecewise linear compensation). Principle is as follows:

$$N = \begin{bmatrix} A^T P A + H^T P_H H & C^T \\ C & 0 \end{bmatrix} \quad (5)$$

where A is for the design matrix of real observation equations, P for the weight matrix, $H = \begin{bmatrix} H(1,sm) & \dots & 0 \\ \vdots & \ddots & \vdots \\ 0 & \dots & H(15,sm) \end{bmatrix}$ for the design of pseudo-observation equations.

$$b = \begin{bmatrix} A^T P o c + H^T P_h o c h \\ b_c \end{bmatrix} \quad (6)$$

$$m_0 = (v^T P v + v_H^T P_H v_H) / (n_{obs} + n_{constr} - n_{unk}) \quad (7)$$

$x = N^{-1}b$, $K_x = m_0 N^{-1}$, x is a parameter vector and K_x for the variance-covariance matrix of the estimates.

After VIE_LSM calculation, 'clock break' can be corrected and some unusual observations can be surveyed.

PWLO estimates of VieVS are in a good agreement with those from other space geodetic techniques. VIE_LSM module provides SINEX input and datum free normal equations for global solutions in DATA/LEVEL2 directory. This will be used by VIE_GLOB for global solution.

VIE_GLOB module

VIE_GLOB module has the capability to estimate parameters that are common to all VLBI sessions from a so-called global solution. Reduction and stacking of parameters will be applied here. It is based on a division of the normal equation system into two parts. In the first part those parameters are concentrated, which will be kept in the global matrix, and in the second part parameters are ordered, which will be estimated only from a single session:

$$\begin{bmatrix} N_{11} & N_{12} \\ N_{21} & N_{22} \end{bmatrix} \cdot \begin{bmatrix} dx_1 \\ dx_2 \end{bmatrix} = \begin{bmatrix} b_1 \\ b_2 \end{bmatrix} \quad (8)$$

where dx_1 is the parameter of global solution and dx_2 is the parameter of reduction. dx_2 can be expressed as follows:

$$dx_2 = N_{22}^{-1} \cdot b_2 - N_{22}^{-1} N_{21} \cdot dx_1 \quad (9)$$

Take the equation (9) into the equation (8) and resolve it:

$$N_{11} \cdot dx_1 + N_{12} N_{22}^{-1} \cdot b_2 - N_{12} N_{22}^{-1} N_{21} \cdot dx_1 = b_1 \quad (10)$$

$$(N_{11} - N_{12} N_{22}^{-1} N_{21}) \cdot dx_1 = b_1 - N_{12} N_{22}^{-1} \cdot b_2 \quad (11)$$

Order equation (11) be $N_R \cdot dx_1 = b_R$, then:

$$dx_1 = N_R^{-1} \cdot b_R \quad (12)$$

Therefore, global solution parameters solver out, and result will be stored in globsol_TEST_LEVEL2.mat file at OUT/GLOB directory.

Steps of examples solution and attentions

In this paper, November 3, 2014 was a single day of XE VLBI data type NGS format solver for example. The 14NOV03XE_N004. NGS file was the input.

Examples solution

In the Scheduling menu parameter settings:

Select VLBI2010 for the station network, set 'session start' for November 3, 2014. Height cut-off angle, minimum angular distance and other parameters are set to default values. In the Simulation menu, select cont05_turb_04.dat for the analog parameter file, select slant wet delay, delay and white noise for the simulation parameters. In the Parameter menu, select vtrf2008 for the terrestrial reference frame Superstation file, select icrf2nonVcS for the celestial reference frame Supersource file, ephemeris chosen JPL_421, the mapping function is selected VMF1 type and the observed values of the Quality code limit constraint is set to a value greater than number 9, where it is set to 10.

In Run-> VieVS estimate settings, choose 'Run first solution', so that you can reduce the large clock error from the observed value and repair 'clock break' problem [7]. The new singular value files will be placed in the Outlier directory. Introduce NNT (Not Net Translation) and NNR (No Net Rotation), two state equations to the estimation of the station coordinate adjustment. Three conversion parameters and translation parameters between

GEO

BUSINESS 2015

BUSINESS DESIGN CENTRE LONDON • UK 27 – 28 MAY

www.GeoBusinessShow.com

REGISTER FREE*

Register online today at:
www.GeoBusinessShow.com

The geospatial event for everyone involved in the gathering, storing, processing and delivering of geospatial information.

Organised by:

diversified
COMMUNICATIONS • UK

In collaboration with:

agi

RICS

**THE SURVEY
ASSOCIATION**

**chartered
ices**

ice
Institution of Civil Engineers



GEO Business

@geobusinessshow

#geobiz

EMPOWERING GEOSPATIAL INDUSTRIES

*Exhibition and workshops are free to attend. Registration fee applies for the conference.

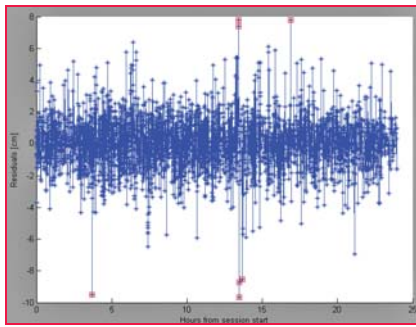


Figure 3: Observation sequence residual plot.

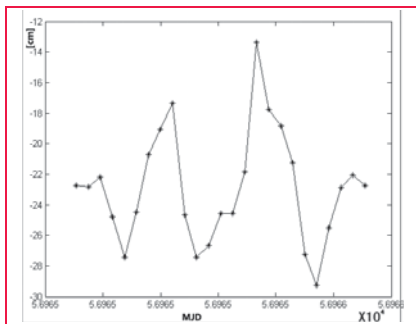


Figure 4: HART15M station pwclk parameter time series.

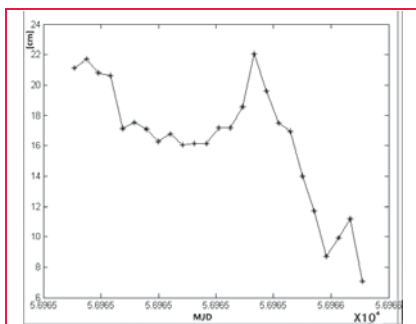


Figure 5: HART15M station zwd parameter time series

priors and adjusted value will be zero.

Figure 3 shows the observation sequence solver of residual plot. It can be seen from the figure in red epoch that the residuals are relatively large. But most are concentrated in the residuals between (-2-2) cm, indicating that the observed data is quite reliable.

Figure 4 and Figure 5 respectively show time series of pwclk (piece-wise linear clock) and zwd (zenith wet delay), two parameters of station HART15M at this observation sequence. Pwclk parameter is shown in Figure 4. It swings up and down in the value -22, fluctuations between the unit of 16. This shows that the clock error is swimming up and down, in line with the trend of white noise time series. Figure 5

Table 1: EOP parameters

EOP PARAMETER	PRIORS	ESTIMATES	STANDARD DEVIATION
XPO/mas	126.579	1.263501341e+2	1.14997e-1
YPO/mas	253.032	2.538387971e+2	1.60712e-1
UT/ms	-392.0232	-3.920217651e+2	4.30678e-3
NUT_X/mas	-0.167	-1.475946538e-1	2.58386e-2
NUT_Y/mas	-0.073	-1.540980496e-1	2.56947e-2

shows the zenith wet delay parameter time series and can be seen from the first drop of wet delay which rose rapidly. The last straight decline is consistent with the result of official online publication of IVS.

Table 1 shows the priori values and estimated values of the five parameters of EOP, and the corresponding standard deviation. As can be seen from the table, the difference between the priori values of the five parameters and estimated value is very small, less than 1mas. This shows that VieVS calculation accuracy is very good.

Attentions

- 1) Before running VieVS, you need to update the time-series of atmospheric non-tidal loading correction for station coordinates, the mapping function VMF1 file and EOP parameter file. Do ensure the latest VLBI data is calculated.
- 2) When you run VIE_SIM module, do not use any of the outlier documents to ensure quality code>9, which is very important for all the observed values for analog simulation.
- 3) If you cannot read the pressure and temperature data stations in the NGS file system, perform automatic calculation with GPT2 (Global Pressure and Temperature model 2) Data.

Conclusions

VieVS as a new VLBI data processing software, which has many new features. Its interface technology, the solver module 'scalability' and automatic 'batch' makes VLBI data processing become more simple and efficient.

This paper uses VieVS to solve NGS format data of VLBI. The numerical experiment shows its advantages and applicability. Its calculating results are consistent with IVS

posted results. It will bring some inspiration for the teaching and using of VieVS.

Acknowledgments

The authors would like to thank the Geodesy and Geophysics Institute of Vienna University of Technology for providing the software of VieVS and the IVS for providing the data. This research was funded by the national '863 Project' of China (No. 2008AA12Z308) and National Natural Science Foundation of China (No. 41374012).

References

- [1] Zhenghang LI, Erhu WEI, et al. Space Geodesy[M], WUHAN: WUHAN UNIVERSITY PRESS, 2010.
- [2] J. Böhm, S. Böhm, T. Nilsson, et al. The New Vienna VLBI Software VieVS [J]. Springer Berlin Heidelberg, 2012,136 (7):1007-1008
- [3] Yuanfei Li, Weiming Zhen. Software related data processing methods [J]. Annals of Shanghai Observatory, Chinese Academy of Sciences, 2004(5): 151-153
- [4] Niell A, et al. VLBI2010: Current and Future Requirements for Geodetic VLBI systems. IVS Memorandum 2006-008v01, 2006.
- [5] L Plank, J Böhm, H Schuh, et al. First steps of processing VLBI data of space probes with VieVS. http://www.hg.tuwien.ac.at/Bibl_Docs/Papers/2011/2011_EVGA_Plank_pa.pdf
- [6] Kikuchi F,et al. VLBI Observation of NarRow Bandwidth Signals from the Spacecraft[J].Earth Planets Space,2004,56:1041-1047
- [7] Spicakova, L. Plank, T. Nilsson, J. Bohm, and H. Schuh. Terrestrial reference frame solutions with the Vienna VLBI Software VieVS. In: Proceedings of the 20th EVGA Meeting in press (this volume), 2011. ▴

GEMNet project

Ordnance Survey is teaming up with the Satellite Applications Catapult, an independent technology and innovation company, on the GEMNet project to understand the nature and extent of interference on GNSS. GEMNet's primary objective is to discover the magnitude and characteristics of GNSS interference, and support UK industry in developing solutions to eliminate the effect of this interference on GNSS receivers. The project has several objectives including collating compelling and independent evidence of interference on GNSS receivers; developing an early understanding of the impact of interference on GNSS users and target industry organisations to join future phases of the project. The results gained will support industry and academic efforts to develop ways to combat threats for transport, critical infrastructure and many other applications.

India's first GIS Map-based real estate report

CommonFloor has come up with GIS Map-based real estate report which highlights key trends witnessed in Chennai real estate market in 2014. Titled "Real Insights 2014: Annual Realty Report," besides the usual analysis on property sizes and prices, the report also evaluates the overall rental market (rental yield), top localities based on user preference and fastest moving rental markets as per consumer demand, amongst others. Additionally, the report also highlights the key emerging trends that will shape realty market in 2015. www.commonfloor.com

Yotta Launches In-Cab Waste Management Solution

A new in-cab waste management system from Yotta is set to transform the delivery of refuse collection services. Mayrise In-Cab uses a vehicle mounted mini-PC to integrate with the Mayrise Waste back office system giving frontline staff access to the latest service and reference information. Utilising GPS, mobile and WiFi technology the Yotta solution

further supports crews in the field with real time messaging, reporting and event logging. The integrated mobile and back office system also allows office based staff to monitor the progress of crews in the field with their location and logged events displayed in real time against a map backdrop. www.yotta.co.uk

Man held for videography without permission in Varanasi, India

A navigation information service provider's employee had to spend a night in police lock up after he tried to collect data of city localities through videography recently. The employee had


failed to seek district administration's prior permission for the task.

According to reports, a car with three video cameras and other equipment was found moving on city roads. The car raised people's suspicion who immediately informed the police. Later, the police seized the car and arrested the person handling cameras and other equipment.

It was found that the person was working for 'mapmyindia', a company engaged in digital map data, navigation, tracking, GPS and GIS based systems integration services. It was later found that the company has license from the Government

ICAO Remotely Piloted Aircraft Systems (RPAS) Symposium
 ICAO Headquarters, Montréal, 23-25 March 2015


RPAS2015



Remotely piloted or piloted: sharing one aerospace system

ICAO's RPAS Symposium will provide a unique opportunity for States, international organizations, and stakeholders to identify how existing aviation rules need to evolve to meet the challenges inherent in welcoming the RPAS community and to examining the alignment between ongoing RPAS development and supporting regulatory provisions. The symposium will also showcase the opportunities created by

the integration of RPAS into the global civil aerospace system, and an industry exhibition will showcase the breadth of existing technologies and the thriving research and development activities currently underscoring this new sector of the aerospace industry. For programme and registration information please be sure to visit the ICAO website at: www.icao.int/meetings/rpas


ICAO
SAFETY

of India and other agencies concerned for data collection. He was later released. <http://timesofindia.indiatimes.com/>

Surat Municipal Corporation makes its Web GIS services public

Surat Municipal Corporation (SMC) from the state of Gujarat, India has launched a GIS portal for the public to gain access to Town Planning maps and to apply for development permissions for a plot or a property. This newly launched initiative is available to public at <http://gis.suratmunicipal.org/>. Users can register using a mobile number and a valid email address to access the services.

National Agency for Cadastre and Land Registration Romania to update its IT system

Teamnet International, the IT & GIS solutions provider has won a RON 43,03 million contract to update IT system of National Agency for Cadastre and Land Registration, Romania. The project that would be implemented over a timeframe of 15 months aims to strengthen integrated cadastre and land registry system to be compatible with INSPIRE Directive E-Terra3. *Mediafax*

Esri adds geodemographic information for 57 countries

Esri announced that geodemographic information for 57 additional countries has been added to its ready-to-use ArcGIS apps including Esri Business Analyst Online (BAO) and Esri Community Analyst. Up-to-date population, income, employment, and consumer spending information helps businesses—including retailers, real estate brokers, merchandisers, supply chain managers, and marketers—better understand local markets all around the world. The newly added countries include those in Latin America and Africa, bringing the total number of countries to 137. In addition, Canadian data has been updated to include 2014 updates, and Australia, France, Germany, and India now have advanced datasets and new reports including household, population, and summary data.


Yemen to launch digital agricultural, soil and water maps

President of the Agricultural Research Corporation of Yemen, Dr. Mansour Mohammed has announced that it will launch the agricultural map, soil and water maps of the Republic of Yemen during the current year 2015. He said that the launch of this map will bring in a significant economic boom to agricultural investment in general, and agriculture and food production in particular. The digital maps will cover the whole Yemeni territory with information on soil and plants, nature and the climate that will be a great tool to investors, decision-makers and local authorities who can obtain digital information for any area in the map easily. *althawranews.net*

Advanced data management capabilities to NGA by BAE

The National Geospatial-Intelligence Agency (NGA) has awarded BAE Systems the Information Store (iSToRE) contract to provide advanced data management capabilities to support the National System for Geospatial Intelligence (NSG). The iSToRE is the NSG's knowledge management solution that consolidates, stores, and archives geospatial intelligence products, making data easily accessible to multiple agencies and defense commands worldwide. *www.baesystems.com*

BMW and HERE's latest collaborations

BMW has announced the latest applications it has enabled with help of HERE related to maps, navigation and collaboration. The BMW i3 is equipped with cloud-based connectivity and a HERE app that synchronises digital devices such as a smartphone with the vehicle's navigation system. Right from planning trips over mobile or a PC to syncing those trips with the car navigation system, updating maps on the fly and sharing tips with family or friends - these are some of the new capabilities. The app further goes onestep ahead, and even can monitor the fuel levels. 

Robotic arms install remote-sensing instrument on ISS

Robotic flight controllers have successfully installed NASA's Cloud Aerosol Transport System (CATS) aboard the International Space Station. It is a LIDAR (Light Detection and Ranging), remote-sensing instrument designed to last from six months to three years. CATS will collect data about clouds, volcanic ash plumes and tiny airborne particles that can help improve our understanding of aerosol and cloud interactions, and improve the accuracy of climate change models. Ground controllers at NASA's Johnson Space Center in the US used one of the space station's robotic arms, called the Special Purpose Dexterous Manipulator, to extract the instrument from the capsule.

The NASA-controlled arm then passed the instrument to a second robotic arm called the Japanese Experiment Module Remote Manipulator System, is controlled by the Japanese Aerospace Exploration Agency. It installed the instrument on the ISS' Japanese Experiment Module, making CATS the first NASA-developed payload to fly on the Japanese module. CATS is currently sending health and status data back to NASA's Goddard Space Flight Center in Greenbelt, Maryland, where the instrument's data would be analysed. *www.business-standard.com/*

FAA allows first real estate company to use drones for aerial photography

Douglas Trudeau of Tierra Antigua Realty in Tucson, Ariz., has become the first real estate agent who can legally use a drone for real estate photography. Trudeau, the FAA announced, is authorized "to fly a Phantom 2 Vision+ quadcopter to enhance academic community awareness and augment real estate listing videos." The Vision+ is currently the top-of-the-line model in DJI's lineup of consumer drones.

In addition, the FAA also granted another exception to Advanced Aviation Solutions in Spokane, Wash., which will use a fixed-wing eBee AG drone from senseFly for monitoring crops. Tierra Antigua and Advanced Aviation Solutions can't just

take their drones for a spin, however. In addition to the pilot, there also has to be an observer around. The pilot also needs to have “an FAA Private Pilot certificate and a current medical certificate, and the UAS must remain within line of sight at all times. <http://techcrunch.com/>

NRSC's Bhuvan to go live soon

Floods in the Uttarakhand state of India gave the National Remote Sensing Centre (NRSC) 24,000 photographs, uploaded in real time from across the disaster zone by affected people, helping ultimately in directing relief operations. In October last year, the NRSC also used an Android app and crowd-sourced over 3,000 photographs of Cyclone Hudhud, helping the Andhra Pradesh government assess the damage.

Bhuvan, the NRSC's pet project, is a crowd-sourced medium where the centre asks people to upload photographs, with time and location, on the web. The NRSC then uses remote sensing

technology to spot the location and use the resource. The mobile app-based platform assembles all photographs under the weblink <http://www.bhuvan.nrsc.gov.in> <http://indianexpress.com/>

Drones to keep an eye on Noida

Noida police in India is all set to use a remote-controlled aerial camera to keep a vigil on traffic and potential law-breakers in the city. They have prepared the proposal too. The drones under consideration are those equipped with infra-red and other systems to enable the cops to 'see' even at night. <http://timesofindia.indiatimes.com/>

NASA's SMAP instrument

NASA is set to launch Soil Moisture Active Passive (SMAP) satellite as part of the ESSP (Earth System Science Pathfinder) program. The overall objective of SMAP is to monitor global soil moisture mapping with unprecedented resolution, sensitivity, area coverage, and revisit times of 3 days or less.

The radiometer provides more accurate soil moisture but a coarse resolution of about 40 kilometers [25 miles] across,” said JPL's Eni Njoku, a research scientist with SMAP. “With the radar, you can create very high resolution, but it's less accurate. To get both an accurate and a high-resolution measurement, we process the two signals together. The instrument's three main parts are a radar, a radiometer and the largest rotating mesh antenna ever deployed in space. *NASA Jet Propulsion Lab*

Pix4D Version 1.3, provides GPU support

Pix4Dmapper V1.3 update features NVIDIA GPU support for faster processing. For initial processing, GPU support will improve processing speed from 10% to 75%, depending on image content and project size. Other feature update includes support for creates a full 3D textured mesh that can be exported in OBJ and PLY format and be used for Fly-through animations. ▽

POWER AND PRECISION AT YOUR FINGERTIPS

EZSURV® POST-PROCESSING SOFTWARE PROVIDES YOU WITH:

- ▶ Access to more than 8,000 CORS stations data all around the world
- ▶ Support multiple receiver native data format
- ▶ State-of-the-art processing engine
- ▶ Easy-to-use application
- ▶ Flexible licensing mechanism
- ▶ White Label version available for manufacturers

U.S. Army interested in eLoran PNT

The United States Army is soliciting information for eLoran receivers for the warfighter, either stand-alone or integrated with GPS. The Jan 14 Request for Information (RFI) provides an outline for the potential use of the receivers in Army and other Department of Defense maritime, aviation, or vehicular platforms and for position and timing purposes. Primary technical areas the Army is interested in include the receiver specifications; its use for maritime, aviation, vehicles, and timing; SWaP-C considerations for an integrated GPS and eLoran receiver; potential benefits of one-way messaging capabilities using the eLORAN data channel; signal tracking where GPS is unavailable (indoors, under water, in urban environments); and how quickly a demonstration could be held.

Lobbyist behind anti-Russian tactic to derail Glonass

© Sputnik/ Alexandr Kryazhev US lobbyist is behind a campaign to derail a proposal being considered by the US government's main communications agency to use Russian satellites to help first responders more accurately locate 911 calls from cell phones, the director of government affairs for the National Emergency Number Association Trey Forgety told Sputnik. Under the US Federal Communications Commission's (FCC) proposal, Russia's GLONASS satellite system would be added to the US satellite GPS system to double the coverage of satellites, thereby increasing the probability and accuracy of finding someone making a 911 call. <http://sputniknews.com>

Welch backs legislation on GPS data

Rep. Peter Welch, joined by Sen. Ron Wyden (D-OR), Sen. Mark Kirk (R-IL), Rep. Jason Chaffetz (R-UT) and Jon Conyers Jr. (D-MI), reintroduced the Geolocation Privacy and Surveillance Act (GPS Act). The legislation creates clear rules about when law enforcement agencies can access and track Americans' electronic location data.

"Cell phones are in the pockets and purses of most Americans," said Welch. "While

tracking technology has transformed our lives in many positive ways, it also poses a risk to privacy through potential misuse of tracking data. The time has come to modernize our statutes to reflect the technology of our age. This bipartisan legislation protects Americans' right to privacy while ensuring law enforcement officials are able to do their important jobs."

Courts have issued conflicting opinions about whether the government needs a warrant to track Americans through their cell phones and other GPS devices. The Supreme Court unanimously ruled in 2012's U.S. vs. Jones case that attaching a GPS tracking device to a vehicle requires a warrant, but it did not address other digital location tracking, including through cell phones, OnStar systems and consumer electronics devices.

The GPS Act applies to all domestic law enforcement acquisitions of the geolocation information of individual Americans without their knowledge, including acquisitions from private companies and direct acquisitions through the use of 'Stingrays' and other devices. It would also combat high-tech stalking by creating criminal penalties for surreptitiously using an electronic device to track a person's movements, and it would prohibit commercial service providers from sharing customers' geolocation information with outside entities without customer consent. <https://vtdigger.org/>

GPS trackers could help ease prison overcrowding

The Judiciary of Guam is hoping to test a program that would put GPS tracking on a handful of pretrial detainees. If successful, it could be one way to ease the ever-growing population at the Department of Corrections. In a recent report, the Office of Public Accountability attributed overpopulation to the high number of pretrial detainees who are confined awaiting their day in court. The report suggested that alternatives to confinement could be a significant step in reducing the strain of overpopulation. One possible alternative is GPS monitoring. www.guampdn.com

Russian airline approved for GNSS Landings

Russia's S7 Airlines has received approval for three Boeing 737-800s to perform landings using GNSS, becoming the country's first carrier to do so, reports Air Transport World. More than 50 airports in Russia have installed equipment allowing global positioning landings (GLS). Russia's State Air Transport Management Corp. plans to certify 10-15 airports per year for GLS landing.

Glonass Company set up by Russian Government

Russian President Vladimir Putin in July 2014 ordered the government to develop and adopt a roadmap for the creation of an open joint-stock company "GLONASS" with 100-percent state participation. According to the plan, the property complex of the state automated information system "ERA-GLONASS" will be transferred to the share capital of the newly created company. Deputy Prime Minister Dmitry Rogozin in September welcomed the establishment of the company, calling it a first step in the commercialization of space-based services.

Beidou system sees slow expansion

Beidou Navigation Satellite System has been in service for two years but the adoption of the system has been slow. With a positioning accuracy of 10 meters, a velocity accuracy of 0.2 meters per second and a timing accuracy of 10 nanoseconds, Beidou has become the third major navigation system in the world. Beidou uses both satellites and ground-based facilities to improve its accuracy. Beidou has been adopted in key areas concerning China's national security, such as transportation, weather, agriculture and land management, as well as in foreign countries, including Thailand and Myanmar. Despite the Chinese government's plan to install the Beidou system on chartered vehicles, buses and trucks carrying dangerous materials in eight provinces, Tianjin and the Pearl River Delta between 2014 and 2015 but the actual implementation has been less than ideal. www.wantchinatimes.com

Where is your vehicle? your package? your machine? **Find it with TraceME!**

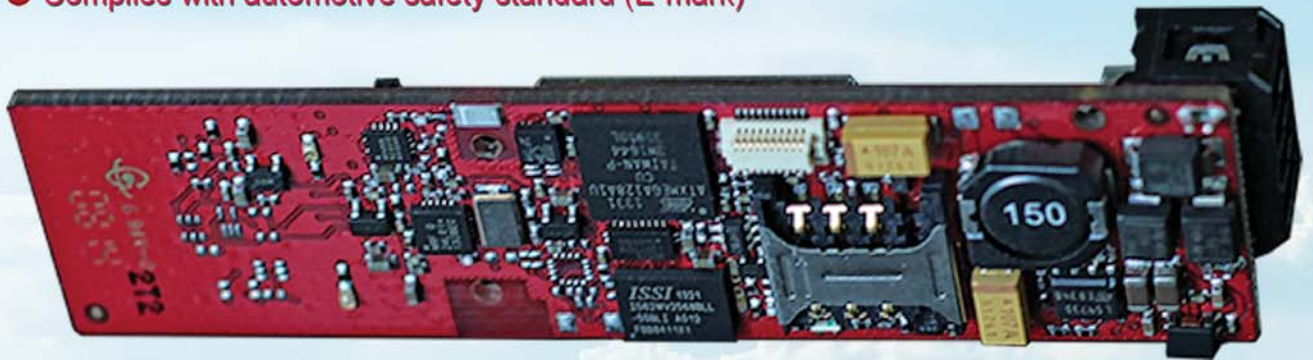
Introducing the new TM-203

The TM-203 is the newest addition to our family of TraceME products.



Unique features:

- Very small fully-featured GPS Tracker (87 x 22 x 7 mm)
- Weighs only 15.5 grams, including GPS, GSM and RF antennas
- Advanced power saving, down to 3uA
- Location-based positioning (LBS) inside buildings
- Portable or externally connectable to integrate multiple sensors
- On-board sensors for compass, temperature and acceleration
- Worldwide coverage: Quad-band GSM/GPRS • Glonass/GPS • Wifi
- Complies with additional standards for insurance benefits (e.g. SCM and Incert)
- Complies with automotive safety standard (E-mark)



We would like to invite you to have a look around our website and get inspired by the possibilities of what KCS TraceME products can bring to your project. Whether you need a solution for personal tracking, trace and control vehicles, object protection or more advanced M2M solutions, KCS TraceME can deliver it.

GPS/GPRS enabled GPS Tracker with advanced I/O. This will allow you to remotely track & trace and/or control a huge diversity of objects, machines and/or vehicles. KCS TraceME is absolutely the most versatile and adaptive Track-n-Trace solution in the market today. Our clients use the TraceME hardware for the most diverse tasks. It is truly an all-round performer and exceeds anything in the market currently available.

- KCS TraceME is available in different form factors (Key fob, OEM., Aluminum & custom made casing);
- GPRS, UMTS, SMS, GSM, Wi-Fi, RFID, E-mail;
- Fully configurable administration tool;
- Event driven, can run custom code, remotely configurable;
- Connect M2M to any device;
- G-shock detection, temperatures, tilt, motion, iButtons, mobile phones, camera's;
- See the rest of the site for the full options!

Please contact us if you want to discuss your ideas!

OEM & Distributor requests are welcome!

www.Trace.ME

All trademarks mentioned herein belong to their respective owners.

DAT/EM Systems releases 7.1

DAT/EM Systems International® released the 7.1 edition of DAT/EM software products including Summit Evolution™, Landscape™, Capture™, MapEditor™, Ortho+Mosaic™, Airfield3D™ and Contour Creator™. The advancements in the 7.1 DAT/EM Photogrammetric Suite represent the latest evolution in technology and are based on customer input and growth within the geospatial industry. datem.com/release7-1

FARO launches FARO Scanner Freestyle^{3D}

FARO Scanner Freestyle^{3D} is an easy, intuitive device for use in Architecture, Engineering and Construction (AEC), Law Enforcement, and other industries. It is equipped with a Microsoft Surface™ tablet and offers unprecedented real-time visualization by allowing the user to view point cloud data as it is captured. It scans to a distance of up to three (3) meters and captures up to 88K points per second with accuracy better than 1.5mm. The patent-pending, self-compensating optical system also allows users to start scanning immediately with no warm up time required. www.faro.com/Scanner/in

Standards work to begin by RTCA on new GNSS-related aviation devices

The RTCA, a nonprofit association that supports and coordinates volunteers developing consensus-based standards, does its work via a large number of committees. Special Committee 159 (SC-159), which will handle the standards for the new receivers, focuses on equipment that uses the GPS.

The Federal Aviation Administration (FAA) asked RTCA last year to develop minimum operational performance standards (MOPS) for a higher quality inertial reference system (IRU)-like device based on an attitude and heading reference system (AHRS). This standard would use integrated GNSS inputs for corrections and alignment. Equipment based on these standards would give aircraft self-contained capability to coast through areas

with GNSS interference without relying on ground-based navigation systems. Such equipment would enhance the aircraft's navigation robustness, improve area navigation (RNAV) operations during GNSS disruptions, and reduce the FAA's costs to maintain ground infrastructure.

Multi-GNSS receiver module for wearables

SkyTraq Technology has introduced a stand-alone multi-GNSS receiver module in a compact 7 x 7 millimeter form factor, the Venus828F, designed with a sensor hub function for wearable and "Internet of Things" (IoT) applications. It is capable of communication with multiple satellite systems and tracking up to 28 satellites concurrently. The compact LGA module integrates all the necessary components for wearables and IoT, forming a complete working GNSS receiver, including GNSS chipset, 0.5ppm TCXO, Flash memory, LDO regulator, DC/DC switching regulator, and passive components. It only requires external antenna and power supply to output accurate position, velocity, and time

GPS sport watches in India by TomTom

TomTom, has forayed into the India wearable market with a range of GPS-enabled sport watches. The range, which includes four smart watches delivers real-time information like time, distance, heart rate, pace, speed and calories burnt to runners, cyclists and swimmers. <http://www.thehindu.com>

FOIF offers A50 GNSS survey receiver

Chinese company FOIF is offering a new survey receiver, the A50. With the A50, the company is focused on developing a smart design for a receiver to make it lightweight, yet powerful, making it easy to use for fieldwork. Besides Bluetooth, wireless radio, and mobile network (2G and 3G), Wi-Fi feature was added to broaden data communications for GNSS. The A50 is designed to provide excellent performance, with a high-sensitivity GNSS module. It not only

Trimble News

Trimble® TerraFlex™ Advanced

An enhanced edition of its TerraFlex field data capture software, which manages asset collection and update activities for everyday geospatial requirements. Organizations across a variety of industries, including environmental management, utilities and government agencies, can deploy a common workflow for field workers to collect or inspect their assets efficiently using TerraFlex Advanced.

Trimble® Rapid Positioning System

A simplified layout solution for building construction professionals. It includes the Trimble RPT600 Layout Station to layout points and capture as-built measurements and Trimble Field Link 2D software running on a performance tablet to control the layout station.

Timing Portfolio for Mobile Telecom

Trimble has introduced a new portfolio of GNSS-based time and frequency products to address the synchronization needs of the fast-growing 4G LTE (Long Term Evolution) small-cell telecom market. Trimble timing solutions provide increased holdover capabilities and more robust signals with multi-constellation GNSS technology with which to sync wireless networks efficiently. The new product line-up includes: The Mini-T GG Disciplined Clock, The Trimble 360 multi-GNSS receiver, The surface mount ICM SMT 360 timing module.

Coillte Selects Trimble Forestry

Ireland's state-owned forest company, Coillte, will implement Trimble's Forestry Logistics solution to provide central dispatch management services for its timber deliveries across Ireland. Coillte has begun a comprehensive redesign of its business-operating model. A key result of the redesign process was the decision to implement central dispatch systems and services. Trimble was selected for its field-proven forestry logistics and log truck dispatching, and in particular, Trimble's experience in supporting the transition to a more optimal timber delivery process, part of Trimble's Connected Forest strategy.

has sophisticated onboard software, but also optional application programs such as FOIF FieldGenius and Carlson SurvCE, providing multiple field solutions.

US Army Corps of Engineers Selects SimActive for Drones

SimActive, a developer of photogrammetry software, has been selected by the United States Army Corps of Engineers (USACE). They join professionals across the globe using Correlator3D™ with UAV imagery.

“Military organizations have been instrumental to our products’ development since inception”, said Dr Philippe Simard, President of SimActive. “It is a milestone for us to welcome the USACE as users of Correlator3D™.”

GPS to Track Antarctica's Ice Migration in Real Time

Antarctica's melting ice sheets have been a major contributor to global sea level increases over the last decade, and the

losses are expected to accelerate over the next two centuries. But researchers attempting to study the rate at which these sheets move and melt have been hamstrung by conventional monitoring methods. That's why a team from the UBL's Laboratoire de Glaciologie has gone ahead and connected one such ice sheet to the Internet of Things.

To obtain a more accurate and timely understanding of the situation, researchers from the UBL have installed a series of GPS sensors and phase-sensitive radar along the Roi Baudouin ice shelf in Dronning Maud Land, East Antarctica. These devices will monitor the sheet's shifts in real-time, providing climatologists with daily, not weekly, updates. *Gizmodo*

Clock modules get timing from GPS, GLONASS and BeiDou

NEO-M8T and LEA-M8T are precision timing modules from u-blox, that work concurrently from GPS, GLONASS and BeiDou, and are Galileo-ready. Accuracy is said to be within 20ns

and the receivers autonomously cold start on a -148dBm signal or, when aided (see below), -157dBm (GPS and GLONASS, or 151dBm for GPS and BeiDou). 12.2 x 16.0mm NEO-M8T is intended for applications such as geophones used for seismic field measurements. LEA-M8T is 17.0 x 22.4mm. www.electronicweekly.com

MegaFon, MTS start joint Parental Control location service

Russian mobile operators MTS and MegaFon have completed the integration of their location services for retail subscribers. Location using their Parental Control services is now available on both networks, using LBS. MTS subscribers are able to use the service via SMS, a dedicated website, or using a mobile application for Android and iOS-powered devices. MegaFon customers can access the service over SMS, the USSD menu, a dedicated website, or via a mobile app for Android-powered mobile devices. www.telecompaper.com ▴



European
Navigation
Conference

2015

Technology - Innovation - Business

Centre de Congrès Cité Mondiale
Bordeaux - France



07 – 10 April 2015

CONFERENCE TOPICS

The 2015 ENC conference will be hosted by the Institut Français de Navigation (IFN) and TOPOS Aquitaine and will be held April 7 through 10 at Centre de Congrès Cité mondiale in Bordeaux, France.

Five good reasons to be there:

- Organized under the auspices of the European Group of Institutes of Navigation (EUGIN)
- High-level scientific activities highlighted during the conference
- Meet all key players in the navigation area and be informed about latest developments in navigation, positioning systems and techniques
- Topics covering a wide range of applications to meet evolving needs across ever-more diverse uses (drones, in-door navigation, etc.)
- Highlighting the resilience and robustness of user equipment which are necessary to prevent end-users from vulnerability

A plenary session will be held to inform the community of the status of the major GNSS programs, including a special focus on Galileo that will be facing early-phase challenges. Several parallel sessions will cover up-to-date topics in navigation.

Registration for the conference is possible as from 1 September 2014 via the conference website.

ABOUT BORDEAUX

Bordeaux is the world's capital of wine and a UNESCO World Heritage Site since 2007. The city is an 18th century architectural gem and counts up to 350 historic monuments.

Bordeaux and the Aquitaine region are long-time and sustainable investors in the space industry and are the co-host of "Aerospace Valley", the international cluster for competitiveness. Aquitaine is a leading region for per capita R&D investment and develops the potential for innovation of start-ups in avionics, space, composite and photonics sectors. Bordeaux is also welcoming the largest inertial confinement fusion experiment in Europe called Laser Mégajoule.

More information : <http://www.enc2015.eu>

For any further details, please contact the conference secretariat at conference.secretariat@enc2015.eu



SUBSCRIPTION FORM

YES! I want my **Coordinates**

I would like to subscribe for (tick one)

☐ 1 year ☐ 2 years ☐ 3 years

12 issues 24 issues 36 issues

Rs.1200/US\$80 Rs.2100/US\$145 Rs.2700/US\$180

**SUPER
saver**

First name

Last name

Designation

Organization

Address

City Pincode

State Country

Phone

Fax

Email

I enclose cheque no.

drawn on

date towards subscription

charges for Coordinates magazine

in favour of 'Coordinates Media Pvt. Ltd.'

Sign Date

Mail this form with payment to:

Coordinates

A 002, Mansara Apartments

C 9, Vasundhara Enclave

Delhi 110 096, India.

If you'd like an invoice before sending your payment, you may either send us this completed subscription form or send us a request for an invoice at iwant@mycoordinates.org

MARK YOUR CALENDAR

March 2015

AUVSI's Unmanned Systems Europe

3 - 4 March 2015

Brussels, Belgium

<http://www.auvsi.org/UnmannedSystemsEurope/Home/>

Locate15

Brisbane, Australia

10 - 12 March

www.locateconference.com

Remotely Piloted Aircraft Systems Symposium

23 to 25 March 2015

Montréal, Canada

<http://www.icao.int/meetings/rpas/>

Munich Satellite Navigation Summit 2015

24 - 26 March

Munich, Germany

www.munich-satellite-navigation-summit.org

April 2015

European Navigation Conference 2015

7 - 10 April

Bordeaux, France

<http://enc-gnss2015.com/>

The World Cadastre Summit, Congress & Exhibition

20-25 April

Istanbul, Turkey

<http://wcadastre.org/page/45-en-home>

Interexpo GEO-Siberia-2015: Open-Source Geospatial Solutions for Public Benefits

20 - 22 April

Novosibirsk, Russia

http://expo-geo.ru/event/4-Interekspo_GEO-SIBIR/

2015 Pacific PNT Conference

20 - 23 April

Honolulu, HI United States

www.ion.org/

The 9th International Forum on Satellite Navigation & NAVITECH-2015 exhibiton

April 22-23

Moscow, Russia

<http://www.glonass-forum.com/>

May 2015

AUVSI's Unmanned Systems 2015

4-7 May

Atlanta, USA

<http://www.auvsi.org/>

RIEGL LiDAR 2015 Conferences

5 - 8 May

Hong Kong and Guangzhou, China

www.riegllidar.com/

MundoGeo Connect

May 5 to 7, 2015

Sao Paulo - Brazil

<http://mundogeoconnect.com/2015/en/>

Baska GNSS Conference 2015

10 - 12 May

Baska, Krk Island, Croatia

www.baskagnssconference.org

36th International Symposium on Remote Sensing of Environment

11-15 May

Berlin, Germany

<http://www.isrse36.org>

FIG Working Week and General Assembly

Sofia, Bulgaria

17 - 21 May

www.figure.net

GEO Business 2015

27 - 28 May

London, UK

<http://geobusinessshow.com/>

June 2015

HxGN LIVE Las Vegas 2015

1 - 4 June

Las Vegas, Nevada USA

<http://hxgnlive.com/las.htm>

TransNav 2015

17 - 19 June

Gdynia, Poland

<http://transnav2015.am.gdynia.pl>

Advancing Geographic Information Science: The Past and Next Twenty Years

College of the Atlantic, Bar

Harbor, Maine, USA

June 29 - July 3

<http://giscienceconferences.org/vespucci2015week2/>

July 2015

GI_Forum 2015

July 7 - 10

Salzburg, Austria

www.gi-forum.org

IGNSS 2015

14-16 July

Queensland, Australia

www.ignss.org

13th South East Asian Survey Congress

28 - 31 July, Singapore

www.seasc2015.org.sg

August 2015

UAV-g 2015

30 August - 2 September

Toronto, Canada

www.uav-g-2015.ca

September 2015

ION GNSS+

14-18 September

Tampa, Florida, USA

www.ion.org

INTERGEO 2015

15 - 17 September

Stuttgart, Germany

www.intergeo.de/intergeo-en/



Unlock Your Full Potential

- Built on IntelliCAD® 8
- 64-bit and 32-bit versions
- Improved performance
- DWG 2013 support (AutoCAD® 2013, 2014, 2015)
- Layer states and filters
- Quick-select
- Adaptive grid
- New 3D orbit commands
- Dynamic licensing
- AutoMAP plotted descriptions
- AutoMAP substitution codes
- Google Earth™ KML export
- Leica codelists & ghost points
- Line/curve/tie table selections
- COGO bearing rotation display
- Draw cluster error vectors
- More .xyz point cloud formats

MicroSurvey CAD 2015 is now available, and you owe it to yourself to try it!

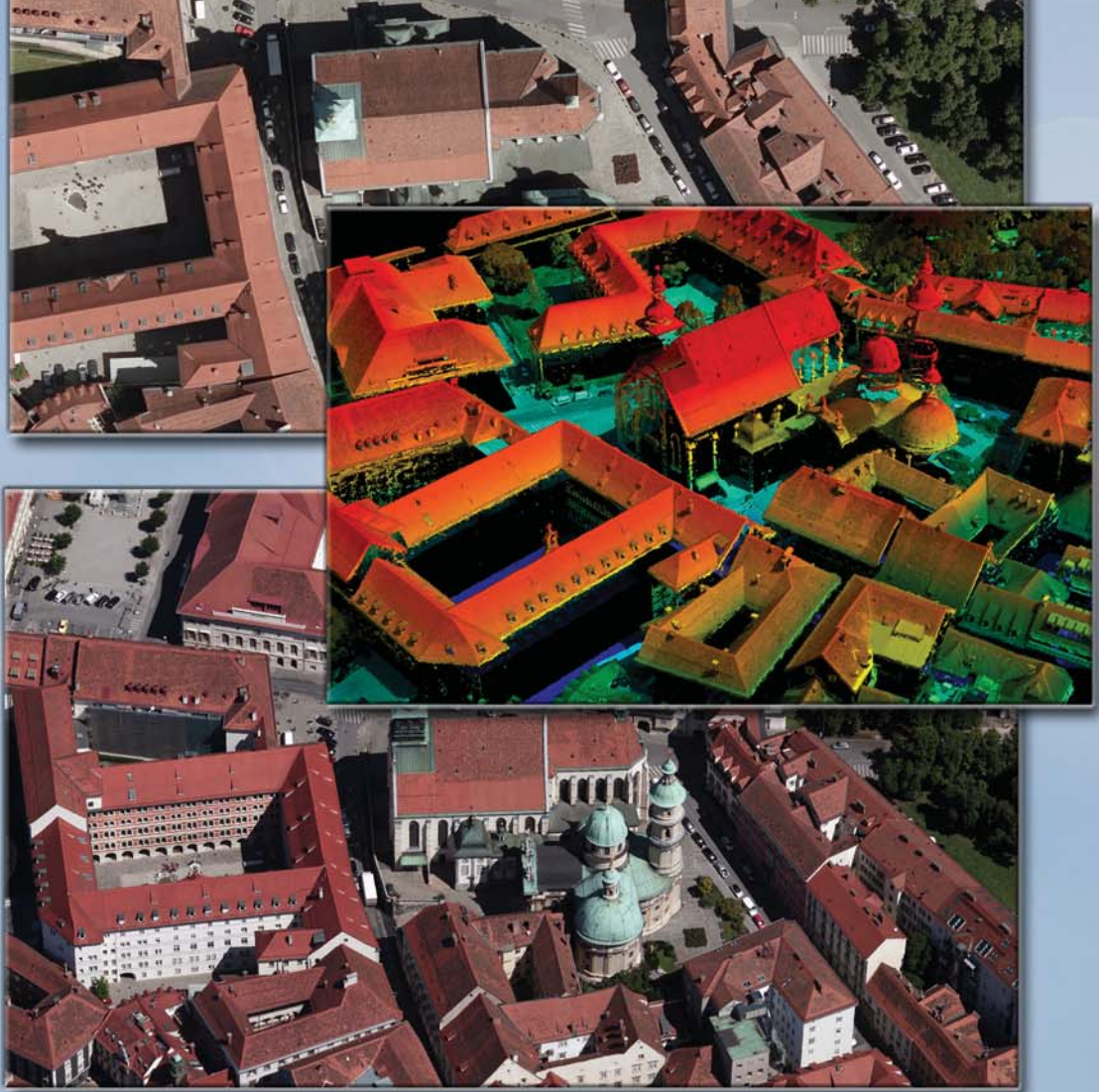
Unlock the full potential of your workstation with the 64-bit version of MicroSurvey CAD. Harness the power and capabilities of the integrated IntelliCAD 8 engine, and experience faster drafting and calculation operations while working with larger drawings, more points, and an overall more powerful MicroSurvey CAD than ever before.

Download a free demo from our website: www.microsurvey.com



© MicroSurvey is registered in the U.S. Patent and Trademark Office by MicroSurvey Software Inc. MicroSurvey is part of Hexagon.
Google Earth is a trademark of Google Inc.
AutoCAD is a registered trademark of Autodesk, Inc., in the USA and other countries.

We have you covered



from all angles.

Need a large format camera system for low-altitude, corridor missions? High-altitude ortho collections? Something in between?

Need to be able to collect oblique imagery? How about oblique and nadir imagery in panchromatic, color and near-infrared all in the same pass?

Need a software system that will allow you to take that aerial imagery and create point clouds in LAS format, digital surface models, and orthomosaics? **No problem.**

The UltraCam series of large format photogrammetric digital aerial sensors includes systems of varying image footprints and focal lengths. Whether you need multi-spectral nadir imagery or obliques—or both from the same camera—we have a system for you.

Meanwhile, our highly automated UltraMap photogrammetric workflow software enables you to process UltraCam data to Level 3, radiometrically corrected and color-balanced imagery, high-density point clouds, DSMs, DSMorthos and DTMorthos.

We've got you covered.



ULTRACAM  Microsoft